

Influence of ABCA1 and ABCA7 on the lipid microenvironment of the plasma membrane

Dissertation

zur Erlangung des akademischen Grades
doctor rerum naturalium
(Dr. rer. nat.)
im Fach Biologie

eingereicht an der
Mathematisch-Naturwissenschaftlichen Fakultät I
der Humboldt-Universität zu Berlin

von
Dottore Magistrale in Biotecnologie Industriali
Anna Pia Plazzo
geb. 17.10.1981 in San Giovanni Rotondo, Italien

Präsident der Humboldt-Universität zu Berlin
Prof. Dr. Dr. h.c. Christoph Marksches

Dekan der Mathematisch-Naturwissenschaftlichen Fakultät I
Prof. Dr. Lutz-Helmut Schön

Gutachter: 1. Prof. Dr. Andreas Herrmann
 2. Prof. Dr. Thomas Günther-Pomorski
 3. Prof. Dr. Thomas Eitinger

Tag der mündlichen Prüfung: 12.06.2009

Alla mia famiglia

Zusammenfassung

Der ABC-Transporter ABCA1 ist unmittelbar in die zelluläre Lipidhomeostase einbezogen, in dem er die Freisetzung von Cholesterol an plasmatische Rezeptoren, wie ApoA-I, vermittelt. Trotz intensiver Untersuchungen ist dieser molekulare Mechanismus nicht verstanden. Verschiedene Studien deuten daraufhin, dass durch die Aktivität von ABCA1 bedingte Veränderungen in der Lipidphase der äußeren Hälfte der Plasmamembran (PM) wichtig für die Freisetzung des Cholesterols sind.

In der vorliegenden Arbeit wird die Lipidumgebung von ABCA1 in der PM lebender Säugetierzellen unter Anwendung der Fluoreszenzlebenszeitmikroskopie von fluoreszierenden Lipidsonden untersucht. Es wurde eine breite Verteilung der Fluoreszenzlebenszeiten der Sonden gefunden, die sensitiv gegenüber Veränderungen der lateralen und transversalen Organisation der Lipide ist. Im Einklang mit Studien an riesengroßen unilamellaren Vesikeln und Plasmamembranvesikeln weisen unsere Ergebnisse die Existenz einer größeren Vielfalt submikroskopischer Lipiddomänen auf.

Die FLIM-Untersuchungen an ABCA1 exprimierenden HeLa-Zellen weisen eine die Lipidphase destabilisierende Funktion des Transportes aus. Dieses wurde unterstützt durch die Lipidanalyse von Fraktionen der PM. Auf der Basis unserer Untersuchungen und früheren Daten stellen wir die Hypothese auf, dass die Exponierung von Phosphatidylserin (PS) auf der Zelloberfläche ein zentrales Ereignis der ABCA1 bedingten Veränderungen ist. Allerdings zeigen vergleichende Studien an ABCA7 exprimierenden Zellen, dass dies nicht ausreicht, um die ABCA1 verursachten Veränderungen in der Lipidpackung der PM zu erklären.

Unsere Ergebnisse beweisen, dass die Fähigkeit von ABCA1, den Cholesterolefflux zu vermitteln, auf durch den Transporter bedingte Veränderungen in der LP der PM zurückzuführen sind, die unabhängig von der Bindung von ApoA-1 sind und dieser vorausgehen. Diese Veränderungen sind notwendig für die Lipidierung von ApoA-1 und der Generierung von HDL-Partikeln.

Schlagerörter: ABCA1, Plasmamembran, Cholesterol, Lipiddomänen, FLIM

Abstract

The ABCA1 transporter organizes cellular lipid homeostasis by promoting the release of cholesterol to plasmatic acceptors such as ApoA-I. Despite intensive investigation, the molecular mechanism of such a process has not yet been clarified.

In the present study we report on the analysis of the ABCA1 lipid microenvironment at the plasma membrane of living cells, by a novel approach based on fluorescence lifetime imaging microscopy (FLIM). In the plasma membrane of mammalian cells, a broad fluorescence lifetime distribution sensitive to treatments interfering with the membrane lateral and transbilayer organization was found. In agreement with investigations in giant unilamellar vesicles and giant plasma membrane vesicles, our results are consistent with the existence of a large variety of submicroscopic lipid domains.

Based on that, FLIM in HeLa cells expressing ABCA1 revealed the destabilizing function of the transporter on the lipid arrangement at the membrane, indicating that lipid packing was a primary target of ABCA1 activity. This was corroborated by the analysis of plasma membrane fractions isolated by density fractionation. On the basis of our analysis and previous data, we speculate that the exposure of phosphatidylserine on the cell surface is a central event for ABCA1-dependent modifications. However, a comparative study of cells expressing ABCA7, the member of the ABCA subfamily with the highest homology to ABCA1, revealed that exposure of PS alone cannot account for the detected effects.

Collectively, our data suggest that the ability of ABCA1 to promote cholesterol efflux is independent and precedes its actual binding to ApoA-I. Rather, ABCA1-induced plasma membrane modifications are necessary for the lipidation of ApoA-I and the generation of high density lipoprotein particles.

Key Words: ABCA1, plasma membrane, cholesterol, lipid domain, fluorescence lifetime imaging

List of abbreviations

ABC	ATP binding cassette	Lo	Liquid ordered
ACAT	Acyl-CoA cholesteryl acyl transferase	LXR	Liver X receptor
ADP	Adenosine diphosphate	MALDI-TOF	Matrix assisted laser desorption ionization-time of flight
ALD	Adrenoleukodystrophy	M β CD	Methyl- β -cyclodextrin
Apo	Apolipoprotein	MDR	Multi drug resistance
ATP	Adenosine triphosphate	Mg ²⁺	Magnesium
BSA	Bovine serum albumine	MLV	Multilamellar vesicle
BSEP	Bile salt efflux pump	MRP	Multi drug resistance protein
Ca ²⁺	Calcium	MS	Mass spectrometry
cAMP	Cyclic adenosine monophosphate	NBD	[N-(7-nitrobenz-2-oxa-1,3-diazol-4-yl)amino]
CE	Cholesterol esters	NBF	Nucleotide binding fold
Cer	Ceramide	PA	Phosphatidic acid
CFTR	Cystic fibrosis transmembrane conductance regulator	PC	Phosphatidylcholine
CHO	Chinese hamster ovary	Pgp	P glycoprotein
CNX	Calnexin	PKA, C	Protein kinase A, C
ConA	Concanavalin A	PL	Phospholipids
CVD	Cardiovascular disease	PM	Plasma membrane
DHB	2,5-dihydroxybenzoic acid	PO	Palmitoyl-oleoyl
DO	Di-oleoyl	PPAR	Peroxisome proliferator-activated receptor
DP	Di-palmitoyl	PS	Phosphatidylserine
DRM	Detergent resistant membranes	PSM	N-palmitoyl-D-sphingomyelin
ER	Endoplasmic reticulum	RCT	Reverse cholesterol transport
FL	Flotillin	Rho	Rhodamine
FLIM	Fluorescence lifetime imaging microscopy	RXR	Retinoid X receptor
FRAP	Fluorescence recovery after photobleaching	SD	Standard deviation
FRET	Förster resonance energy transfer	SEM	Standard error of the mean
GP	Generalized polarization	SM	Sphingomyelin
GPMV	Giant plasma membrane vesicle	SMase	Sphingomyelinase
GPI	Glycosylphosphatidylinositol	SSM	N-stearoyl-D-sphingomyelin
GUV	Giant unilamellar vesicle	TAP	Transporter associated with antigen processing
HDL	High density lipoprotein	TCR	T cell receptor
HEK	Human embryonic kidney	TD	Tangier disease
IDL	Intermediate density lipoprotein	TfR	Transferrin receptor
LacCer	Lactosyl ceramide	TMD	Transmembrane domain
Ld	Liquid disordered	VLDL	Very low density lipoprotein
LDL	Low density lipoprotein	WHAM	Wisconsin hypoalpha mutant

Index

Zusammenfassung	III
Abstract	IV
List of abbreviations	V
1 Introduction	1
1.1 The plasma membrane	1
1.1.1 The repertoire of membrane lipids	1
1.1.2 Phase separation in model membranes	3
1.1.3 Lipid rafts in the plasma membrane	5
1.1.4 Lipid asymmetry and protein-mediated lipid translocation	6
1.2 ATP-Binding Cassette (ABC) transporters	8
1.2.1 General features	8
1.2.2 Domain organization and transport cycle	9
1.2.3 ABC transporters and the transport of lipids	10
1.2.4 The ABCA subfamily	12
1.2.4.1 ABCA1: the key controller of cholesterol efflux	14
1.2.4.2 ABCA7: a molecule with unknown function	14
1.3 ABCA1	16
1.3.1 General features	16
1.3.1.1 Once upon a time	16
1.3.1.2 Topological model	17
1.3.1.3 Regulation of ABCA1	18
1.3.1.4 Tissue and intracellular distribution of ABCA1	19
1.3.2 Physiological function of ABCA1	20
1.3.2.1 Liver ABCA1: lipid efflux and HDL formation	21
1.3.2.2 Macrophage ABCA1 and atherosclerosis	22
1.3.2.3 ABCA1 and engulfment of apoptotic cells	23
1.3.3 Mechanism of ABCA1-mediated lipid efflux	24
1.3.3.1 Lipid efflux to ApoA-I	24
1.3.3.2 ABCA1/ApoA-I interaction	25
1.3.3.3 ABCA1 and membrane domains	25
2 Aim of the study	27
3 Material and methods	28
3.1 Material	28
3.1.1 Chemicals and reagents	28
3.1.2 Biological material	30
3.2 Methods	31
3.2.1 Molecular biology	31
3.2.2 Cellular biology	31
3.2.2.1 Cell culture	31
3.2.2.2 Cell transfection	32
3.2.2.3 Cell treatments	32
3.2.2.4 Radiolabelling of cells and cholesterol efflux	33
3.2.2.5 Cholesterol subcellular distribution	33
3.2.3 Microscopy	34
3.2.3.1 Labelling of cells with NBD-lipid analogues	34
3.2.3.2 Labelling of actin microfilaments with phalloidin	34
3.2.3.3 Confocal laser scanning microscopy	34

3.2.3.4	Fluorescence lifetime imaging microscopy (FLIM)	35
3.2.3.5	Fluorescence lifetime determination	35
3.2.3.6	Fluorescence recovery after photobleaching (FRAP)	37
3.2.4	Biochemistry	38
3.2.4.1	Preparation of MLVs and GUVs	38
3.2.4.2	Preparation of GPMVs	38
3.2.4.3	Detergent-free isolation of lipid rafts	39
3.2.4.4	SDS-Polyacrylamide gel electrophoresis (SDS-PAGE)	40
3.2.4.5	Cholesterol, phospholipid and protein determination	40
3.2.4.6	MALDI-TOF mass spectrometry	41
3.2.4.7	Laurdan spectroscopy	42
3.2.4.8	Annexin V and ApoA-I binding	42
3.2.4.9	Outward redistribution of C6-NBD-PS and C6-NBD-PC	43
4	Results	44
4.1	FLIM of C6-NBD lipid analogues – a tool to study the lateral heterogeneity of membranes	44
4.1.1	Visualization of lipid domains by fluorescence lifetime of C6-NBD-PC in GUVs	44
4.1.2	Partitioning of C6-NBD-PC and other lipid analogues in GPMVs	46
4.1.3	Lifetime distribution of C6-NBD-PC in GPMVs	49
4.1.4	Lifetime distribution of C6-NBD analogues in cellular membranes	51
4.1.4.1	Lifetime distribution of C6-NBD analogues in HepG2 cells	52
4.1.4.2	Lifetime distribution of C6-NBD analogues in HeLa cells	53
4.1.4.3	Effect of ionomycin, cytochalasin D and sphingomyelinase on C6-NBD-PC lifetime	56
4.2	Influence of ABCA1 on the lipid microenvironment at the plasma membrane	59
4.2.1	Impact of ABCA1 on the plasma membrane lateral organization	59
4.2.1.1	ABCA1 expression in HeLa cells	59
4.2.1.2	ABCA1 activity affects the physicochemical properties of the cell surface	60
4.2.1.3	Efflux of cholesterol to M β CD and ApoA-I	63
4.2.1.4	C6-NBD-PC lifetime in condensed membranes: activated Jurkat cells	64
4.2.1.5	Lateral mobility of C6-NBD-PC	66
4.2.2	ABCA1 partitioning in GPMVs	68
4.2.3	Fractionation of the plasma membrane	71
4.2.3.1	Raft partitioning and ABCA1 activity	71
4.2.3.2	Lipid composition of plasma membrane fractions	74
4.2.3.3	Lipid order of plasma membrane fractions	78
4.2.4	ABCA1 and ABCA7: similarities and differences	80
5	Discussion	85
5.1	FLIM of C6-NBD lipid analogues: a tool to study the lateral heterogeneity of membranes	85
5.1.1	Visualization of lipid domains by fluorescence lifetime of C6-NBD-PC in GUVs	85
5.1.2	Fluorescence lifetime of C6-NBD-PC in GPMVs	86
5.1.3	Fluorescence lifetime of C6-NBD-PC in cellular membranes	88
5.2	Influence of ABCA1 on the lipid microenvironment at the plasma membrane	90
5.2.1	ABCA1 affects the lateral organization of the plasma membrane	90
5.2.2	Mechanism of ABCA1-dependent destabilization of raft domains	91
	Bibliography	95
	Acknowledgement	110
	Publications	111
	Eidesstattliche Erklärung	112

1 Introduction

1.1 The plasma membrane

Eukaryotic cells use about 5% of their genes to synthesize thousands of different lipids [1]. The main biological functions of lipids include energy storage, acting as structural components of cell membranes, and participating in signalling pathways. Triacylglycerols and steryl esters, stored in adipose tissue, constitute the major form of energy storage in animals and provide a reservoir of fatty acid and sterol components that are needed for the biogenesis of membranes. Second, the amphipathic character of polar lipids is at the basis for the formation of cellular membranes. This compartmentalization enables the segregation of the internal constituents of the cell from the external environment and the restriction of specific chemical reactions into organelles. In addition to this barrier function, lipids provide membranes with the potential for budding, tubulation, fission and fusion, properties that are fundamental for the biological processes [2]. Finally, lipids can act as first and second messengers in the processes of signal transduction. The most important example is the phosphoinositide system, which is involved in many different processes including cell proliferation, hormone secretion, smooth muscle contraction and transduction of visual information. Indeed, the production and inactivation of inositol lipids is controlled by almost a hundred of (isoforms of) kinases and phosphatases.

1.1.1 The repertoire of membrane lipids

The main classes of eukaryotic membrane lipids are glycerolipids, sphingolipids and sterols.

Glycerolipids are based on glycerol with two fatty acid chains linked at position 1 and 2 (**Fig. 1**). A *cis*-double bond is usually present in the fatty acid that is linked at position 2, causing a kink in the acyl chain and decreasing the packing density of the lipid. A phosphate can be attached at position 3 (forming phosphatidic acid, PA). This phosphate can carry a head group, which either produces a zwitterionic lipid (PC, PE), or gives a net acidic charge (PS, PI). The most abundant phospholipid in eukaryotic membranes is PC (>50%).

Sphingolipids are based on a sphingosine, with a saturated C16-C26 fatty acid linked via an amide bond, yielding ceramide (Cer). The linkage of a phosphocholine headgroup to Cer forms sphingomyelin (SM). Alternatively, addition of glucose or galactose gives rise to glucosylceramide (GluCer) or galactosylceramide (GalCer), respectively. Sphingolipids have saturated tails that allow them to be in a more packed configuration, with cholesterol filling the spaces between the acyl chains and increasing the density of lipid packing [3,4].

Sterols are the major non polar lipids of cell membranes, with cholesterol predominating in mammals and ergosterol in yeast. They are based on a planar and rigid four-ring structure. Besides being a fundamental constituent of cellular membranes, cholesterol is also a precursor molecule for the production of bile salts and steroid hormones.

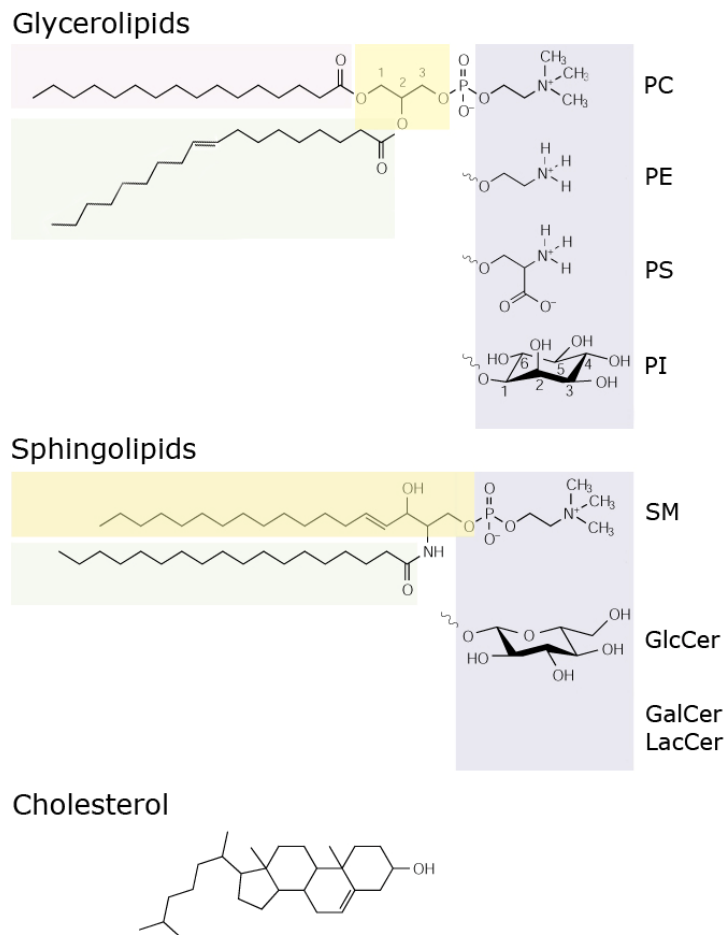


Fig. 1: Structure of mammalian membrane lipids. The main eukaryotic membrane lipids are glycerophospholipids, sphingolipids and cholesterol. The most abundant glycerolipid is PC, which consists of glycerol (yellow shading), two fatty acid chains on the sn-1 and sn-2 position and phosphate carrying the headgroup choline (blue shading). A *cis*-double bond, usually present in the fatty acid that is linked at the sn-2 position, causes a kink in the acyl chain and increases the membrane area of the lipid. The phosphosphingolipid SM and the glycosphingolipid GlcCer have a ceramide backbone, consisting of a sphingoid base, such as sphingosine (yellow shading), linked to a fatty acid via an amide bond. Addition of glucose or galactose to Cer gives rise to GlcCer or GalCer, respectively. LacCer: lactosyl ceramide.

1.1.2 Phase separation in model membranes

Membrane lipids can occur in various phases depending on their structure and environment. At a temperature that is characteristic of the particular lipid species (defined as melting temperature, T_m), phospholipids (PL) can undergo a phase transition from a gel phase (or solid-ordered, S_o) to a liquid disordered (L_d) phase. In the gel phase the lateral mobility of the lipids is highly restricted, with the acyl chains mainly in all-*trans* configuration, packed together in a rigid conformation. In the L_d phase, the lateral mobility of the lipids increases and the acyl chains become disordered. If the membrane contains sufficient amount of cholesterol, the formation of a third phase, the liquid ordered (L_o) phase, is possible. This phase is characterized by a high degree of acyl chain ordering, typical of the gel phase, but with a relatively fast diffusion of lipids, only two- to three-fold slower than in the L_d phase [5].

Appropriate mixtures of SM, unsaturated PL and cholesterol at the opportune temperature can form membranes with coexisting L_d and L_o phases. The L_d phases are enriched with unsaturated PL, whereas cholesterol and sphingolipids preferentially accumulate to the L_o phase [6,7,8]. The interaction of cholesterol with the fatty acid chains of sphingo- or phospholipids leads to a higher degree of order and, accordingly, to a more stretched configuration of the fatty acid chains, responsible for the local increase in the thickness of the bilayer.

Although it is not completely clear how cholesterol drives the formation of a L_o phase, several explanations have been proposed. The packing of cholesterol with the saturated acyl chains of sphingolipids is entropically more favorable than with unsaturated acyl chains [9]. Moreover, possible hydrogen bonding between the hydroxyl group of cholesterol and the amide group of sphingolipids and ceramides can also contribute to this preferential association [10,11,12]. It was suggested that, in a bilayer, the non polar cholesterol relies on the coverage provided by the headgroup of polar phospholipids to avoid the unfavorable free energy of its contact with water [13]. This explanation is often referred to as the “umbrella model”. Alternatively, cholesterol was suggested to form reversible, condensed complexes of defined stoichiometry with sphingolipids and saturated phospholipids [14,15]. The uncomplexed sterol molecules, *i.e.* those that exceed the association capacity of the bilayer lipids, are proposed to have a high escape tendency [14], likely because of enhanced projection into the aqueous compartment. This tendency is also referred to as cholesterol chemical activity. Recently, based on molecular dynamics simulations, Pandit *et al.* proposed that cholesterol molecules may assist the process of domain formation by decreasing the line tension between L_o and L_d domains. This conclusion was based on the observation that, in the ternary system DOPC/SM/cholesterol 1/1/1, cholesterol preferentially localized at the interface

between the ordered SM region and the disordered DOPC region, without showing any preference for SM or DOPC [16].

The process of phase separation has been extensively studied in giant unilamellar vesicles (GUVs), as in these membranes the formation of large, micrometer-scale domains ($> 200 \mu\text{m}$) can be directly visualized by using fluorescent dyes that differentially partition into the two phases (**Fig. 2A**). In biomembranes, it has been questioned whether such phase separation could be hampered by the presence of thousands of different lipid species and membrane proteins. However, this was recently demonstrated not to be the case, as giant plasma membrane vesicles (GPMVs) directly prepared from cells by chemically induced blebbing spontaneously separate into coexisting fluid phases at temperatures $\leq 25^\circ\text{C}$ (**Fig. 2B**) [17,18].

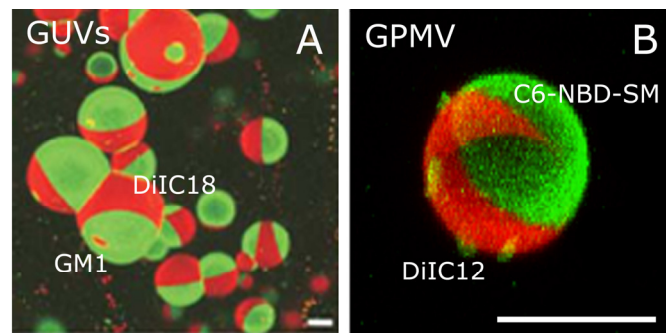


Fig. 2: Phase separation in GUVs (A) and GPMVs (B). (A) GUVs prepared from DOPC/SM/cholesterol (1/1/1) can undergo phase separation into a Ld (red) and Lo (green) phase. Coexisting phases can be visualized by the addition of fluorescent probes that preferentially enrich into one phase (in this case, the Ld phase is visualized by DiIC18 and the Lo phase by GM1-ctxB-488). This figure is taken from [19]. (B) GPMVs prepared from mammalian cells are also able to form distinct phases. In this case the Ld phase, in red, is visualized by the enrichment of DiIC12 and the Lo phase, in green, by the preferential accumulation of C6-NBD-SM (own result). Bars correspond to $10 \mu\text{m}$.

Very recently, Lingwood *et al.* demonstrated that the cross-linking of the ganglioside GM1 could also induce phase separation at 37°C in plasma membrane spheres (PMS) prepared by cell swelling procedures [20]. The authors conclude that the plasma membrane is compositionally poised for raft activation at physiological temperature and that this underlines its capacity to be selectively stimulated to evoke a large-scale lateral reorganization.

These results demonstrate that the complex mixture of lipids and proteins in biological membranes can support fluid/fluid phase coexistence, and are consistent with the presence of nanoscopic Ld/Lo fluctuations in the plasma membrane of living cells [21].

1.1.3 Lipid rafts in the plasma membrane

Research into lateral heterogeneity in cell membranes started more than three decades ago. After the presentation of the fluid mosaic model of the plasma membrane in 1972, which denoted the membrane as a uniform, fluid phospholipid bilayer with proteins dispersed at low concentration [22], the concept of the lateral segregation of lipids first came up in 1987 from van Meer and Simons, who proposed the necessity of lipid domains to explain the sorting of sphingolipids in the Golgi apparatus [23,24]. Few years later, Brown and Rose showed that, after treating cells with cold, non-ionic detergents such as Triton X-100, GPI (glycosylphosphatidylinositol) -anchored proteins and sphingolipids could be recovered in the low density, detergent insoluble fractions [25]. Similarly, detergent resistant membranes (DRM) prepared from model membranes were found to be enriched in cholesterol and sphingolipids and to contain a subset of GPI-anchored proteins [26]. These observations, among others, led to the assumption that the plasma membrane is organized into microdomains, with structure similar to that of the L_0 phases of model membranes, dispersed among lipids in a L_d phase [12]. These “rafts” were proposed to function as platforms for proteins and to serve trafficking and signalling events.

As the limitations of the detergent-based biochemical approaches became evident (see [27] for a review), since it was shown that detergent extraction can even induce formation of microdomains *per se* [28], detergent-free techniques developed to isolate lipid rafts. These techniques are considered more faithful indicators of the native situation in the membrane, although recent work has pointed out that also the application of mechanical stress and the induction of membrane tension can induce coalescence of microdomains [29].

The development of sophisticated biophysical techniques has led to the idea of the plasma membrane as a very heterogeneous and dynamic composite, with raft proteins organized into nanoclusters with radii of 5-20 nm [30,31,32,33]. For instance, based on homo-FRET and fluorescence anisotropy measurements on the surface of CHO cells, GPI-anchored proteins have been suggested to localize in small clusters with about three to four copies [30]. In a recent study, FRET measured between carbocyanine lipid probes has been used to investigate the lateral organization of lipid components in the plasma membrane of living cells [34], supporting the existence of nanometer-scale phase heterogeneity of lipids.

In addition, the sensitivity of the fluorescence lifetime to local properties of lipid bilayers has been recently used to study the lateral organization of lipids in GUVs and in the plasma membrane of living cells [35,36,37]. The newest development comes from the group of Hell [38]. These authors demonstrate, by using stimulated emission depletion (STED) far-field fluorescence nanoscopy, that

sphingolipids and GPI-anchored proteins, but not phosphoglycerolipids, are transiently trapped in cholesterol-mediated molecular complexes, residing within areas with diameters < 20 nm.

From this picture, it emerges that, although the research in this field started already many years ago, the evaluation of the raft organization on biological membranes has been difficult because of the lack of proper tools, able to reliably measure fluctuating nanoscale heterogeneities with minimal or no disturbance [5]. However, a new epoch of investigations has recently started and will follow, along with the advances in the biophysical techniques and imaging methodologies.

1.1.4 Lipid asymmetry and protein-mediated lipid translocation

Besides lipids, the other fundamental constituents of the plasma membrane are proteins, which constitute approximately an equal mass to lipids [39]. Membrane proteins can contribute to the organization and to the physical properties of the plasma membrane by their mere presence or by influencing the distribution of lipids. Reciprocally, also lipids can affect the distribution and function of membrane-associated proteins (for reviews, see [40,41]).

It is long known that in the plasma membrane of animal cells, lipids are asymmetrically distributed between the two leaflets, with PC and SM enriched in the exoplasmic leaflet and PE and PS in the cytosolic leaflet (reviewed in [42]). Whereas SM and glycosphingolipids are basically present only in the outer leaflet, and PS only in the inner leaflet, PC and PE have less pronounced asymmetrical distributions. Conversely, the transbilayer distribution of cholesterol remains unclear. Cholesterol was proposed to be enriched in the exoplasmic leaflet, due to its high affinity for SM [6], to be symmetrically distributed [43,44] or even preferentially present in the cytoplasmic leaflet of erythrocytes [45].

Three classes of proteins are involved in the maintaining and regulation of the transbilayer asymmetry: lipid flippases, lipid floppases and scramblase proteins (**Fig. 3**). Flippases and floppases use the energy derived from the hydrolysis of ATP to drive the translocation of specific phospholipid species towards or away from the cytosolic leaflet, respectively.

Flippases are members of the type 4 subfamily of P-type ATPases, whereas members of the superfamily of ATP binding cassette (ABC) transporters are thought to be floppase candidates.

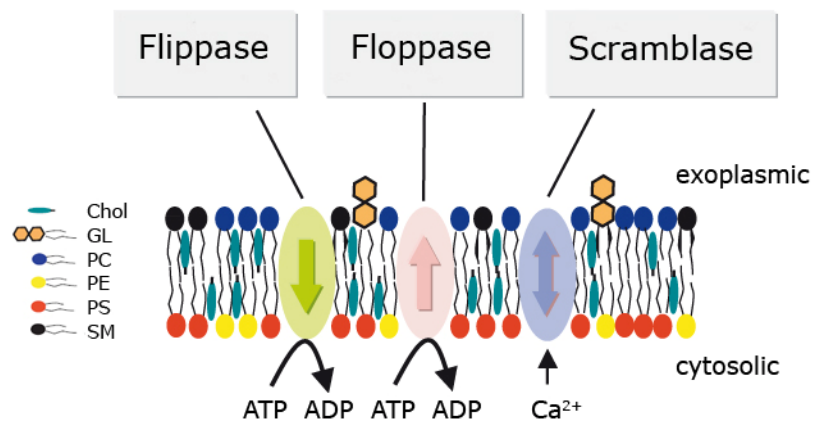


Fig. 3: Lipid asymmetry in the plasma membrane of mammalian cells. This asymmetric lipid arrangement is thought to derive as the result of the action of ATP-dependent proteins that move specific lipids towards (flippases) or away from the cytosolic leaflet (floppases). Cellular activation triggered by cytosolic calcium can collapse the lipid asymmetry by the transient activity of an ATP-independent scramblase. The figure is adapted from [46].

Scramblases are calcium-dependent, bidirectional activities involved in the elimination of the plasma membrane phospholipid asymmetry in critical cellular events like cell activation, injury and apoptosis. Efforts have been made to isolate and clone the potential scramblase PLSCR1 [47]. Moreover, its function as a phospholipid translocase has been recently challenged [48].

1.2 ATP-Binding Cassette (ABC) transporters

1.2.1 General features

The superfamily of ATP-binding cassette (ABC) transporters is one of the largest family of proteins known. It comprises a large number of transporters, channels and regulators, with representatives in all phyla, from prokaryotes to humans [49].

ABC transporters are highly conserved, multispan transmembrane molecules that use the energy derived from ATP hydrolysis to translocate a wide variety of substrates across different cell membranes. Substrates can be sugars, inorganic ions, amino acids, peptides, proteins, lipids and various organic and inorganic compounds. These processes are fundamental for many aspects of cell physiology, including uptake of nutrients, elimination of waste products, generation of metabolic energy, antigen processing, bacterial immunity, cholesterol and lipid trafficking, developmental stem cell biology and cell signalling [50].

The human ABC transporter family consists of 49 members divided into 7 subfamilies, denoted ABC A-G, based on their sequence similarity and structural homology [51]. The high physiological importance of these proteins is underlined by the fact that mutations in their genes are tightly related to genetic disorders. Indeed, most insights into their functions come from the analysis of loss-of-function diseases and genetically modified mice.

Structurally, ABC proteins can be divided into two groups: full-size transporters, which consist of two similar structural units covalently bound, and half-size transporters, composed of single units that form active homo- or heterodimers. One structural unit consists of a nucleotide binding fold (NBF), or ATP binding cassette, and of transmembrane domains (TMDs). The NBFs are highly conserved among all ABC transporters. They contain characteristic motifs, the Walker A and the Walker B regions, typically separated by 90-120 amino acids, and a third, short and highly-conserved motif, called the signature C, located just upstream of the Walker B site. The Walker A and Walker B motifs are found in most proteins that hydrolyze ATP; conversely, the signature C motif is unique for ABC transporters. The TMDs can vary considerably between different ABC proteins. They consist of α -helices which can cross the phospholipid bilayer multiple times, usually from 6 to 11, and are believed to provide for substrate specificity [52].

1.2.2 Domain organization and transport cycle

The eukaryotic ABC proteins typically possess two NBFs and two TMDs. However, many variations in this topographical arrangement are also observed (Fig. 4). The class of (TMD-NBF)₂ represents the full-size transporters, and can be found in the ABCB (also called MDR/TAP), ABCC (MRP/CFTR) and in the members of the ABCA subfamily. Possibly, a third transmembrane domain, TMD₀, composed of five helices, is attached to the N-terminus of several members of the ABCC family. This configuration is designated as TMD₀(TMD-NBF)₂ arrangement.

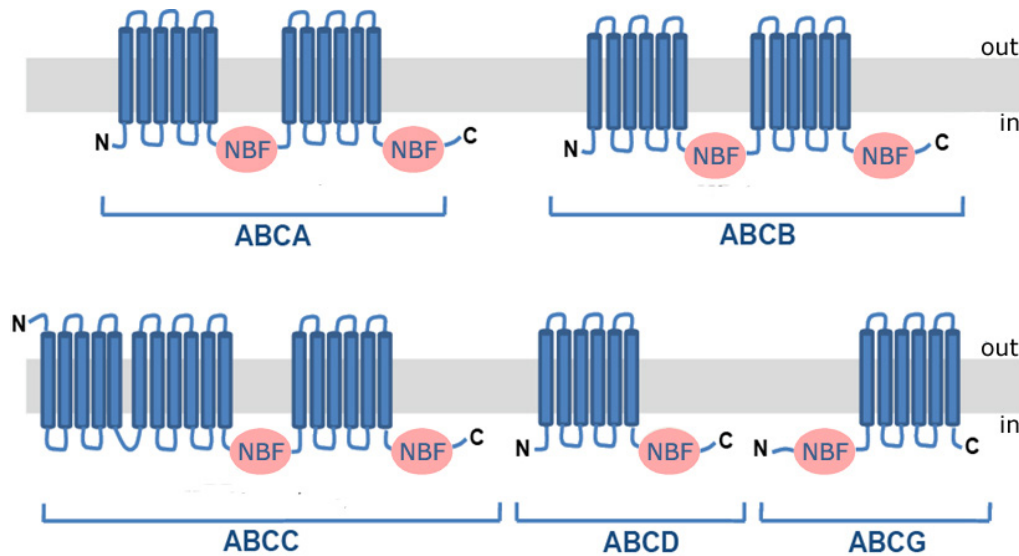


Fig. 4: Domain organization of the human ABC protein subfamilies involved in membrane transport. Transmembrane domains (TMDs) are shown as membrane-spanning helices and nucleotide binding folds are indicated as NBF. The most common arrangement of the members of the indicated subfamilies is shown. ABCE and ABCF subfamilies are not represented, as they are composed of only NBFs and are not involved in any transport function.

Two variations of half transporters are represented among the human ABC proteins: TMD-NBF configuration is present in the ABCB subfamily, in the ABCD (ALD) subfamily of peroxisomal transporters and, in “reverse” configuration, in the ABCG (White) subfamily. ABC proteins of the subfamilies E and F possess only nucleotide binding folds and, therefore, are likely not involved in membrane transport, but rather have regulatory functions [50].

The mechanism used by ABC transporters to drive the substrate translocation has not yet been completely defined. Biochemical, structural and genetic studies have led to the “ATP switch model”, so called because it hypothesizes a switch between two main conformations of the NBFs, an open and a closed one. This model is depicted in Fig. 5 [53,54]. In the first step, the binding of the ligand to a high-affinity pocket formed by the TMDs induces a conformational change in the NBFs, which enhances their affinity for ATP. Two molecules of ATP bind, cooperatively, to generate the close

dimer. The energy released by the formation of the NBF closed dimer causes a conformational change in the TMDs that drives the translocation of the substrate. ATP hydrolysis initiates the resetting of the transporter to its basal configuration, by destabilizing the closed NBF dimer. Finally, the sequential release of P_i and ADP restores the transporter to the open NBF dimer configuration, ready for the subsequent cycle.

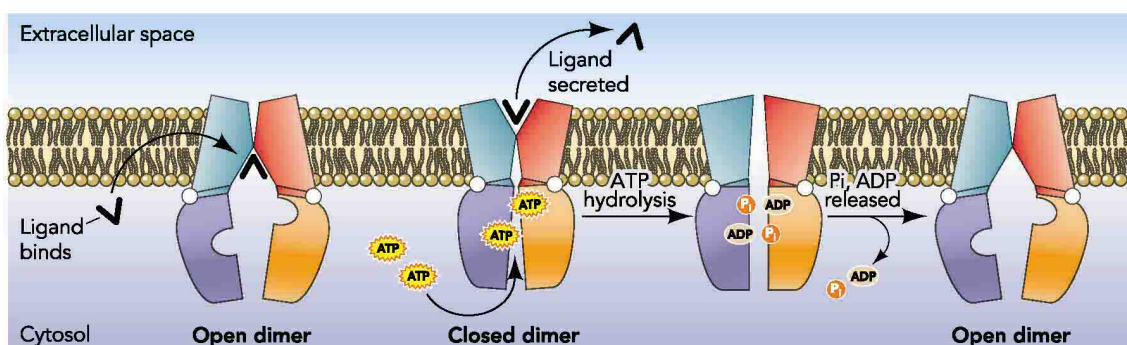


Fig. 5: The ATP switch model for ABC transporters [54]. In its basal state, the transporter has the NBFs in an open dimer configuration, with low affinity for ATP. The transport cycle is initiated by binding of the substrate to its high affinity site on the TMDs from the inner leaflet of the membrane. The affinity for ATP is increased, and two ATP molecules bind to generate the closed dimer. This closed NBF dimer induces a conformational change in the TMDs, which drives the translocation of the substrate. The hydrolysis of ATP destabilizes the closed NBF dimer and the sequential release of P_i and ADP restores the transporter to its basal configuration.

1.2.3 ABC transporters and the transport of lipids

The fact that several ABC proteins were found to be mutated in lipid-linked diseases suggested their potential involvement in lipid transport. However, it was first in 1992 that Higgins and Gottesman formulated the hypothesis that ABCB1 (also called MDR1 or Pgp) was a 'floppase' capable to transport drugs from the inner to the outer leaflet of the lipid bilayer or to the external medium [55]. Since then, a large body of evidence has been accumulating, indicating that ABC proteins can transport lipids across cellular membranes and, in few cases, also in model membranes containing the purified proteins. The specificity in the transport function is reflected in the tissue distribution of the different proteins. At the cellular level, all biological membranes except the nuclear membrane possess ABC transporters, although the vast majority is expressed at the plasma membrane.

The multi-drug resistance protein ABCB1/MDR1 Pgp was shown to expel a variety of short-chain and long-chain (NBD- and radiolabelled) lipids and amphiphilic drugs from the cell [56,57,58]. Among endogenous lipids, outward transport of PAF (platelet-activating factor, a short-chain PC) was suggested [59]. However, ABCB1 was unable to restore transport of PC into the bile of mice lacking *Mdr2* [60], the homologous to human *ABCB4* in mouse. ABCB4 (MDR2/3 Pgp) is

responsible for secretion of PC into the bile, as the bile of mice lacking this protein displays absence of this lipid [60]. In addition, ABCB4 was shown to exclusively transport short-chain NBD analogues of PC in transfected cells [58], differently from the broad substrate specificity of ABCB1. Therefore, the question was raised whether natural long-chain PC is indeed a substrate of ABCB1.

In the process of bile formation, another essential step is the excretion of bile salts, which is mediated by ABCB11 (BSEP), the major canalicular bile salt export pump in man. This process occurs in concert with the translocation of PC. Indeed, mutations in either *ABCB4* or *ABCB11* cause a familial cholestatic liver disease [61].

Members of the D subfamily of ABC transporters localize in the peroxisomal membrane and are involved, as homo- and/or heterodimers, in the β -oxidation of long and very long chain fatty acids, in the synthesis of bile acids and cholesterol plasmalogens, in the metabolism of amino acids and purines and in the generation and degradation of hydrogen peroxide [62]. These proteins are thought to be involved in the transport of fatty acids into the peroxisomal matrix [63,64]. Mutations in *ABCD1/ALDP* result in the X-linked neurometabolic disorder adrenoleukodystrophy [65], characterized by elevated levels of very long chain fatty acids in the nervous system [66].

A number of members of the ABCG family are thought to be implicated in the transport of steroids, phospholipids and toxins. ABCG1 acts, as a homo- or heterodimer, possibly with ABCG2, as a regulator of cholesterol and phospholipid transport in macrophages [67]. In fact, its gene expression was described to be induced during cholesterol influx and suppressed by lipid efflux via high density lipoproteins (HDLs). Inhibition of ABCG1 expression resulted in reduced HDL-dependent efflux of cholesterol and PC. It was proposed that ABCG1 and ABCG4 act in concert with ABCA1 in the removal of excess cholesterol from macrophages [68]. In this process, ABCA1 would mediate the transport of cholesterol to lipid-poor apolipoprotein A-1 (ApoA-I), whereas ABCG1 and ABCG4 to HDL.

Defects in ABCG5 and ABCG8 are the cause of sitosterolemia, an inherited lipid metabolic disorder characterized by hyperabsorption and decreased biliary excretion of dietary sterols [69,70]. These two half transporters are localized to the apical membrane of enterocytes and hepatocytes and likely function as heterodimers to promote efflux of sterols into the bile [71,72,73]. Since cholesterol was argued not to require a transporter to redistribute between the two leaflets of the plasma membrane, it was proposed that ABCG5/G8 may function as a “liftase”, pushing the substrate out of the bilayer and making it available for extraction [74]. Wang *et al.* recently purified ABCG5/G8 from mouse liver and reconstituted sterol transfer in membrane vesicles [75].

To date, many ABC transporters that are supposed to have a role in lipid transport belong to the ABCA subfamily. An overview of the members of this subgroup and of the related genetic disorders can be found to follow.

1.2.4 The ABCA subfamily

In 1994, the group of G. Chimini reported the identification of two novel mammalian ABC transporters by a PCR-based approach, named ABC1 (later ABCA1) and ABC2 (ABCA2) [76]. Both proteins were found to possess novel features compared to the other members of ABC transporters known, namely the presence of a large regulatory domain interrupted by an extra hydrophobic segment. Therefore the novel ABCA subclass was defined. In the following years, a large group of transporters sharing similar features were identified [77,78,79].

The ABCA subfamily consists of 17 full size proteins. They all have a broad tissue distribution, with the exceptions of ABCA3, predominantly expressed in the lung, ABCA4, which is selectively expressed in the retina, ABCA12, mostly found in the skin epidermis and ABCA17, in testis [80].

ABCA1 is the defective gene in Tangier Disease (TD), an inherited HDL deficiency characterized by very low levels of HDLs in the plasma, peripheral accumulation of cholesterol and increased incidence of atherosclerosis. This protein will be extensively described in section 1.3.

ABCA2 is predominantly expressed in the brain and in neural tissues [81]. This protein was shown to be associated with lysosomes, where it may play an important role in neuronal lipid transport [82,83]. Recent works have also indicated a relationship between ABCA2 and Alzheimer's disease [84].

ABCA3 was described to be predominantly expressed in alveolar type II cells in the lung [85]. Staining of the lung tissue with ABCA3-specific antibodies suggested that this protein is specifically concentrated in the membrane of lamellar bodies. These are lysosome-like structures that store pulmonary surfactant, a mixture of phospholipids and proteins which reduce the surface tension at the air-liquid interface. ABCA3 is hypothesized to have a role in the excretion of the lipid fraction of the pulmonary surfactant and is associated with a neonatal respiratory failure [86]. The transport process appears to depend on the lipidation of an amphipatic, helical acceptor protein, surfactant protein B [87].

Defective *ABCA4*, also known as ABCR or Rim protein, is responsible for Stargardt's disease, a form of macular degeneration [79]. Mutations in the *ABCA4* gene have also been attributed to some cases of cone-rod dystrophy, retinitis pigmentosa, and age-related macular degeneration. ABCA4 is

localized in the photoreceptor outer segment disc membranes of the retina, where it is thought to have a role in the visual cycle mediating the recycling of all-*trans*-retinal to 11-*cis*-retinal. Studies on the ATPase activity of the reconstituted ABCA4 suggested, as a substrate, all-*trans*-N-retinylidene-PE, the lipid product generated from the photobleaching of rhodopsin [88].

ABCA5 is expressed in brain, lung, heart, and thyroid gland. Subcellular localization analysis showed the accumulation of the protein in lysosomes and late endosomes [89]. At present, the function of ABCA5 is poorly understood.

ABCA6, *8*, *9* and *10* transporters have a striking sequence similarity and are therefore referred to as “ABCA6-like transporters”. They are thought to represent a subgroup more recently emerged in the evolution of the ABCA family [90]. A potential role for these proteins in macrophage lipid homeostasis was suggested [90,91,92].

ABCA7 has been reported to mediate efflux of cellular phospholipids in response to stimulation by apolipoprotein A-I (ApoA-I), similarly to ABCA1. However, both its involvement in cholesterol efflux and its physiological function are still controversial [93]. A more detailed description of ABCA7, with highlighted similarities and differences to ABCA1, is presented in 1.2.4.2.

ABCA11 is a pseudogene.

ABCA12 has been linked to two congenital keratinization disorders: lamellar ichthyosis and the more severe harlequin ichthyosis. The latter is characterized by a profound thickening of the keratin layer in the fetal skin. Recent studies in *abca12* knock out mice revealed a reduction in skin linoleic esters of long chain omega-hydroxy-ceramides and a corresponding increase in their glucosyl ceramide precursors. As omega-hydroxy-ceramides are required for the barrier function of the skin, these results establish that ABCA12 activity is needed for the generation of long chain ceramide esters, which are essential for the development of a normal skin structure and function [94].

ABCA13 is the largest ABC transporter described to date. The *ABCA13* gene maps to chromosome 7p12.3. This region is genetically linked to Schwachman-Diamond syndrome, a genetic disorder that affects the pancreas, and to a locus involved in T-cell tumor invasion and cancer metastasis [95]. At present, the exact function and substrates of this protein are unknown.

Recently, four new members, *ABCA14-17*, were added to the ABCA subfamily, but they have only been cloned from mouse and rat. All these proteins are predominantly expressed in testis, which suggests that their function may be related to testicular development and/or spermatogenesis [84]. Indeed, ABCA17 was found to be localized, by *in situ* hybridization, in germ cells in the seminiferous tubulus. When the protein was transfected in HEK293 cells, it localized to the endoplasmic reticulum (ER). Metabolic labelling analysis revealed a reduction, in this cell line, in

the amount of esterified lipids, suggesting that ABCA17 may function in the regulation of the lipid composition in the sperm [96]. The human ortholog of the murine *abca17* was recently identified, although it was suggested to be a transcribed pseudogene [97].

In conclusion, during the past years evidence has been accumulating suggesting that ABCA transporters are needed in critical functions in human physiology, which, when defective, lead to several pathological conditions. These proteins appear to mediate the translocation of lipid compounds across different biological membranes. Potential substrates of ABCA transporters include phospholipids (ABCA1, ABCA3, ABCA4, ABCA7), cholesterol (ABCA1) and sphingolipids (ABCA12). However, many members still lack the identification of their potential substrates. The molecular details of the process of substrate translocation await, as well, further clarification.

1.2.4.1 ABCA1: the key controller of cholesterol efflux

ABCA1 is the prototype of the A subfamily of ABC proteins and probably one of the most studied ABC transporters. Since its discovery as the mutated gene in TD, a HDL deficiency syndrome, it has undergone through intensive investigation. A detailed description of the protein structure, of its regulation and of the proposed models for its function is presented in section 1.3.

1.2.4.2 ABCA7: a molecule with unknown function

ABCA7 is the member of the A subfamily with the highest homology to ABCA1 (54% based on amino acid identity). It is highly expressed in the thymus and in other immune and hematopoietic tissues [98]. In addition, strong expression in the brain has also been reported [99,100]. This expression pattern is substantially different from that one of ABCA1, which is, conversely, ubiquitously expressed, with a preferential localization in the liver [101].

Given the central role of ABCA1 in the formation of HDL particles, it was assumed that ABCA7 may also function in lipid or cholesterol metabolism. Indeed, transfection of ABCA7 in several mammalian cell lines mediates efflux of phospholipids (and cholesterol) to apolipoproteins such as ApoA-I (reviewed in [93]), which is the initial step in the production of HDLs. However, deficiency of ABCA7 in mice does not cause evident phenotypic alterations [100], whereas the loss of ABCA1 in mice or humans leads to a dramatic decrease in circulating HDL levels. Genetic knockdown of *abca7* in mouse peritoneal macrophages did not affect phospholipid or cholesterol efflux to ApoA-I. Moreover, in macrophages isolated from *abca1* knockout mice, ApoA-I-stimulated phospholipid efflux was not detected [102]. These results are inconsistent with a residual role of ABCA7 in lipid

efflux *in vivo*, and its physiological function remains essentially unknown. Efflux of cholesterol is still controversial. Whereas some groups reported no cholesterol efflux to ApoA-I [102,103], others showed low but positive cholesterol release [99,104,105]. A second isoform of ABCA7, so called Type II, has been described [99]. This isoform was shown to mediate neither cholesterol nor phospholipid release and appeared to be mainly localized in the ER when transfected in HEK293 cells, in contrast to the plasma membrane localization of the Type I protein.

Given the high levels of ABCA7 expression in platelets [106], a possible role for this protein in the secretion of various lipid mediators was also suggested. Moreover, the observation that ABCA7 is upregulated during the differentiation of keratinocytes [107] may indicate its potential role in epidermal lipid reorganization.

Very recently, ABCA7 was shown to stimulate efflux of cellular cholesterol to ApoE discs and to regulate the processing of the amyloid precursor protein *in vitro*, inhibiting the production of β -amyloid peptides [108]. Therefore, a role for this transporter in the brain lipid metabolism was proposed.

1.3 ABCA1

1.3.1 General features

1.3.1.1 Once upon a time...

In 1960s, in a small isle some kilometers west of the eastern shore of Virginia, Tangier Island, the case of a child with unusually large tonsils of grey-yellowish colour was reported. Histopathological examination revealed the presence of many foam cells accumulating cholesteryl esters along the surface of the tonsils and the patient showed almost completely absence of HDLs in the plasma. This disease was named Tangier disease (TD).

At that time, little was known about lipoprotein physiology and its link to atherosclerosis. However, already in the 70s, the discovery of a receptor for low density lipoproteins (LDLs) and the finding of its deficiency in familial hypercholesterolemia pointed out the crucial role of LDL particles in atherosclerosis [109]. Some years later, plasma HDL cholesterol level was inversely related to the risk of coronary heart disease (CHD) [110]. This observation confirmed the hypothesis previously drawn that HDLs act as shuttles in a process termed reverse cholesterol transport (RCT), in which excess cholesterol is removed from peripheral tissues, such as the arterial wall, and transported to the liver for excretion [111]. Early on, HDL binding sites were also described in fibroblasts. Interestingly, the density of the HDL binding sites was found to be reciprocally related to the cellular levels of cholesterol [112,113]. This gave rise to the hypothesis that TD was caused by a defect, or deficiency, in one HDL receptor. In the following years more than 40 HDL binding proteins were described, but none of them was proved to be missing or not functional in TD [114,115,116].

It was finally in the mid 1990s that 4 groups independently reported that Tangier cells were impaired in the efflux of cholesterol and phospholipids not to HDL particles, but to lipid-free or lipid-poor ApoA-I [117,118,119,120]. Other 5 years had to pass until the genetic defect in TD could be identified to chromosome 9q31 and to the ATP binding cassette transporter A1 [121,122,123].

Nowadays, ABCA1 is known to be responsible for the efflux of cellular phospholipids and cholesterol to ApoA-I, which is the first and rate-limiting step in the formation of HDL particles and in the process of reverse cholesterol transport. Mutations in *ABCA1* gene lead to two HDL-deficiency syndromes: familial hypoalphalipoproteinemia, in its heterozygous form, and TD, in its homozygous or compound heterozygous form. Impairment of ABCA1 is associated with a large spectrum of signs, including large, orange tonsils, peripheral neuropathy, enlarged spleen and liver, development of atherosclerosis and early and increased onset of cardiovascular disease [124]. However, despite intense investigations, the exact molecular mechanism by which ABCA1 drives this process has not yet been fully clarified.

1.3.1.2 Topological model

ABCA1, as all the members of the A subfamily of ABC transporters, is a full-size protein. It has a symmetrical structure, with two transmembrane domains (TMDs) consisting of 6 helices and two nucleotide binding folds (NBFs). The NBFs possess the conserved sequences present in many proteins that utilize ATP, the Walker A and the Walker B motifs, and the Signature C motif, a sequence unique of ABC transporters (**Fig. 6**). The NH₂ terminus of ABCA1 is predicted to be at the cytosolic side of the membrane. All members of the ABCA subfamily present two large extracellular loops, located between the transmembrane segments 1 and 2 and between 7 and 8. These loops are highly glycosylated and can be linked by one or more cysteine bonds [125,126].

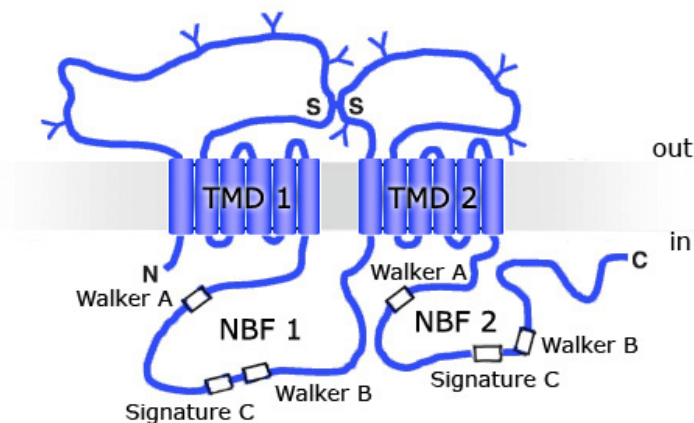


Fig. 6: Topological model of ABCA1. Full-length ABC transporters of the A subfamily are composed of two hydrophobic transmembrane domains (TMDs), each containing six α -helices, and two nucleotide binding folds (NBFs). The NBFs contain conserved motifs, namely the Walker A, Walker B and Signature C, characteristic of all ABC transporters. This topological model is based on studies on ABCA1 and its close homologue ABCA4 [101,125,127] (Y indicates the approximate glycosylation sites, S-S indicates one predicted disulfide bond).

A missense mutation in one of the conserved cysteine residues in the second extracellular loops (C1478R) was shown to cause TD. This highlights the importance of the formation of disulfide bonds, which play a crucial role in protein folding and stability [123]. Furthermore, the quaternary structure of ABCA1 is also important for its function, as transition from dimers into highly oligomeric forms has been observed during the ATP catalytic cycle [128].

1.3.1.3 Regulation of ABCA1

ABCA1 expression is highly controlled at both transcriptional and posttranscriptional level. A fundamental role in the regulation of the *ABCA1* gene is played by nuclear orphan receptors [129]. They are a large group of ligand-dependent transcription factors characterized by an amino-terminal domain responsible for DNA binding and transcriptional activation, and by a carboxy-terminal ligand-binding domain. Among them, the major regulator of lipid homeostasis is the liver X receptor (LXR) [130]. LXR, that functions as a heterodimer with the retinoid X receptor (RXR), is activated by a wide range of hydroxylated cholesterol metabolites and intermediates including oxysterols [131,132]. This likely provides the cells with a “read-out” of the unesterified cholesterol content, as LXR can trigger the activation of various mechanisms that protect the cells from cholesterol overload, including the transcription of many ABC transporters such as ABCA1 and ABCG1 [131]. Conversely, RXR binds and is activated by retinoic acid. RXR receptors typically do not function alone, but rather serve as regulators of several metabolic pathways [133].

Peroxisome proliferator-activated receptors (PPARs) also participate in the up-regulation of ABCA1 expression [134,135]. Conversely, down-regulation of ABCA1 transcription is achieved by the activation of pregnane X receptors (PXR), or through thyroid hormone receptor (TR)/RXR dimers [135] and geranylgeranyl phyrophosphate (ggPP) [136].

In mouse, but not in human, macrophages, expression of ABCA1 is induced by cAMP analogues [137]. The cAMP responsive element was recently identified in intron 2 of the murine *abca1*, whereas the human *ABCA1* gene is not responsive due to a disruption in this element caused by an 8-basepair insertion [138].

Besides being controlled by orphan receptors and by intracellular cAMP levels, PKC-dependent phosphorylation, hormone-sensitive lipase activity and certain fatty acids can also modulate ABCA1 expression [139]. In addition, pro-inflammatory cytokines, tumor necrosis factor α , interleukin-1 β and interferon- γ were shown to down-regulate the LXR-mediated enhancement of ABCA1 expression [140], whereas transforming growth factor β induces ABCA1 expression [141].

In addition to ABCA1 mRNA abundance, the protein levels are also strictly regulated. ABCA1 is rapidly degraded by calpain-mediated proteolysis, with an estimated $t_{1/2}$ of about 1 h. This proteolytic degradation is promoted by the presence, in one of the cytoplasmic loops of ABCA1, of a sequence that resembles a PEST motif, which targets proteins for degradation [142]. The binding of ApoA-I to the protein is necessary to slow ABCA1 rapid degradation. Conversely, unsaturated fatty acids were shown to reduce the macrophage ABCA1 content by enhancing its degradation rate [143]. Direct interaction of ABCA1 with the β 1-syntrophin through the protein-protein interaction

PDZ binding motif also stimulated ABCA1 activity and reduced its degradation rate [144]. Recently, one subunit of the serine palmitoyltransferase enzyme, SPTLC1, was co-purified with ABCA1 and found to negatively regulate its function [145].

1.3.1.4 Tissue and intracellular distribution of ABCA1

ABCA1 is expressed in several tissues in humans, such as the liver, intestine, trachea, lung, adrenal gland, spleen, heart and uterus of pregnant women [129,146]. In some of these tissues, the expression is steroid-dependent [147]. Moreover, ABCA1 can be found in cells of the myeloid lineage, such as activated monocytes, macrophages and foam cells of atherosclerotic lesions, whereas in mice it has been detected in both peritoneal and bone marrow-derived macrophages. ABCA1 expressed in the liver and in the intestine is responsible for the formation of essentially all circulating HDL particles, whereas the impairment of ABCA1 function leads to accumulation of cholesterol mainly in macrophages [148].

When expressed in several cell lines, ABCA1 is mainly localized at the plasma membrane and in intracellular compartments corresponding to the Golgi apparatus, early and late endosomes and lysosomes [149,150]. In polarized hepatocytes, ABCA1 was shown to be localized at the basolateral membrane [151], where it contributes to the maintaining of circulating HDL levels.

The localization of the protein at the cell surface is in agreement with its hypothesized function in lipid transport. However, intracellular ABCA1 could also be involved in the efflux of lipids. Indeed, the existence of a complex intracellular trafficking pathway was described, in which ABCA1-containing lipid vesicles rapidly traffic between intracellular sites and the plasma membrane [152,153]. This trafficking pathway may play, as well, important roles in modulating ABCA1 transport activity and formation of HDL particles [154].

1.3.2 Physiological function of ABCA1

Since its discovery, several functions have been attributed to ABCA1. When it was first identified, it was reported to have a role in macrophage engulfment of apoptotic cells through exposure of PS on the outer leaflet of the plasma membrane [155]. Later on, its identification as the mutated gene in TD has highlighted its role in cholesterol efflux.

Cholesterol, besides being one of the essential components of the plasma membrane, is also a precursor for the synthesis of bile acids and all steroid hormones. Cholesterol can be introduced with the diet and synthesized *de novo* from almost all animal cells. However, it cannot be completely catabolized, and therefore, it has to be transported into the bile for its elimination. In humans, approximately two thirds of cholesterol is transported by LDLs, about 20% by HDLs and the rest by VLDLs. LDLs contribute to the loading of cells with cholesterol through receptor-mediated endocytosis. Conversely, HDLs function as cholesterol acceptors and promote its efflux out from the cells.

In the intestine, cholesterol (C) absorption across the enterocytes is performed on the apical surface by the Niemann-Pick C1-like1 protein (NPC1L1) (**Fig. 7**). On the same membrane, the heterodimers ABCG5/G8 mediate the transport of cholesterol in the opposite direction (see also section 1.2.3). ABCA1 is localized at the basolateral membrane, where it mediates the efflux of cholesterol and phospholipids to ApoA-I to form nascent HDLs (**Fig. 7, 1**). Similarly, in the liver hepatocytes, ABCA1 functions at the basolateral surface (**2**) to form nascent HDL particles. In addition, hepatocytes secrete cholesterol esters (CE), formed by the reaction of acyl-CoA cholesterol acyl transferase (ACAT), to produce nascent VLDL particles. Also in this case, at the apical membrane, the dimer ABCG5/G8 transports cholesterol into the bile canaliculi. Finally, ABCA1 prevents the overloading of macrophages with cholesterol, delivered from modified LDLs through scavenger receptors, by transporting it out of the cell (**3**).

A more detailed description of these steps, as well as the experimental evidence that allowed drawing the described model is presented in the chapters to follow.

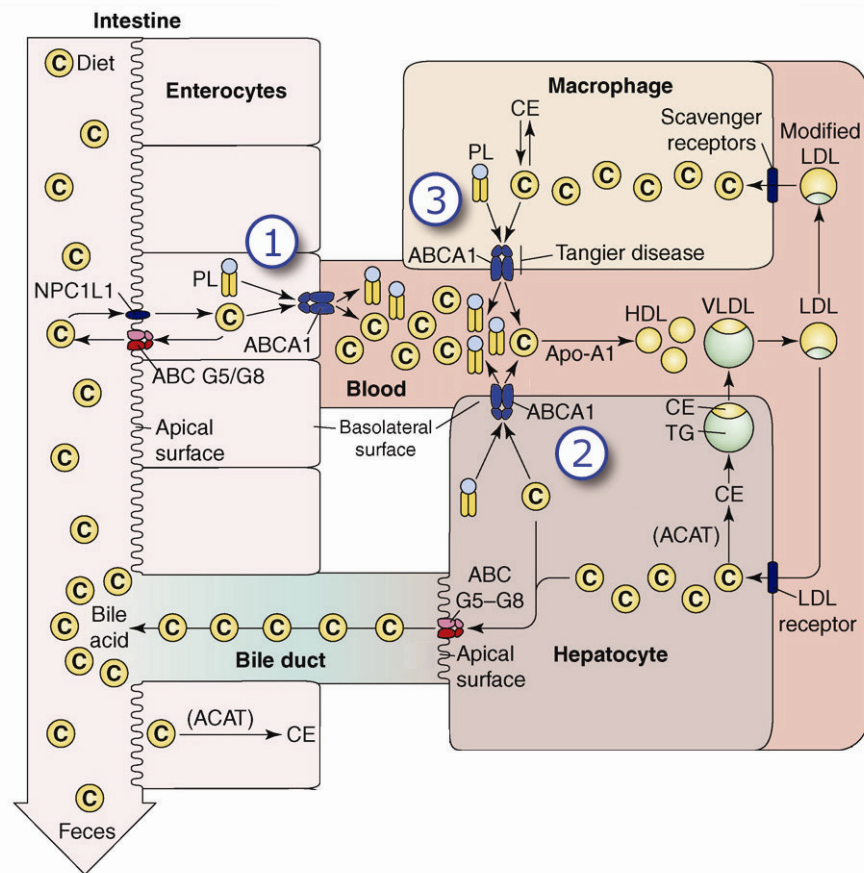


Fig. 7: Cholesterol and phospholipid transport by ABCA1 in the intestine, liver and macrophages. A detailed description of the figure is presented in the text and in the following sections. C: cholesterol, CE: cholesteryl esters, TG: triglycerides, PL: phospholipids, NPC1L1: Niemann-Pick C1-like1 protein 1, ACAT: acyl-CoA cholesteryl acyl transferase, HDL: high density lipoprotein, LDL: low density lipoprotein, VLDL: very low density lipoprotein. This figure is adapted from [148].

1.3.2.1 Liver ABCA1: lipid efflux and HDL formation

HDLs are one of the 5 major groups of lipoproteins (chylomicrons, VLDL, IDL, LDL, HDL) which enable cholesterol and triglycerides to be transported within the blood stream. They consist of about 50% apoproteins, where ApoA-I and ApoA-II are the most abundant, 20% of free and esterified cholesterol, 15% of phospholipids and 5% of triglycerides. One of the major functions of HDLs consists in the transport of cholesterol from peripheral tissues to the liver for elimination into the bile, process called reverse cholesterol transport [101]. The starting step in the process of formation of HDL particles is the efflux of cholesterol and phospholipids to lipid-free or lipid-poor ApoA-I, which is controlled by ABCA1. Therefore, ABCA1 is a major determinant of circulating plasma HDL levels. Fundamental knowledge about the physiological function of this protein has been gained from the observation of the clinical phenotypes of patients affected by TD or familial hypoalphalipoproteinemia. These patients display almost null or reduced level of plasma HDLs,

respectively, and high risk of developing atherosclerosis. In the clinical phenotypes wide heterogeneity is observed [156]. This has been proposed to be a consequence of different mutations in ABCA1, that give rise to the large spectrum of effects observed. To date, 73 *ABCA1* mutations have been identified [157], the majority of which are in the extracellular and intracellular loops of the protein. In addition, numerous single nucleotide polymorphisms in *ABCA1*, that are associated with mild changes in HDL levels, have been described [156].

The generation of animal models with inactivated ABCA1 has largely contributed to the accumulating evidence of the involvement of this protein in HDL and lipoprotein metabolism. *Abca1* knock out mice have phenotypes similar to those with TD [149], although few different features, such as differences in the distribution of accumulated lipids and difficulties in breeding [158], are present. Investigations of *abca1* transgenic mice demonstrated that overexpression of ABCA1 in the liver increases the levels of HDLs [159,160].

A natural animal model of TD exists, the Wisconsin hypoalpha mutant (WHAM) chicken. This animal shows impaired transport of cholesterol introduced with the diet from the intestine to the blood stream [161], highlighting the importance of the ABCA1 pool localized in the intestine. Moreover, the chicken displays normal ApoA-I secretion, but fast clearance, similarly as in *abca1* knock out mice or in TD patients [162].

1.3.2.2 Macrophage ABCA1 and atherosclerosis

Atherosclerotic cardiovascular disease is the primary cause of death in the Western countries. Atherosclerosis is a progressive inflammatory disease characterized by the accumulation of lipids and fibrous elements in the arteries [140]. This leads to the formation of plaques that can cause a narrowing of the lumen of arteries, eventually leading to their complete blockage. Macrophages have a central role in atherogenesis, the process of plaque formation. Deposition of excessive amounts of cholesterol in macrophages leads to their transformation into foam cells, a hallmark of atherosclerosis. Since macrophages cannot limit their uptake of cholesterol via scavenger receptors [163], cholesterol efflux is the central mechanism to prevent development of atherosclerotic lesions.

An inverse relationship between HDL levels and the risk of atherosclerosis has been established [164]. ABCA1 expressed in macrophages prevents them from becoming overloaded with cholesterol by transporting it out of the cells. The role of ABCA1 in atherosclerosis was established by studying mice specifically deficient in macrophage ABCA1 [165]. In these animals, an increase in atherosclerotic lesions was observed, in spite of normal HDL levels. Along the same line, overexpression of macrophage ABCA1 was shown to protect against atherosclerosis, with minimal

effect on plasma lipoproteins [166]. This suggests that the macrophage ABCA1 plays its atheroprotective function independently from its role in maintaining plasma HDL levels.

1.3.2.3 ABCA1 and engulfment of apoptotic cells

Engulfment is a specialized form of phagocytosis dedicated to the clearance of cell corpses generated by the apoptotic program. This process is mainly performed by locally recruited macrophages. One of the signals used from apoptotic cells to be “eaten” is the exposure of PS, normally confined in the inner leaflet, to the outer leaflet of the plasma membrane, alone or bound to bridging molecules [167].

A role of ABCA1 in engulfment is suggested by several studies. The ability of peritoneal macrophages to engulf apoptotic thymocytes was impaired by blocking ABCA1 function with antibodies interfering with the NBF [155]. A close structural relative of ABCA1 was identified as the product of *ced-7*, one of the engulfment genes in the nematode *C. elegans* [168]. In addition, using *in vivo* loss-of-function and *in vitro* gain-of-function models, it was shown that ABCA1 promotes Ca^{2+} -induced exposure of PS at the plasma membrane, as determined by a prothrombinase assay, membrane microvesiculation and measurement of transbilayer redistribution of spin-labelled phospholipids. Consistently with a role of ABCA1 in engulfment, knock out mice showed defective engulfment during development and in adult life [149].

The lipid transport activity of ABCA1 may also be involved in other cellular processes, such as endocytosis. Indeed, an enhanced endocytotic activity in Tangier disease cells, associated with an impairment of PS exposure, was assessed [169]. Moreover, both receptor-mediated and fluid-phase endocytosis were shown to be reduced in cells expressing ABCA1 [170].

1.3.3 Mechanism of ABCA1-mediated lipid efflux

1.3.3.1 Lipid efflux to ApoA-I

ABCA1 promotes the cellular efflux of phospholipids (mainly PC and SM) and cholesterol to ApoA-I. Although this was already recognized 10 years ago, to date, the exact molecular mechanism involved in the ABCA1-dependent mobilization of lipids has not yet been established.

There is considerable disagreement as to whether ABCA1 promotes the direct efflux of both PL and cholesterol to ApoA-I, or whether ABCA1 is primarily a phospholipid transporter and stimulates cholesterol efflux only after generating a lipidated ApoA-I, which would, then, function as an acceptor for cholesterol. Smith *et al.* reported concomitant phospholipid and cholesterol efflux in macrophages after induction of ABCA1 expression by cAMP [171]. Other studies have provided evidence that apolipoproteins simultaneously remove PL and cholesterol from cells by microsolvubilizing the plasma membrane [172,173].

On the other hand, based on a large body of experimental evidence, it was also suggested that efflux of phospholipids and cholesterol are uncoupled events. For instance, Fielding *et al.* reported dissociation between PL and cholesterol efflux to ApoA-I in the presence of the ABC transporter inhibitors vanadate and okadaic acid [174]. Recently, an inhibitor of PKA (protein kinase A) was shown to block cholesterol but not PL efflux [175]. Cholesterol depletion from membranes by cyclodextrin abolished ABCA1-mediated cholesterol efflux but did not affect efflux of PL [176]. In addition, in the same study, no binding of a photoactivable cholesterol analogue to ABCA1 was detected. An increased ability of ApoA-I to promote cholesterol efflux, after being transferred from ABCA1-transfected HEK293 cells to ABCA1-deficient cells, was reported [174,176], but it could not be confirmed by another study in BHK cells [177]. These results suggest that ABCA1 may promote the efflux of only phospholipids and that cholesterol efflux occurs indirectly. Indeed, ABCA1 was shown to induce exposure of PS on the outer leaflet of the plasma membrane [170,178]. This event was proposed to alter the general properties of the membrane and to be at the basis of the impact of ABCA1 on the lipid physiology of the cell [149].

Interestingly, it was recently described that the phospholipid translocation activity of ABCA1 induces bending of the membrane bilayer to create highly curved sites to which ApoA-I can bind [179]. These highly curved sites may represent unstable regions at the membrane, prone to microsolvubilization by ApoA-I. The authors speculated that the binding of ApoA-I may be enhanced by the presence of PS molecules translocated to the exofacial leaflet by ABCA1. It was indeed reported that PS enhances vesicle curvature [180] and binding of ApoA-I to synthetic vesicles [179]. ApoA-I binding to protruding structures in the plasma membrane was previously shown by Lin and

Oram [173]. In the same study, it was also shown that these structures were absent in fibroblasts isolated from a subject with TD.

1.3.3.2 ABCA1/ApoA-I interaction

The interaction between ABCA1 and ApoA-I is of fundamental importance in the process of cellular lipid efflux. However, the nature of this molecular interaction is not fully understood.

Chemical cross-linking studies suggest that a direct binding between these two molecules occurs [127,137]. If this is the case, this interaction should be of low specificity, as ABCA1 can facilitate cholesterol transfer also to many amphipathic proteins [181]. Fitzgerald *et al.* have demonstrated that the extracellular loops between the transmembrane segments 1 and 2 and between 7 and 8 of ABCA1 can be the ones responsible for the binding to ApoA-I. However, there is no clear correlation between this binding and the efflux of lipids. In fact, a mutant ABCA1 protein (T590S) that binds to ApoA-I, but that does not promote lipid efflux, was described [182,183]. This implies that the binding of ApoA-I to ABCA1 may be necessary but is not sufficient to promote cholesterol efflux. Moreover, a simple receptor-ligand interaction would not explain why the ATPase activity of ABCA1 is required for the binding [178]. Corroborating this hypothesis, the diffusion parameters of membrane-associated ApoA-I indicate an interaction with membrane lipids rather than proteins [178].

A second model proposes that the lipid translocase activity of ABCA1 can modify the lipid distribution at the plasma membrane, creating a site required for the docking of ApoA-I [178]. Indeed, the identification of a “high-capacity binding site” at the plasma membrane was recently reported [184]. Interestingly, another group demonstrated that ABCA1 activity creates two types of binding sites for ApoA-I at the cell surface [185]. A first, low-capacity site involves direct ApoA-I/ABCA1 interaction and has regulatory functions stabilizing the transporter. Conversely, a second, high-capacity site at the membrane, created by the activity of ABCA1, involves the binding of a larger pool of ApoA-I that functions in the assembly of nascent HDL particles.

1.3.3.3 ABCA1 and membrane domains

In addition to its role in the lipidation of ApoA-I, ABCA1 was recently reported to influence cholesterol packing at the plasma membrane. Oram and colleagues first documented that ABCA1-expressing cells are more susceptible to cholesterol oxidase [177], an enzyme that preferentially modifies cholesterol in disordered membrane domains [186]. They proposed that ABCA1 redistributes cholesterol to cell surface domains readily accessible to apolipoproteins. In another study, ABCA1 expression in BHK cells was shown to alter the micro-organization of the plasma

membrane, whereas this alteration was not observed upon expression of a non-functional mutant transporter [187]. Based on detergent- and non detergent-based fractionation methods, the authors concluded that ABCA1 activity expands the non-raft membrane fraction.

Furthermore, macrophages isolated from *abca1* knock out mice were shown to exhibit increased lipid rafts [188], as visualized by labelling the cells with two probes, the θ -toxin derivative BC θ , which selectively binds to membrane cholesterol in lipid rafts [189], and the fluorescent polyethylene glycol cholesteryl ether fPEG-chol, which can bind to cholesterol-rich membranes [190].

Very recently, it was reported that, in the absence of ApoA-I, ABCA1 expression leads to the release of cholesterol/phospholipid rich non HDL microparticles, which was prevented by rigidifying the plasma membrane with wheat germ agglutinin [191]. The authors speculated that this process can derive from the ABCA1-induced bending of the membrane.

In conclusion, the intense study performed on ABCA1 in the last nine years has provided a huge amount of data. A final model for its function has to take in consideration several evidence: i) ABCA1 is required for the efflux of lipids and cholesterol to ApoA-I; ii) ApoA-I is able to bind, at least in a small pool, to ABCA1, even though this binding is not sufficient to trigger lipid efflux; iii) ABCA1 expressing cells show highly curved membrane protrusions to which ApoA-I preferentially binds and iv) enhanced exposure of PS on the outer leaflet of the plasma membrane; v) ABCA1 influences the micro-organization of the plasma membrane through its ATPase activity.

2 Aim of the study

ABCA1 is a member of the ABC transporter superfamily with extremely high physiological importance, as mutations in its gene are associated with HDL deficiency and premature development of atherosclerosis. Atherosclerosis is the primary cause of heart disease and, in the Western countries, is the underlying cause of about 50% of all deaths [140]. Thus, it is critical to understand the exact molecular mechanism of ABCA1 function. Despite the intensive study over the last nine years, there is still no clear picture of how and where ABCA1 mediates the transfer of cholesterol and phospholipids to ApoA-I. Strong evidence indicates that this transfer of lipids occurs at the plasma membrane. In particular, an increasing body of work has emerged proposing that ABCA1 can form lipid domains at the cell surface even in the absence of ApoA-I, even though controversy is still present concerning the nature of such domains. To date, no study assessing the lipid microenvironment of ABCA1 in living cells was performed, also because of the lack of tools suitable to study a complex time- and space-fluctuating system such as the plasma membrane.

The aim of this study was i) to develop a new fluorescence lifetime-based approach that allows investigating the domain structure in the plasma membrane of living cells and ii) to apply this technique for studying the influence of ABCA1 on the lipid microenvironment at the plasma membrane. The strategy chosen was to characterize this technique in systems with increasing complexity as a basis for the interpretation of the study in the cell plasma membrane. GUVs would constitute a well controlled and characterized system that allows the direct visualization of lipid domains by fluorescence microscopy, whereas GPMVs would highlight the influence of a highly heterogeneous protein and lipid composition.

The characterization of the fluorescence lifetime in the plasma membrane of cells would allow evaluating the influence of ABCA1 on its physicochemical properties, integrating the previously proposed models for ABCA1 function. In parallel, the use of well established biochemical approaches would permit the comparison, corroboration and integration of the results. Not less important, this would underline the suitability of new biophysical approaches to study the influence of membrane proteins on the lateral and transbilayer arrangement of lipids.

3 Material and methods

3.1 Material

3.1.1 Chemicals and reagents

Chemicals, reagents and devices were purchased as indicated. All solvents (chloroform, methanol and acetonitrile) were obtained in highest commercially available purity from Fluka GmbH (Schnelldorf, Germany) and used as supplied. Indium tin oxide (ITO) coated glass slides were from Präzisions Glas & Optik (Iserlohn, Germany). High performance TLC plates were from Merck (Darmstadt, Germany). Common buffers and reagents used for SDS-PAGE and Western blotting analysis are indicated in **Table 1**.

Table 1: Common buffers used for SDS-PAGE and Western Blotting analysis.

SDS-PAGE			
<i>Gel composition</i>	<i>Resolving</i>		<i>Stacking</i>
	<i>6%</i>	<i>10%</i>	<i>3%</i>
dH ₂ O	5.3 ml	4 ml	2.3 ml
30% acrylamide/bisacrylamide (Rotiforese, Carl Roth, Karlsruhe, Germany)	2 ml	3.3 ml	300 µl
0.5 M Tris/HCl, pH 6.8			750 µl
1.5 M Tris/HCl, pH 8.8	2.5 ml	2.5 ml	
10% SDS (w/v)	100 µl	100 µl	30 µl
10% APS	100 µl	100 µl	30 µl
TEMED	8 µl	4 µl	3 µl
Sample buffer(2x)			
10% SDS		2 ml	
8 M Urea		4.8 g	
0.5 M Tris/HCl, pH 6.8		2.5 ml	
β-mercaptoethanol		560 µl	
1% glycerol		100 µl	
0.01% bromophenol blue		1 µl	
dH ₂ O		until 10 ml	
Western Blotting			
Antibody dilution buffer	1% milk, 0.1% Tween-20 in DPBS		
Washing buffer	DPBS, 0.1% Tween-20		
Blocking buffer	5% milk, 0.1% Tween-20 in DPBS		

Lipids and lipid analogues used were purchased from Avanti Polar Lipids (Alabaster AL, USA) and used without further purification. They are indicated in **Table 2**.

Table 2: Lipids and lipid analogues used. All are purchased from Avanti Polar Lipids (see reference numbers).

Lipid (analogue)	Description	Ref.
DOPC	1,2-Dioleoyl- <i>sn</i> -Glycero-3-Phosphocholine	850375
SM (brain)	(2S,3R,4E)-2-acylaminooctadec-4-ene-3-hydroxy-1-Phosphocholine	860062
Cholesterol		700000
C6-NBD-PC	1-Palmitoyl-2-[6-[(7-nitro-2-1,3-benzoxadiazol-4-yl)amino]hexanoyl]- <i>sn</i> -Glycero-3-Phosphocholine	810130
C6-NBD-PS	1-Palmitoyl-2-[6-[(7-nitro-2-1,3-benzoxadiazol-4-yl)amino]hexanoyl]- <i>sn</i> -Glycero-3-Phospho-L-Serine (Ammonium Salt)	810192
C6-NBD-LacCer	N-[6-[(7-nitro-2-1,3-benzoxadiazol-4-yl)amino]hexanoyl]-D-Lactosyl-b1-1'-Sphingosine	810226P
C6-NBD-PA	1-Palmitoyl-2-[6-(<i>N</i> -(7-nitrobenz-2-oxa-1,3-diazol-4-yl))-phosphatidic acid (C6-NBD-PA)]	810173
Rho-DOPE	1,2-Dioleoyl- <i>sn</i> -Glycero-3-Phosphoethanolamine- <i>N</i> -(Lissamine Rhodamine B Sulfonyl) (Ammonium Salt)	810150

Media and buffers used for propagation of *E. coli* and for culturing of mammalian cells are indicated in **Table 3**.

Table 3: Common media and buffers used for *E. coli* propagation and mammalian cell culture.

Medium/Buffer	Description/Origin
LB medium	10 g/l Bacto™ Tryptone, BD Biosciences, Heidelberg, Germany 5 g/l Bacto™ Yeast extract, BD Biosciences 5 g/l NaCl 0.1% 1 M NaOH (v/v)
LB agar	LB medium + 15 g/l agar
DMEM	Dulbecco's modified Eagle's medium, PAN Biotech, Aidenbach, Germany
RPMI 1640	Biochrom, Berlin, Germany
FCS	Foetal calf serum, Invitrogen, Karlsruhe, Germany
Trypsin-EDTA	PAN Biotech
DPBS	Dulbecco's phosphate buffered saline, PAN Biotech

Antibodies against human or mouse transferrin receptor and Rab5 were a kind gift of P. Pierre, M. Pierres and H.T. He (CIML, Marseille, France). OKT3 antibody was a kind gift of C. Freund (FMP, Berlin, Germany). Antibodies against ABCA1 and related molecules were provided by D. Trompier and M. Pierres (CIML, Marseille, France). Primary and secondary antibodies used are indicated in **Table 4**. Proteins were transferred to nitrocellulose membranes (Amersham, Freiburg, Germany) and signals were detected with ECL reagents (Amersham).

Table 4: Primary and secondary antibodies used for the detection of the indicated molecules by Western blotting and confocal microscopy.

Antibody	Description	Ref.
<i>Primary antibodies</i>		
β -COP	Rabbit, monoclonal; 1:500	Sigma (Lyon, France)
Calnexin	Mouse, monoclonal; 1:200	Stressgen (Ann Arbor, Michigan, USA)
Calreticulin	Rabbit, monoclonal; 1:2000	Calbiochem (Darmstadt, Germany)
Caveolin	Rabbit, polyclonal; 1:1000	BD Biosciences (Heidelberg, Germany)
CD-14	Rat, monoclonal; 1:250	Pharmingen (san Diego, CA, USA)
Flotillin-1	Mouse, monoclonal; 1:200	BD Biosciences (Le Pont de Claix, France)
Hsp70	Rabbit, polyclonal; 1:100	Abcam (Cambridge, United Kingdom)
LAMP 2	Mouse, monoclonal; 1:500	Pharmingen (san Diego, CA, USA)
<i>Secondary antibodies</i>		
HRP-conjugated	Anti-rabbit,-mouse,-rat (goat); 1:10000	Jackson Immunoresearch (West Grove, PA, USA)
TRITC-labelled	Anti-mouse IgG (goat); 1:1000	Sigma (Taufkirchen, Germany)

3.1.2 Biological material

A short description of the *E. coli* strain used for plasmid propagation as well as of the mammalian cell lines used is reported in **Table 5**.

Table 5: *E. coli* strains and mammalian cell lines used (ATCC: American type culture collection).

Cell line	Description	Ref.
<i>E. coli strains</i>		
DH5 α	F ⁻ endA1 recA1 hsdR17(r _k ⁻ m _k ⁺) supE44 λ ⁻ thi-1 gyrA(Na1) relA1 Φ 80 lacZ Δ M15 Δ (lacZY A-argF)	
<i>Mammalian cell lines</i>		
HeLa Tet Off	Human cervical epithelioid carcinoma-derived cell line that expresses the tetracycline-controlled transactivator (tTA). High-level gene expression system can be generated by transfecting these cells with a plasmid that expresses the gene of interest under the control of a suitable Tet Response Element. Doubling time is approximately 20 h during log phase. Adherent, elongated cells with filopodia.	630905 (Clontech)
HepG2	Human hepatocellular liver carcinoma cell line. Adherent, epithelial-like cells growing as monolayers and in small aggregates. Doubling time is approximately 50-60 h.	HB 8065 (ATCC)
Jurkat, clone E6-1	Human T cell leukemia. Round cells growing singly or in clumps in suspension. Doubling time is approximately 25-35 h.	TIB-152 (ATCC)
MDCKII	Madin-Darby canine kidney cells. Adherent, epithelial-like cells growing as monolayers and aggregates. Doubling time is 30-35 h.	CCL-34 (ATCC)

3.2 Methods

3.2.1 Molecular biology

Competent bacteria (50 μ l) were incubated with 1 ng of plasmidic DNA (whose volume was kept less than 10% of the total volume) for 10 min on ice before placing them at 42°C for 90 s. The tube was then transferred on ice for 2 min before adding 800 μ l of LB medium and subsequently incubating for 30 min at 37°C under mixing (1400 rpm). 50 μ l of this solution were spread on LB agar plates with 100 μ g/ml ampicillin and incubated for 16 h at 37°C. One colony was then selected and let grow in a flask with LB medium overnight. Plasmids were purified with the Plasmid Maxi Kit (Qiagen, Hilden, Germany). Sample concentration and purity was determined by spectrophotometric analysis at 260 nm and 280 nm, respectively, with a Nano-Drop spectrophotometer (Eppendorf, Hamburg, Germany). Plasmidic DNA was kindly provided by Dr. G. Chimini, CIML, Marseille, France.

3.2.2 Cellular biology

3.2.2.1 Cell culture

HeLa Tet-Off cells, HepG2 and MDCKII cells were grown in Dulbecco's modified Eagle's medium (DMEM) supplemented with 10% foetal calf serum (FCS), penicillin, streptomycin and sodium pyruvate (all from Invitrogen, Karlsruhe, Germany) and maintained at 37°C under 5% CO₂. HepG2 cells were grown in cell culture flasks coated with collagen A (Biochrom, Berlin, Germany).

Jurkat E6-1 cells were cultured in suspension below a concentration of 2×10^5 cells/ml in RPMI 1640 medium supplemented with 2 mM L-glutamine (both Biochrom AG, Berlin, Germany), 2 g/l sodium pyruvate and 10% FCS and maintained at 37°C under 5% CO₂. Jurkat cells were kindly provided by C. Freund (FMP, Berlin, Germany).

Aliquot of cells at early passage were stored in liquid nitrogen at -196°C in DMEM supplemented with 20% FCS and 10% DMSO (Sigma, Taufkirchen, Germany). Frozen cells were rapidly thawed and cultured for at least 2 days before seeding as needed. Cells were counted with a Fuchs-Rosenthaler hemocytometer.

3.2.2.2 Cell transfection

Plasmids containing ABCA1, ABCA7 and the respective variants fused with EGFP, EYFP or ECFP were generated in pBI vector (Clontech, Mountain View, CA, USA) [149]. All constructs were verified by sequencing. For transient transfection, cells at the third passage were thawed and grown for 10-16 h before transfection.

Transient transfection with ABCA1, ABCA1MM and ABCA7, tagged with the indicated fluorescent proteins, was performed on a 60-70% confluent monolayer of HeLa Tet-Off cells with 5 µg of plasmid DNA in ExGen 500 (Euromedex, Souffelweyersheim, France) according to the manufacturers' instructions. Briefly, 5×10^5 HeLa Tet-Off cells were incubated overnight with the transfection mix (5 µg of pBI ABCA1-GFP and 100 ng of pTK-Hyg mixed with 20 µl of ExGen 500 in 0.15 M NaCl) and then seeded as required. Transfection efficiency was monitored by flow cytometry (FACScan, BD Biosciences) before seeding. Typically, transfection efficiency was about 40%. Cells were utilized for microscopy about 60 h post-transfection.

Transient transfection with Hemagglutinin-cerulean was performed similarly. In this case, microscopy analysis of cells was done about 48 h post-transfection, when the majority of the protein localized to the plasma membrane. Hemagglutinin-cerulean plasmid was kindly provided by S. Engel (Free University, Berlin, Germany).

For creation of stable-transfected cells, hygromycin B (20 µg/ml, Sigma, Taufkirchen, Germany) selection was started 48 h after transfection. Three-week-old individual cell clones were picked with cloning cylinders and subsequently expanded on the basis of GFP-positive cells, visualized by fluorescence microscopy. Cells were cultured for few passages in complete medium containing 20 µg/ml hygromycin B.

3.2.2.3 Cell treatments

For treatment of Jurkat cells with antibodies or sphingomyelinase, 0.5×10^6 cells were pelleted (5 min; 200 g). For activation with OKT3 antibody, the pellet was resuspended in 25 µl RPMI 1640 and 25 µl OKT3 for 20 min at 37°C. Cells were again pelleted to remove unbound antibodies and incubated with 200 µl RPMI 1640 containing 4 µl TRITC-labelled anti-mouse IgG (diluted 1:100) for 10 min. For sphingomyelinase treatment, the pellet was resuspended in 200 µl RPMI 1640 containing 0.1 U/ml sphingomyelinase (from *Staphylococcus aureus*; Sigma-Aldrich, Taufkirchen, Germany) and subsequently incubated for 30 min at 37°C. Labelling of the cells was achieved by resuspending the pellet with 200 µl 2.5 µM C6-NBD-PC (in RPMI 1640) and incubated for 10 min on ice. To remove the staining solution, the cells were again pelleted and resuspended in 200 µl PBS.

Cytochalasin D treatment was performed on HeLa cells (10^5) grown in glass bottom microwell dishes (MatTek, Ashland, MA, USA). Cells were treated with $0.4 \mu\text{M}$ solution of cytochalasin D in complete medium for 10 min at 37°C before labelling with C6-NBD-PC as described in section 3.2.3.1.

Ionomycin treatment was performed for 10 min at 37°C in DPBS with Ca^{2+} and Mg^{2+} at the indicated concentrations or in DPBS without Ca^{2+} and Mg^{2+} . The calcium-chelating agent EGTA was used at a concentration of 1 mM. In each case, control samples were prepared in which cells were subjected to the same treatments but in the present of the solvent alone (DMSO, EtOH or medium).

3.2.2.4 Radiolabelling of cells and cholesterol efflux

For measurement of cholesterol efflux, 10^6 cells were seeded on 6-well tissue culture plates and grown for one day. Cells were labelled with $1 \mu\text{Ci/ml}$ of [^3H]-cholesterol (GE Healthcare, Freiburg, Germany) in DMEM containing 1 mg/ml BSA for 24 h. After extensive washing with DPBS or DMEM, cells were either incubated on ice with 1 ml of an ice-cold 5 mM M β CD solution in DPBS for 1 min or with 10 $\mu\text{g/ml}$ ApoA-I in DMEM supplemented with 0.1% FCS for 16 h. The medium was collected and the cells washed with additional 200 μl of DPBS, subsequently pooled together with the medium. The medium was centrifuged (1000 g, 7 min, 4°C) to remove cell debris and cholesterol crystals. Cells were dissolved in 600 μl of 0.1 M NaOH solution at room temperature for 30 min. Radioactivity in media and cells was measured by liquid scintillation counting (Lumasafe Plus, Lumac Lsc. B.V, Groningen, The Netherlands) with a Canberra-Packard 1600TR liquid scintillation analyzer (Dreieich, Germany). Cholesterol efflux rate was calculated as the percentage of radioactivity in the medium relative to the total radioactivity in cells and medium.

3.2.2.5 Cholesterol subcellular distribution

For determination of subcellular [^3H]-cholesterol distribution, $\sim 10^6$ cells were labelled with $0.5 \mu\text{Ci/ml}$ of [^3H]-cholesterol for 24 h in DMEM, 1 mg/ml BSA. After washing with cold buffer A (250 mM sucrose, 2 mM EDTA, 40 mM Tricine, pH 7.8, Complete Protease Inhibitor Cocktail, Roche, Basel, Switzerland), cells were scraped into 3 ml of cold buffer A and spun down by centrifugation before being resuspended into 1 ml of buffer A. Cells were homogenized with a dounce homogenizer and centrifuged (1000 g, 10 min, 4°C) to remove nuclei. The post nuclear supernatant (PNS) was collected and the volume was completed until 2 ml with buffer A. 45–10% continuous sucrose gradients were formed in SW41 tubes (Beckman, Krefeld, Germany) and the 2-ml postnuclear supernatant fractions were layered on the top of the gradients. Gradients were subjected to centrifugation (137000 g, 20 h, 4°C) and 12 fractions of 1 ml each were collected from the top. Equal volumes of each fraction were analyzed by SDS-PAGE, blotted onto nitrocellulose

membranes (Amersham, Freiburg, Germany) and probed for the indicated proteins. [³H]-cholesterol levels in each fraction were analyzed by mixing 300 µl of sample with 2 ml of liquid scintillation mixture and radioactivity was detected using a Canberra-Packard 1600TR liquid scintillation analyzer. The refraction index of the fractions was measured using a Bausch & Lomb refractometer at 20°C.

3.2.3 Microscopy

3.2.3.1 Labelling of cells with NBD-lipid analogues

Aliquots of NBD-labelled phospholipid analogues, stored at -20°C in chloroform or chloroform/methanol (1/1), were transferred into a glass tube and dried under a nitrogen flow, before being resuspended in DPBS at the desired concentration. 10⁵ HeLa cells seeded on 35 mm glass-bottom microwell dishes (MatTek, Ashland, MA), were washed with cold DPBS and labelled with C6-NBD-PC or C6-NBD-LacCer for 20 min on ice. Cells were then extensively washed with DPBS at 25°C and immediately analyzed by FLIM to ensure that NBD-lipids localized essentially in the outer leaflet of the plasma membrane. HepG2 cells, seeded on poly-D-lysine-coated dishes, were prepared similarly. In this case, all washing steps were done with HBSS (Hank's balanced salt solution, PAN).

3.2.3.2 Labelling of actin microfilaments with phalloidin

Cells grown in glass-bottom microwell dishes were washed with DPBS and fixed for 10 min at room temperature in fixative solution (4% formaldehyde in DPBS, pH 7). Cells were washed, permeabilized with a 0.5% solution of Triton X-100 in DPBS for 5 min and washed again. Staining of actin filaments was performed by incubating the cells with a 100 nM solution of rhodamin phalloidin (Tebu-Bio, Offenbach, Germany) in DPBS for 30 min, at room temperature in the dark. Subsequently, cells were washed and DNA was stained for 30 s with a 100 nM solution of DAPI (Invitrogen) in DPBS. Cells were extensively washed and imaged in DPBS at room temperature.

3.2.3.3 Confocal laser scanning microscopy

Confocal laser scanning microscopy was performed using an inverted Fluoview 1000 microscope (Olympus, Tokyo, Japan) and a 60 x (N.A. 1.35) oil immersion objective at 25°C, if not stated otherwise. Images with a frame size of 512 x 512 pixels were acquired. GFP and NBD fluorescence were excited with the 488 nm laser line of an Ar-ion laser; fluorescence emission was recorded between 500 nm and 600 nm. CFP was excited with a 440 nm diode laser and detected between 460 nm and 490 nm. EYFP was excited at 515 nm using an Ar laser and detected between 530 and 630

nm. The red rhodamine, Texas Red and TRITC fluorescence was excited with a 559 nm diode laser and recorded from 570 to 670 nm. When multiple dyes were used, the appropriate settings were determined to avoid overlap between the different signals.

3.2.3.4 Fluorescence lifetime imaging microscopy (FLIM)

Images were taken by confocal laser scanning microscopy using an inverted Fluoview 1000 microscope (Olympus, Tokio, Japan) with a 60x (N.A. 1.35) oil-immersion objective at 25°C. Images with a frame size of 512 x 512 pixels were acquired. For confocal images of NBD-labelled cells, NBD-fluorescence was excited with a 488 nm Ar-ion laser and recorded between 500 and 530 nm. FLIM images were acquired by a commercial FLIM upgrade kit (PicoQuant, Berlin, Germany). NBD was excited with a pulsed diode laser (pulse width: 60 ps; pulse frequency: 10 MHz; 4 μ s/pixel) with a wavelength of 468 nm. Emission was recorded using a 540/40 bandpass filter. Single photons were registered with a single photon avalanche photo diode (SPAD). For each image, 50-70 frames were acquired with an average photon count rate of $\sim 2-4 \times 10^4$ counts/s. Images were pseudocolor-coded according to the average lifetime (τ_{av}) of the pixels, defined as

$$\tau_{av} = \frac{\sum_i \alpha_i \cdot \tau_i^2}{\sum_i \alpha_i \cdot \tau_i}$$

where α_i is the respective amplitude.

3.2.3.5 Fluorescence lifetime determination

For the analysis of fluorescence lifetime parameters of NBD-analogues in mammalian cells, cell membrane compartments were selected applying an intensity threshold to exclude fluorescence from background or cytoplasm (**Fig. 8A**). If necessary the selection was refined manually to exclude regions not associated with the membrane.

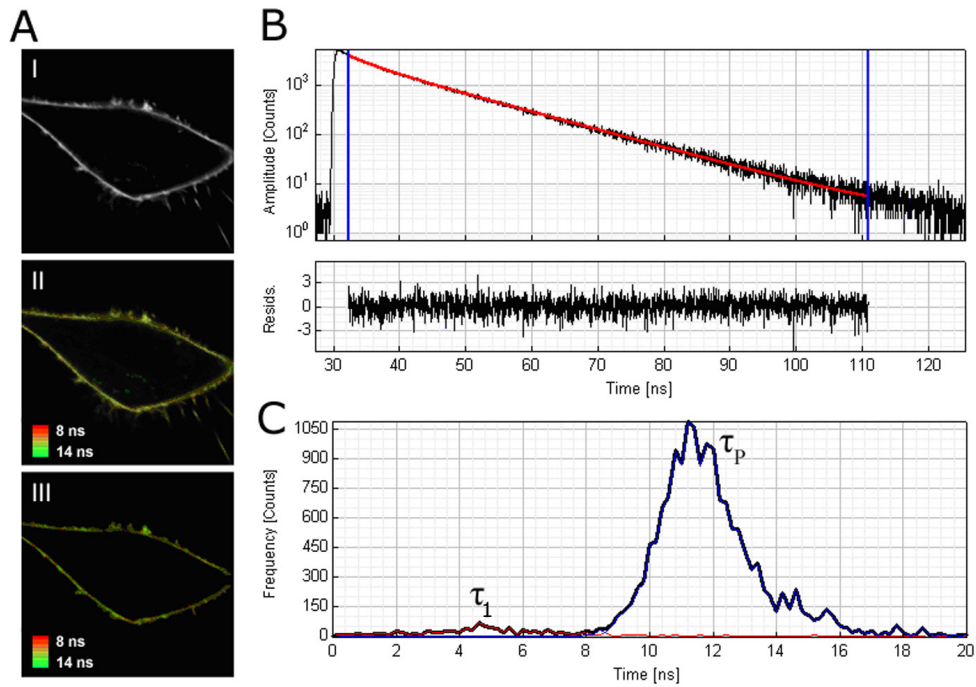


Fig. 8: Determination of fluorescent lifetimes in the plasma membrane of HeLa cells. Images were taken by exciting the NBD fluorescence at 468 nm with a pulsed diode laser as described in 2.2.3.4. (A) The intensity image (A,I) and the average lifetime image shown as pseudocolor image (A,II see scale) of a typical cell are displayed. From this image, the plasma membrane was selected (III) and the fluorescence overall decay curve was generated (B). The part of the curve non affected by the instrument response function (approximately from 3 ns after the beginning of the pulse) was fitted with a biexponential decay function (red line) obtaining τ_1 and τ_p . The lower plot shows the weighted residuals. For construction of the lifetime histograms (C), 2 x 2 or 3 x 3 pixels in the selected region of interest were binned and the fitting procedure was repeated for each binned pixel using the lifetime parameters obtained from the overall decay curve as starting parameters. In the histograms the intensity weighted frequencies ($\alpha_i \times \tau_i$) are plotted.

For the selected regions of interest (ROI), an overall fluorescence decay curve was generated by summing up the photons registered for that region. From the decay curve only the part not affected by the instrument response function (IRF) was used (“tail-fit”, approximately from 3 ns after beginning of the pulse). A typical decay profile in the plasma membrane of HeLa cells with the biexponential fitting and the weighted residual distribution is shown in **Fig. 8B**). Using a nonlinear least squares iterative fitting procedure, fluorescence decay curves were fitted as a sum of exponential terms to obtain the fluorescence lifetimes of the NBD-group:

$$F(t) = \sum_i \alpha_i \exp(-t/\tau_i)$$

where $F(t)$ is the fluorescence intensity at time t and α_i is a pre-exponential factor representing the intensity of the time-resolved decay of the component with lifetime τ_i . Typically, adequate fitting of fluorescence decays in cellular membrane, *i.e.* the plasma membrane and intracellular membranes, was achieved with three lifetimes. However, two lifetimes (τ_1 and τ_p , see “Results” for further

details) already provided sufficient quality of fit when considering fluorescence decays originating only from analogues in the plasma membrane. Due to the tail-fit method, the short component τ_1 detected for NBD (see result section) might be underestimated. Quality of fits was judged by the distribution of the residuals and the χ^2 value. For construction of lifetime histograms (**Fig. 8C**), 2 x 2 or 3 x 3 pixels in the selected regions of interest were binned and the fitting procedure described above was repeated for each binned pixel, using the lifetime parameters obtained from the overall decay curve as starting parameters. In the histograms the intensity weighted frequencies ($\alpha_i \times \tau_i$) are plotted.

Analysis of fluorescence lifetimes in GUVs and GPMVs was performed similarly.

3.2.3.6 Fluorescence recovery after photobleaching (FRAP)

FRAP measurements were performed at 25°C with a 60 x (N.A. 1.35) oil-immersion objective using an Olympus Fluoview 1000 microscope. Regions were selected in the apical membrane of cells with similar expression levels of the wild type or mutant form of ABCA1. After 8 scans (scan speed 4 $\mu\text{s}/\text{pixel}$) at 1% laser power, a circular spot of 1.2 μm radius was bleached for 10 ms with 100% laser power. Under these conditions, 70-80% of NBD fluorescence was bleached. The subsequent recovery of fluorescence was recorded at low laser power (1%) for about 90 s, with an interval of 0.3 s between each postbleach scan. This experimental set up provided minimal bleaching during the measurement. All FRAP measurements were performed at 25°C to minimize the influence of membrane traffic events on the fluorescent recovery. Analysis was performed in Origin 7.5 (OriginLab Corp.). Recovery curves were fitted with an approximation of the theoretical recovery curve:

$$F(t) = F_0 + F_r / (t + \tau)$$

The diffusion coefficient (D) was calculated from the recovery time by the formula: $D = \omega^2 \gamma / 4t_{1/2}$ (ω : radius of the focused circular laser beam, γ : correction factor for the amount of bleaching [192]); mobile fraction (Mf) was given by $Mf = (I_\infty - I_0) / (I_i - I_0)$ [193]. At least 12-20 cells were measured in each experiment.

3.2.4 Biochemistry

3.2.4.1 Preparation of MLVs and GUVs

Multi Lamellar Vesicles (MLVs) were prepared by resuspending dried lipids in Hepes buffer (145 mM NaCl, 10 mM Hepes, pH 7.4), followed by vigorous vortexing.

GUVs were produced from lipid films dried on ITO-coated glass slides by electroswelling, as originally described by Angelova and Dimitrov [194,195]. Lipid mixtures were made from stock solutions in chloroform stored at -20°C. For each preparation, 100 nmol of lipids (including cholesterol) were mixed in 30 µl of chloroform. Single drops of the lipid mixture were pipetted onto two ITO or titanium slides and allowed to spread. To obtain homogeneously distributed lipid films, the solvent was evaporated on a heater plate at 50-60°C. The glass slides were put under vacuum (<10 mbar) for 1 h to remove possible traces of the solvent. The electroswelling chamber was assembled from both lipid-coated ITO slides using 1 mm Teflon spacers. Alternatively, chambers formed from two hollowed titanium sheets were used instead of ITO-coated glass slides, as it was reported by Ayuyan and Cohen that the ITO-coating may catalyse the formation of peroxides from unsaturated lipids [196]. One layer of Parafilm (Pechiney Plastic Packaging, Chicago, IL, USA) was used as insulation.

Chambers were filled with 1 ml of pre-warmed (50-60°C) sucrose buffer (250 mM sucrose, 15 mM sodium azide) with an osmolality of 280 mOsm/kg. An alternating voltage (rising from 0.02 V to 1.1 V over 30 min) with a frequency of 10 Hz was immediately applied. GUVs formed during 2 h incubation at 50-60°C. To detach the vesicles, a voltage of 1.3 V (4 Hz) was applied for 30 min. The vesicles were stored in the dark at room temperature for up to 4 days until use. GUVs were prepared and imaged by Dr. Martin Stöckl. For microscopy, GUVs were diluted 1:3 – 1:5 with glucose buffer (280 mM glucose, 11.6 mM potassium phosphate, pH 7.2) and allowed to settle on a microscopy slide.

3.2.4.2 Preparation of GPMVs

Giant plasma membrane vesicles (GPMVs) or “blebs” were prepared from almost confluent HeLa cells by chemically induced vesiculation as described previously [17,18]. Cells grown in T25 flasks were washed twice with GPMV buffer (2 mM CaCl₂, 10 mM Hepes, 0.15 M NaCl, pH 7.4). To each flask 1.5 ml of freshly prepared GPMV reagent (25 mM formaldehyde, 2 mM dithiothreitol in GPMV buffer) were added. Flasks were incubated for 1 h at 37°C while slowly shaking (60-80 cycles per minute). After incubation, GPMVs that had detached from the cells were gently decanted into a conical glass tube and allowed to settle for at least 30 min on ice. Before imaging, the needed dyes were added to the GPMV suspension resulting in the following final concentrations: R18

(Octadecylrhodamin-B-chlorid, Invitrogen, Karlsruhe, Germany), 0.5 μM ; C6-NBD-PC, 0.8 μM ; Rho-DOPE, 0.8 μM ; C6-NBD-LacCer 0.5 μM ; C6-NBD-SM 2 μM . Images of the equatorial plane of the blebs were taken at 10°C or at 25°C. Temperature was controlled with a water circulating bath.

Concanavalin A-Texas Red (Molecular Probes, Eugene, Oregon, USA) labelling was performed by incubating the cells with a 50 $\mu\text{g/ml}$ solution in GPMV buffer for 5 min at 15°C before formation of blebs. Biotin labelling was performed with Sulfo-NHS-LC-Biotin followed by incubation with Streptavidin Texas Red (both Pierce, Rockford, IL, USA) following the manufacturers' instructions.

To study ABCA1 and ABCA1MM partitioning, GPMVs were prepared from HeLa cells 60 h post transfection with ABCA1 or ABCA1MM tagged with the EGFP or ECFP at the C terminal. The relative domain size was calculated by approximating the vesicle to a circumference and calculating the length of the cord covered by the Ld-like phase, where 1 is the length of the whole circumference. CHO-K1 cells expressing GPI-CFP were kindly provided by S. Scolari.

3.2.4.3 Detergent-free isolation of lipid rafts

Biochemical isolation of lipid rafts was performed accordingly to the detergent-free method developed by Macdonald and Pike [197]. Cells grown in 10 cm tissue culture dishes were scraped into 5 ml of base buffer (20 Tris-HCl, pH 7.8, 250 mM sucrose) with 1 mM CaCl_2 and 1 mM MgCl_2 and washed by centrifugation (1000 g, 5 min, 4°C). Cells were resuspended in 333 μl of base buffer and lysed by mechanical shearing with 20 strokes of a G-25 needle. The PNS was collected after two centrifugation steps (1600 g, 10 min, 4°C). The obtained 666 μl were diluted in 666 μl of 50% OptiPrep solution (Sigma, Lyon, France) made in base buffer, and overlaid with a 6-25% OptiPrep step gradient prepared in base buffer. After centrifugation of the samples at 52000 g in a Beckman SW60 rotor (90 min, 4°C), 18 fractions of 222 μl were collected from the top of the gradient. Equal volumes per fraction were subjected to Western blot analysis. For Laurdan spectroscopy, MALDI-TOF mass spectrometry, cholesterol, phospholipid and protein determination, membrane fractions were prepared from bulk cultures of cells (25×10^6). Refraction index of the fractions was measured using a Bausch & Lomb refractometer at 20°C. Densitometry analysis was performed with AIDA 2.11 software. Analysis of membrane fractions was performed in collaboration with A. Zarubica and Dr. G. Chimini (CIML, Marseille, France).

3.2.4.4 SDS-Polyacrylamide gel electrophoresis (SDS-PAGE)

For separation of proteins, SDS-PAGE was used [198] with the Mini PROTEAN 3 system (Bio-Rad). For investigation of ABCA1, 6% acrylamide/bisacrylamide resolving gels were used, whereas 10% gels were employed to investigate smaller molecules. For stacking gels, 3% acrylamide/bisacrylamide was used. The composition of gels and sample buffer is indicated in **Table 1**. Electrophoresis was run at 25 mA per gel.

3.2.4.5 Cholesterol, phospholipid and protein determination

Cholesterol levels were determined using the Amplex-Red cholesterol assay (Molecular Probes, Leide, The Netherlands) according to manufacturers' instructions.

Lipids were extracted by the method of Bligh and Dyer [199]. Samples were adjusted to volume ratios aqua dest./chloroform/methanol of 0.8/1/2 and kept for 30 min at room temperature after vigorous vortexing. Phase separation was achieved by adding 1 volume each of chloroform and 40 mM acetic acid following by vortexing for 1 min and centrifugation (1000 g, 10 min, 4°C). The upper phase was washed with additional 2 volumes of chloroform followed by vortexing and centrifugation as above. Pooled lower phases were evaporated in glass tubes under a nitrogen stream or under vacuum.

Phospholipid content was determined by measuring the phosphorous amount adapting the method of Hess *et al.* [200]. This assay employs the fact that, at low pH, malachite green forms a complex with phosphomolybdate, which is stabilized by the presence of Tween-20 [201]. Samples and standards containing known amounts of DOPC in chloroform were placed in small 150 µl glass vials (Knauer, Berlin, Germany) and dried under vacuum. 10 µl of 10 N H₂SO₄ and 30 µl of 60% perchloric acid were added to the dried samples. After vortexing, the tubes were heated for 45 min at 200°C in a heating block in order to evaporate the perchloric acid. After cooling down the samples, 75 µl of water and then 400 µl of freshly prepared malachite green working solution were added to the tubes and mixed. Malachite green working solution was prepared by mixing 3 volumes of 0.045% (w/v) malachite hydrochloride (Sigma, Taufkirchen, Germany) with 1 volume of 4.2% ammonium molybdate (w/v) in 4 N HCl for 30 min by magnetic stirring. After filtration through a 0.45 µm filter, 0.02 volumes of 1.5% Tween-20 per volume of filtered solution were added. Samples were transferred to 96 well plates and the absorption at 630 nm was measured on a microplate reader (FLUOstar OPTIMA, BMG Labtechnologies, Offenburg, Germany) after 10 min.

Protein content in the plasma membrane fractions was quantified with the Micro BCA protein assay kit (Pierce, Rockford, USA), according to manufacturers' instructions.

3.2.4.6 MALDI-TOF mass spectrometry

All MALDI-TOF mass spectra were acquired on an Autoflex I mass spectrometer (Bruker Daltonics, Bremen, Germany) with ion reflector. The system utilizes a pulsed 50 Hz nitrogen laser, emitting at 337 nm. The extraction voltage was 20 kV and gated matrix suppression was applied to prevent the saturation of the detector by matrix ions. All spectra were acquired in reflector mode using delayed extraction. A more detailed description of MALDI-TOF MS, in particular of phospholipids, is given in [202]. Spectral mass resolutions and signal-to-noise ratios were determined by the instrument software Flex Analysis 2.4 (Bruker Daltonics). Selected assignments were also confirmed by post source decay fragment ion analysis [203]. The mass spectrometer was calibrated using the molecular ions of a lipid mixtures desorbed from a standard DHB preparation applied next to the spots of interest (positive ion mode). For negative ion detection, the signals of the DHB matrix were used for calibration [204]. Assignments of the most intense peaks are indicated in **Table 6**. MALDI-TOF mass spectrometry experiments were done in collaboration with Dr. Jürgen Schiller (University of Leipzig, Germany).

Table 6: Assignment of the most intense peaks in MALDI-TOF mass spectra of organic extracts of plasma membrane fractions.

Positive ion mass spectra			
<i>Peak position (m/z)</i>	<i>Molecular mass assignment</i>	<i>Peak position (m/z)</i>	<i>Molecular mass assignment</i>
703.6	SM 16:0 + H ⁺	758.6	PC 16:0, 18:2 + H ⁺
725.6	SM 16:0 + Na ⁺	760.6	PC 16:0, 18:1 + H ⁺
732.6	PC 16:0, 16:1 + H ⁺	780.6	PC 16:0, 18:2 + Na ⁺
734.6	PC 16:0, 16:0 + H ⁺	782.6	PC 16:0, 18:1 + Na ⁺
754.6	PC 16:0, 16:1 + Na ⁺	786.6	PC 18:0, 18:2 + H ⁺
756.6	PC 16:0, 16:0 + Na ⁺	808.6	PC 16:0, 18:2 + Na ⁺
Negative ion mass spectra			
<i>Peak position (m/z)</i>	<i>Molecular mass assignment</i>	<i>Peak position (m/z)</i>	<i>Molecular mass assignment</i>
760.6	PS 16:0, 18:1	863.6	PI 18:0, 18:1
788.6	PS 18:0, 18:1	885.6	PI 18:0, 20:4
835.6	PI 16:0, 18:1	887.6	PI 18:0, 20:3
861.6	PI 18:0, 18:2		

3.2.4.7 Laurdan spectroscopy

Laurdan (Molecular Probes, Leide, The Netherlands) solutions in DMSO were added to the membrane fractions isolated with the detergent-free method as described in 2.2.4.3 for 10 min at 25°C. The probe:lipid ratio was kept constant at 1:360. For experiments with MLVs, Laurdan was added to 1 mM lipid solution with constant probe:lipid ratio of 1:1000. Final concentration of DMSO was 0.2 % (v/v). After 10 minutes of incubation, Laurdan was completely incorporated, as assessed by the stabilization of the fluorescence signal. Fluorescence spectra were recorded using an Aminco Bowman Series 2 spectrofluorometer (Rochester, USA) at 25°C, controlled by a water circulating bath. Excitation and emission wavelengths were set at 360 nm and 428 nm, respectively, using 4 nm bandwidth for both.

The fluorescence intensity of Laurdan was quantified by the generalized polarization (GP), which is defined as [205,206]

$$GP = (I_{437} - I_{482}) / (I_{437} + I_{482})$$

where I_{437} and I_{482} are the emission intensities at the corresponding wavelengths.

3.2.4.8 Annexin V and ApoA-I binding

HeLa or MDCKII cells stably expressing ABCA7-YFP cultured in T25 flasks were washed with DPBS supplemented with 24 mM glucose and 10 mM Hepes (mDPBS), trypsinized and washed again. To measure exposure of endogenous PS on the cell surface, about 10^5 cells were incubated on ice in the dark for 10 min with 5 μ l of APC-Annexin V (BD Biosciences, Heidelberg, Germany) in 0.5 ml of binding buffer (10 mM Hepes, 140 mM NaCl, 2.5 mM CaCl_2). Cells were washed and resuspended in 0.5 ml of binding buffer containing 1 μ l of 1 mg/ml stock solution of propidium iodide. Measurements were performed with a FACSCalibur flow cytometer (BD Biosciences) equipped with an Argon laser (488 nm) and a diode laser (630 nm). Data were analyzed with WinMDI software gating on YFP negative (non expressing) and positive (expressing) cells and analyzing APC-Annexin V fluorescence signal. To measure exposure of PS on the outer leaflet of HeLa cells after Ionomycin treatment, Annexin V-FITC was used. In this case, measurements were performed on a FACScan (BD Biosciences).

Fluorescence-based assays for surface binding of cyanilated ApoA-I to ABCA1 were carried out in the laboratory of Dr. Giovanna Chimini as described in [183].

3.2.4.9 Outward redistribution of C6-NBD-PS and C6-NBD-PC

Cells grown in 35 mm dishes were labelled with 1 ml of 10 μ M C6-NBD-PS on ice and incubated at 20°C for 30 min to allow inward movement of the NBD lipid analogues [56,207]. Non inserted analogues were removed by washing cells twice with mDPBS (DPBS supplemented with 24 mM glucose and 10 mM Hepes). Inward redistribution of analogues was initiated by addition of mDPBS pre-warmed to 20°C containing 5 mM diisopropyl fluorophosphates (DFP, Sigma) (as in all following incubations) to prevent hydrolysis of analogues [208]. NBD lipid analogues remaining on the cell surface were extracted twice by incubation with 2% BSA (w/v) in mDPBS for 10 min on ice. After removing the second BSA-containing medium, cells were washed twice with cold mDPBS. For $t=0$ min, cold medium containing 2% BSA and 5 mM DFP in mDPBS was added to the cell dish and incubated for 10 min on ice. To measure C6-NBD-PS outward transport, pre-warmed (37°C) mDPBS with 2% BSA and 5 mM DFP was added to the dish and cells were incubated at 37°C (15, 30 min). The BSA-containing medium was removed and a second extraction with 2% BSA in mDPBS for 10 min on ice was performed.

To measure outward redistribution of C6-NBD-PC, this lipid analogue was biosynthetically produced from C6-NBD-PA. Transport to the outer leaflet of the plasma membrane was measured at 15°C [58]. Cells grown in 35 mm dishes were incubated at 15°C with 1 ml of 25 μ M C6-NBD-PA solution in mDPBS. After 3 h, analogues on the exoplasmic leaflet were removed by washing cells twice with 2% BSA (w/v) in mDPBS for 10 min on ice. Subsequently, cells were incubated at 15°C in 2% BSA solution (1 h, 3 h).

After the incubations, the second BSA back exchange medium was pooled with the first. Cells were scraped into DPBS. For C6-NBD-PS analysis, lipids from media and scraped cells were extracted with isopropyl alcohol (5.5 ml per 1 ml of medium) to prevent substantial loss into the aqueous phase. Samples were centrifuged at 1000 g for 10 min and the supernatant was transferred into new glass tubes and dried under a nitrogen flow. Lipids were dissolved in chloroform:methanol (1:1), applied to TLC plates (Kieselgel 60, Merck) and ran in chloroform:methanol:aqua dest (16:6:1).

For C6-NBD-PC analysis, cells and incubation media were extracted with the method of Bligh and Dyer [199] using 20 mM acetic acid in the aqueous phase. Lipids were subjected to two-dimensional separation (I, chloroform, methanol, 25% ammonium hydroxide (65:25:4, v/v); II, chloroform/acetone/methanol/acetic acid/ water (10:4:2:2:1, v/v)) on TLC plates. NBD fluorescent spots were quantified with a FLA 3000 PhosphoImager (Fujifilm, Dusseldorf, Germany) with the excitation set at 473 nm and emission at 520 nm.

4 Results

In order to assess the influence of ABCA1 on the micro-organization of the plasma membrane, our strategy was to develop a new approach that allowed the identification and characterization of lipid domains in the plasma membrane of living cells.

GUVs and GPMVs were employed as a basis for the interpretation of the data in living cells. Successively, the plasma membrane lipid microenvironment and the effects of its perturbation were investigated.

In the second part of the result section, the application of this approach to the case of ABCA1 is illustrated, followed by the analysis of ABCA1 partitioning in GPMVs and in membrane domains isolated by density fractionation. Finally, a comparative study with ABCA7 is presented.

4.1 FLIM of C6-NBD lipid analogues – a tool to study the lateral heterogeneity of membranes

4.1.1 Visualization of lipid domains by fluorescence lifetime of C6-NBD-PC in GUVs

In our laboratory, a single dye approach based on fluorescence lifetime imaging microscopy (FLIM) was developed to investigate formation of phospholipid domains in artificial and cellular membranes [209]. This technique relies on the intrinsic properties of the NBD group, which shows differential fluorescence lifetimes according to physical properties of the environment in which it is embedded. Parts of the results are shortly illustrated to follow.

To date, giant unilamellar vesicles (GUVs) have been extensively used to study coexisting lipid phase behavior, because their large, micrometer scale domains can be directly observed by fluorescence microscopy. Indeed, GUVs made from appropriate lipid mixtures show formation of laterally segregated domains, which can be visualized by fluorescent compounds that preferentially distribute into one of the domains. Besides, properties such as fluorescent lifetime or generalized polarization, which depend on the environment surrounding the fluorophore, can also be employed to discriminate between coexisting lipid phases [37,210]. Last, the possibility to control the lipid composition of such vesicles is a further advantage that makes them an attractive tool for studying lateral lipid segregation.

GUVs prepared from mixtures of DOPC/SSM/cholesterol 1/1/1 (mol/mol/mol) show coexisting liquid disordered (Ld) and liquid ordered (Lo) phases at 25°C. In these vesicles, the nature of the

different lipid domains can be identified because of the preferential localization of the lipid analogue C6-NBD-PC into the Ld phase [209,211]. This is visualized in the microscopy images as a bright region (Fig. 9A, upper panel).

Apart from the differential localization of the lipid analogue, Ld and Lo phases can be identified by the different fluorescence lifetime of C6-NBD-PC molecules partitioning in such domains. In both the Ld or the Lo phase, the fluorescence decay of C6-NBD-PC shows a bimodal lifetime distribution, with a short (τ_1) and a long (τ_2) lifetime. The long lifetime τ_2 represents the major component of the distribution, whereas τ_1 only provides minor contribution (<5%).

The analysis of the two phases separately revealed that the long lifetime τ_2 is clearly distinct in the Ld and Lo phase, being about 7 ns (τ_{2Ld}) and 11 ns (τ_{2Lo}), respectively, at 25°C (Fig. 9A, lower panel and 9B). In Fig. 9B the histograms of the distribution of τ_2 for each domain and the envelope histogram are presented. Conversely, the short component τ_1 was found not to be sensitive to the lipid phase.

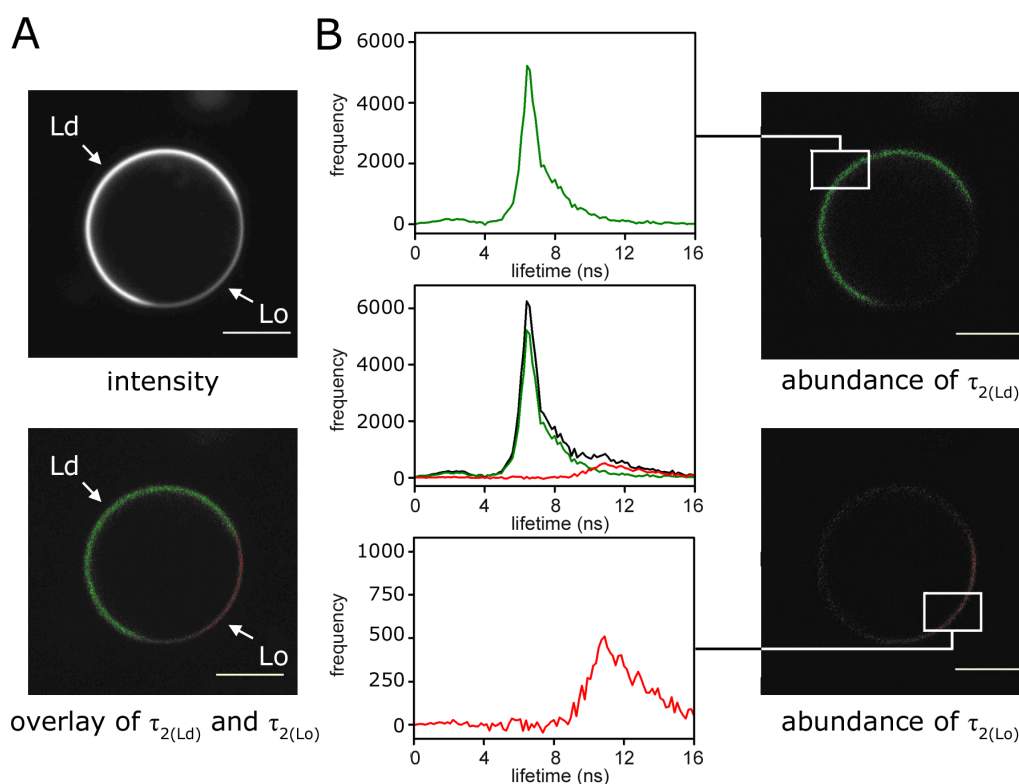


Fig. 9: Fluorescence lifetime of C6-NBD-PC in the Ld and Lo phase of GUVs. (A) Intensity image (top) of C6-NBD-PC in GUVs prepared from DOPC/SM/cholesterol showing the preferential enrichment of this lipid analogue in one phase. At the bottom, the fluorescence lifetime image displaying the lateral distribution of the lifetime components τ_{2Lo} and τ_{2Ld} of C6-NBD-PC is shown. Comparison of the overlay of τ_{2Lo} and τ_{2Ld} with the intensity image shows that τ_{2Ld} is associated with the Ld domain, while τ_{2Lo} is associated with the Lo domain. (B) Images and lifetime histograms of the Ld and Lo domain analyzed separately. For each pixel, the amplitude of the lifetime components τ_{2Ld} or τ_{2Lo} is presented. In addition, the envelope histogram (black line) is shown. White bars correspond to 10 μ m. Images and data were kindly provided by Dr. Martin Stöckl.

The full characterization of the fluorescence lifetime behavior of C6-NBD-PC in model membranes revealed that the longer lifetime component τ_2 is sensitive to the lipid environment. Even for GUVs showing no visible domains, such as vesicles prepared from POPC/PSM/cholesterol 1/1/1, the typical values for τ_{2Ld} and τ_{2Lo} could be recovered from the fluorescence decays. This demonstrates the presence of submicroscopic heterogeneities and confirms that fluorescence lifetime is a proper tool to study the lateral organization and the lipid-dependent physical properties of membranes.

4.1.2 Partitioning of C6-NBD-PC and other lipid analogues in GPMVs

GUVs, being simple model membranes usually composed of three components, allow studying many physical aspects of lipid bilayers thanks to their simplicity and to the possibility to strictly control parameters such as lipid composition. On the other hand, heterogeneity is a fundamental feature of biological membranes. It has been calculated that the mammalian bilayer can possess up to 9,600 species of glycerophospholipids, more than 100,000 species of sphingolipids, thousands of mono/di/triacylglycerol variants and numerous fatty acid- and sterol-based structures [212]. Combined with the great abundance of protein types, this creates a complex and very heterogeneous system.

Giant plasma membrane vesicles (GPMVs) recently emerged as an adequate tool to investigate fluid/fluid phase coexistence and to study the partitioning of lipids and proteins in a biological environment. Such vesicles, obtained from the plasma membrane of cells by chemically induced vesiculation, or “blebbing”, show simple, low-curvature geometries of GUVs and appear free of cytoskeletal constraints and cellular organelles [17]. They have a lipid composition representative of the plasma membrane, with phospholipid:cholesterol ratios of about 2:1 [213,214]. By providing a compositionally rich biological membrane system, they overcome the possible limitations of GUVs, which may fail to capture the multitude of protein-protein and protein-lipid interactions taking place in the plasma membrane. In order to investigate whether the properties of NBD are conserved in vesicles with a complex biological lipid composition, the study of the fluorescence lifetime of C6-NBD-PC was extended to GPMVs.

GPMVs were generated from HeLa cells. These vesicles undergo phase separation into visible, coexisting fluid domains at 25°C (about 40% of the total vesicles formed) or at lower temperatures. Phase separation can be visualized by probes that differentially partition between the two phases, namely the Ld- and the Lo-like phase. C6-NBD-PC was incorporated into the vesicles after their preparation. As previously shown, in GUVs C6-NBD-PC preferentially partitions in the Ld phase [209,211]. Unexpectedly, in GPMVs the lipid analogue did not display an evident heterogeneous

distribution (**Fig. 10A**). The formation and the nature of the different lipid phases were assessed by the non homogeneous distribution of Rho-DOPE. This fluorescent analogue of DOPE was previously shown to preferentially enrich into the Ld-like phase in plasma membrane blebs prepared from rat basophilic leukemia (RBL) mast cells [17,18]. Even vesicles with preferential enrichment of C6-NBD-PC into the Lo-like phase were found (**Fig. 10B**). This indicates that the partitioning of the probe depends not only on the lipid phase, but also on its lipid composition and accompanied modulation of its physical properties (see also discussion, chapter 5.1.2). The lipid-like fluorophore R18, already known to partition almost exclusively into the Ld phase in GUVs [215], was also confirmed to be preferentially enriched in the same phase in GPMVs (**Fig. 10C**). In principle, partition coefficients between coexisting phases could be determined from fluorescence images; however, given the uncertainties in the quantum yields and the difficulties in accurately quantifying fluorescence intensities from the curved surfaces of the vesicles, it was preferable to analyze qualitative information.

In any given sample, not all the vesicles undergo phase separation. This demonstrates that, in some cases, lipids distributed heterogeneously between the vesicles. Those vesicles showing no phase separation were found to be organized mainly as Lo-like phase, as suggested by the enhanced partitioning of C6-NBD-PC in vesicles exhibiting no domain formation as compared to enrichment in the Ld-like phase in blebs with coexisting phases (**Fig. 10C**) and by lifetime measurements. Indeed, τ_2 in those vesicles that show no domain formation was similar to τ_2 measured in the Lo-like phases of vesicles with coexisting domains (description to follow and **Table 7**).

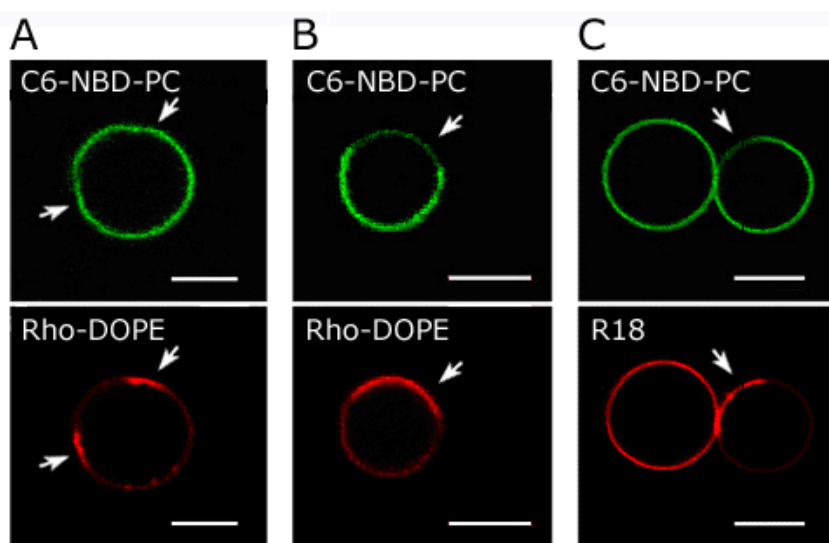


Fig. 10: Partitioning of C6-NBD-PC in GPMVs. C6-NBD-PC incorporated in GPMVs prepared from HeLa cells shows a weak preference for the Lo-like phase, identified by exclusion of Rho-DOPE. Domain-forming vesicles that did not show a preference of C6-NBD-PC for a specific domain were also found (B). R18, already known to be preferentially enriched in the Ld phase in GUVs, was confirmed to prefer the same phase also in GPMVs, as indicated by the complementary staining with C6-NBD-PC (C, vesicle on the right). Vesicles not showing domain formation were also present. At 10°C and 25°C partitioning behavior of the probes was similar. White bars correspond to 5 μm . Arrows indicate the Ld-like phases.

Lo phases in artificial membranes are enriched in sphingolipids, glycosphingolipids and cholesterol. Moreover, GPI-anchored proteins are also considered to be enriched in ordered lipid domains, based on detergent fractionation [10,216] and model membrane studies [217].

To gain insights into the partitioning behavior of these molecules in GPMVs, C6-NBD-SM and C6-NBD-LacCer were incorporated into the vesicles. The analysis of the phase preference revealed that these two lipid analogues display strong enrichment for the Lo-like phase (**Fig. 11**). This suggests that the sphingosine backbone is responsible for this net preference, consistently with model membrane studies [142]. Vesicles in which the analogues were localized in both phases, as described for C6-NBD-PC, were not found.

Similarly, GPI-CFP displayed a marked preference for the Lo-like phase (**Fig. 11C**), in agreement with previous results [18,215]. In this case, blebs were prepared from CHO-K1 cells transiently transfected with this construct [218] (kindly provided by S. Scolari).

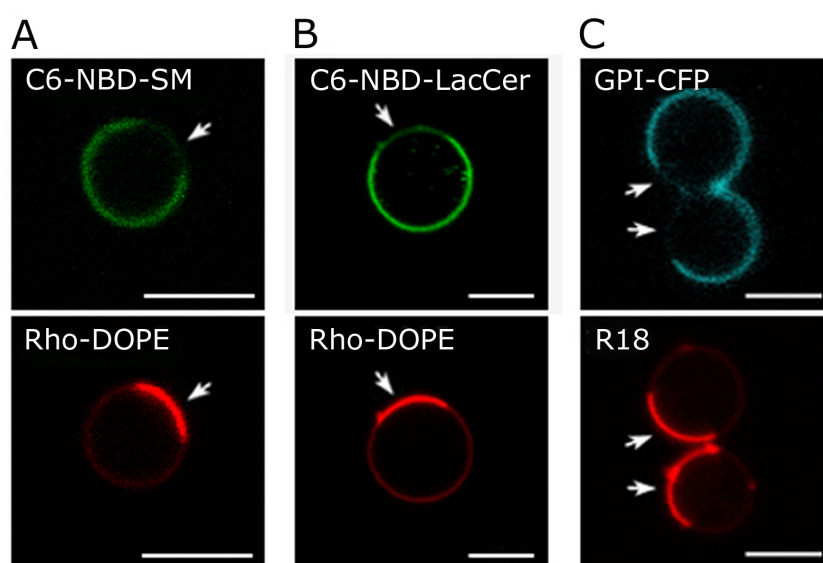


Fig. 11: Partitioning of C6-NBD-SM, C6-NBD-LacCer and GPI-CFP in GPMVs. C6-NBD-SM and C6-NBD-LacCer incorporated in GPMVs prepared from HeLa cells display preferential enrichment in the Lo-like phase, as determined by the complementary partitioning with Rho-DOPE (A and B). Also GPI-CFP, a widely utilized raft marker, prefers the Lo-like phase, as indicated by the complementary staining with R18 (C). Vesicles were visualized at 25°C. White bars correspond to 5 μm . Arrows indicate the Ld-like phases.

4.1.3 Lifetime distribution of C6-NBD-PC in GPMVs

Analysis of fluorescent lifetime of C6-NBD-PC in GPMVs was performed by separately evaluating lifetimes in the Ld- and Lo-like domains. This revealed the presence of a short (τ_1) and a long (τ_2) lifetime component in both phases. Independently of the differential domain-specific distribution of the lipid analogue in comparison with GUVs, lifetime values of τ_2 were similar: at 25°C, C6-NBD-PC lifetime was ~ 6.7 ns in the Ld-like phase and ~ 9.6 ns in the Lo-like phase (**Table 7**). When the vesicles were measured at 10°C, longer lifetimes were detected both for the Ld-like and the Lo-like phase (8.4 ns and 10.8 ns, respectively). This is likely due to an increase in the packing of the acyl chains of the membrane lipids at lower temperatures. Interestingly, lifetime values in vesicles that did not show domain formation were only slightly smaller than values assessed in the Lo-like phase at the respective temperature. This may indicate that such vesicles have an ordered membrane organization and is corroborated by the observation that, in the majority of the cases, the extent of the Lo-like phase covered the larger part of the vesicle surface. Other studies have previously suggested that liquid ordered domains represent the major fraction of the plasma membrane [214,219].

Table 7: Fluorescent lifetime values of τ_2 of C6-NBD-PC in GPMVs prepared from HeLa cells at 25°C and 10°C, before and after cholesterol depletion by M β CD. Data are presented as mean \pm SEM ($n > 6$). The percentage of vesicles showing coexisting phases is also indicated.

	Temperature	$\tau_{2(Ld)}$	$\tau_{2(Lo)}$	τ_2 (no visible domains)	Domain-forming vesicles
		<i>ns</i>	<i>ns</i>	<i>ns</i>	%
-	25°C	6.7 \pm 0.2	9.6 \pm 0.3	9.5 \pm 0.1	40
	10°C	8.4 \pm 0.3	10.8 \pm 0.1	10.3 \pm 0.2	54
M β CD	25°C	7.1 \pm 0.2	9.6 \pm 0.1	8.8 \pm 0.1	21
	10°C	8.2 \pm 0.1	10.3 \pm 0.1	9.3 \pm 0.2	48

In **Fig. 12** the lifetime histograms at 25°C for the Ld-like and Lo-like domain, as well as their envelope histogram, are shown. Even in the case in which GPMVs did not show preferential enrichment of C6-NBD-PC (**Fig. 12A, I**, see arrow), domains could be distinguished by fluorescence lifetime imaging (**Fig. 12A, II and B**). Moreover, fluorescence decay analysis of vesicles for which lipid domains of microscopic size were not observed either by intensity or by lifetime imaging, showed that the lifetime histogram of those vesicles was very similar to the envelope histogram of vesicles forming large domains (**Fig. 12B**, dotted and full black line, respectively).

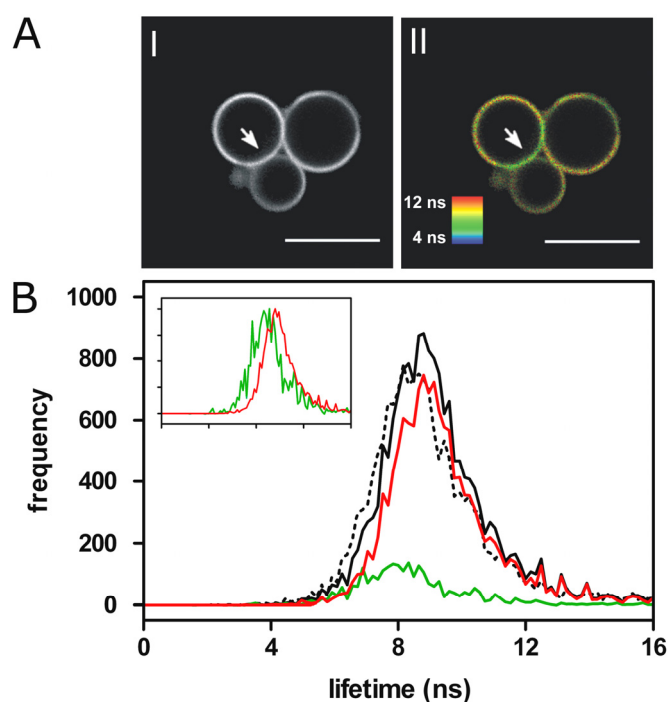


Fig. 12: Fluorescent lifetime of C6-NBD-PC in GPMVs. C6-NBD-PC in blebs prepared from HeLa cells shows only a weak or no domain preference (A, I: intensity image). Nevertheless, Ld (white arrow) and Lo domains can be characterized by lifetime differences (A, II: pseudocoloring according to the average lifetime as indicated in the scale). White bars correspond to 10 μ m. The lifetime histogram for τ_2 for the Ld domain (green line) and Lo domain (red line), as well as their envelope (full line, black), are shown in B. The histogram of lifetime distribution in GPMVs showing no lipid domains (dotted line, black) is very similar to the envelope histogram of GPMVs forming large domains. In the inset, the normalized distribution for the Ld and Lo domains is shown. Measurements were made at 10°C.

Cholesterol is a major determinant of formation of Lo phases. Therefore, we investigated the fluorescence lifetime of C6-NBD-PC in GPMVs formed from cells subjected to cholesterol depletion by M β CD. This treatment did not affect the morphology of the vesicles nor the domains. Similarly, lifetime values in the Ld and Lo domains did not substantially change. Conversely, vesicles that did not show coexisting phases displayed a small reduction in the lifetime values. The percentage of domain-forming vesicles at 25°C was drastically reduced after cholesterol depletion (**Table 7**). As already described, lowering the temperature to 10°C slightly increased the lifetimes.

In conclusion, these results demonstrate that the typical lifetime values for the Ld and Lo domains are conserved in vesicles with large differences in lipid composition, such as GUVs and GPMVs. NBD lifetimes were independent from the preferential enrichment of C6-NBD-PC in a specific domain. In addition, the envelope histograms of vesicles showing or not showing visible domain formation were found to be highly similar. This suggests that submicroscopic lipid domains formed also in the case where micrometer-scale phase separation was not observed.

4.1.4 Lifetime distribution of C6-NBD analogues in cellular membranes

The membrane raft hypothesis proposes that membrane lipid domains, enriched in cholesterol and (glyco-)sphingolipids, form dynamic sorting membrane sites that may function as signalling platforms for membrane proteins [12]. However, controversy concerning size, lifetime and even existence of lipid rafts in the plasma membrane of cells is still present [27]. This skepticism is also raised by the fact that, to date, most conclusions were drawn based on model membrane studies and on detergent fractionation methods, approaches that, although potentially informative, may not reflect the native situation in biological, intact membranes. Typically, in cells large domains have not been observed, suggesting that rafts may be organized at submicroscopic levels, being very small and highly dynamic [5].

We have used our approach based on fluorescence lifetime of NBD lipid analogues to study the presence and properties of lipid domains in the plasma membrane of living cells. Two cell lines were used for this purpose: HepG2 cells originate from the liver, the major site of cholesterol biosynthesis and catabolism, and express many ABC transporters, whereas HeLa cells are a cervical carcinoma cell line. As the latter does not endogenously express ABCA1, it was subsequently utilized to investigate the influence of ABCA1 expression (section 4.2).

4.1.4.1 Lifetime distribution of C6-NBD analogues in HepG2 cells

In a first approach, HepG2 cells were labelled with C6-NBD-PC or C6-NBD-PS. Upon incubation of cells with C6-NBD-PC on ice, lipid analogues were primarily inserted into the outer leaflet of the plasma membrane (**Fig. 13A**). Intracellular staining was very faint if at all present (**Fig. 13A, I**). Several components could be distinguished by analysing the fluorescence lifetime measured at 25°C (**Fig. 13A, III and IV**). Whereas the amplitude of the short lifetime τ_1 around 1.8 ns was very small, we observed two long lifetimes, named τ_i and τ_p , with the maximum of the distribution centered at 6.4 ns and 11.5 ns, respectively (**Fig. 13A, IV**; τ_i : dashed line, τ_p : full line). Image analysis revealed that τ_p was essentially found in the plasma membrane, while τ_i was associated with analogues in intracellular membranes. Indeed, the larger contribution of τ_p compared to τ_i was in agreement with the preferential localization of the analogues in the plasma membrane. Notably, if the analysis was performed selecting only the plasma membrane, then only τ_p was found in addition to τ_i .

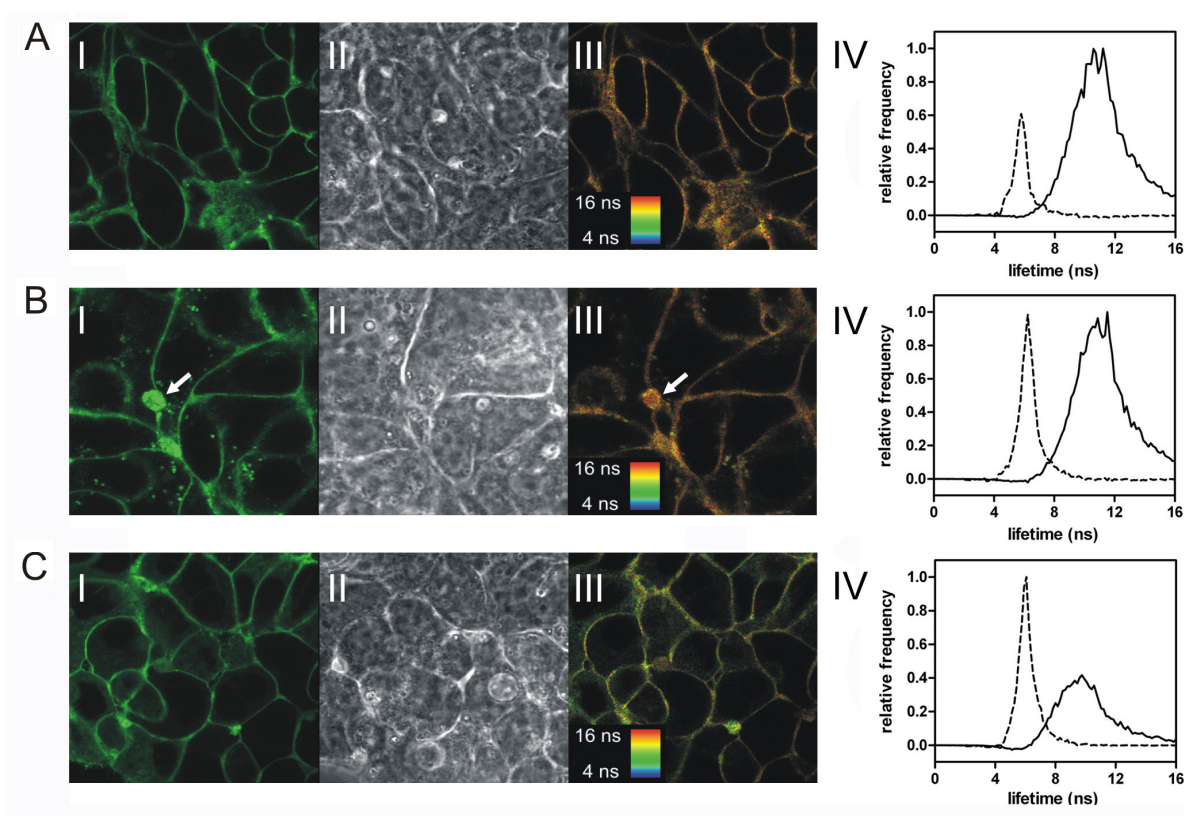


Fig. 13: Fluorescence lifetime of C6-NBD-PC (A and B) and C6-NBD-PS (C) in HepG2 cells. Fluorescence lifetime of the lipid analogues was measured at 25°C immediately after labelling (A,C) and after 1 h of incubation at 37°C (B). (I): confocal fluorescence image; (II): DIC image; (III): average lifetime shown as pseudocolor image (see scale); (IV): histogram of lifetime: τ_i (dashed line) and τ_p (full line). A canicular vacuole, where C6-NBD-PC becomes enriched [220], is indicated by the arrow. Images were taken and analyzed by Dr. Thomas Korte.

The same pattern of lifetimes was observed when cells were incubated, after the labeling procedure, for 1 h at 37°C (**Fig. 13B**). Although the analogue remained mainly confined to the plasma membrane, fluorescent spots in the cytosol started to appear due to its progressive internalization (**Fig. 13B, I**). The fact that the intracellular labelling was enhanced is also indicated by an increase of the contribution of τ_i (**Fig. 13B, IV**). This was due to the transport of the analogues along the endocytic pathway or to slow redistribution across the plasma membrane. Similar lifetimes were observed for C6-NBD-PS (**Fig. 13C**), with a maximum at 6.5 ns and 10.9 ns for τ_i and τ_p , respectively. Again, τ_p essentially originated from analogues in the plasma membrane, whereas τ_i derived from intracellular membranes. However, in this case, the contribution of τ_i was much higher in comparison to C6-NBD-PC, reflecting the enhanced intracellular localization of the analogue of PS. Intracellular staining was even stronger after 1 h of incubation (not shown), due to an aminophospholipid translocase activity which is responsible for transport of PS and corresponding analogues, such as C6-NBD-PS but not PC (analogues), to the cytoplasmic leaflet of the plasma membrane of HepG2 cells, as previously shown [170,221,222]. After translocation, C6-NBD-PS redistributes to intracellular membranes. An efficient transport leading to intracellular staining during the labelling procedure was observed even at low temperatures. Cellular distribution and fluorescence lifetime pattern of C6-NBD-PC or C6-NBD-PS was very similar for HeLa cells (see paragraph to follow). Experiments with HepG2 cells were performed in collaboration with Dr. Thomas Korte.

4.1.4.2 Lifetime distribution of C6-NBD analogues in HeLa cells

In order to have a direct comparison with the values obtained in GPMVs prepared from HeLa cells, C6-NBD-PC fluorescence lifetime was studied in the plasma membrane of the same cellular system. Similarly to HepG2 cells, HeLa cells were labelled with C6-NBD-PC on ice and fluorescence lifetime was promptly measured. At 25°C, proper fitting of the decay curves corresponding to the NBD located in the plasma membrane was achieved with two lifetime components, τ_1 and τ_p , centered at about 3.3 ns and 11.7 ns, respectively. At 10°C, an increase in τ_p to 12.7 ns was measured ($p < 0.0001$, unpaired two-tailed t test), while τ_1 remained essentially unchanged ($p = 0.3$, **Table 8**). This is in agreement with measurements in GPMVs (**Table 7**) and can be attributed to a decreased fluidity of the membrane at lower temperatures. The long component of C6-NBD-PC lifetime at the plasma membrane is considerably higher compared to that found in GPMVs at the same temperature, and even to that measured in the Lo-like phase (compare **Table 7**). This indicates that in the cell parameters other than cholesterol content and lipid and protein composition contribute to the lateral properties of the plasma membrane.

These other parameters may be influenced, for instance, by the cytoskeleton [223] (see also description of cytochalasin D treatment, to follow). Moreover, partial loss of lipid asymmetry occurring during formation of GPMVs may also explain the decrease in the lifetime.

To test whether the lifetime values were dependent on the lipid analogue used, fluorescence lifetime was measured after incorporation of C6-NBD-LacCer in the outer leaflet of the plasma membrane. This lipid analogue is composed of two carbohydrate moieties attached to a ceramide unit, which confer slow redistribution rates across the plasma membrane. The long component τ_p of C6-NBD-LacCer was found to be significantly longer compared to that of C6-NBD-PC ($p < 0.0001$, **Table 8**). This is likely due to the preferential localization of C6-NBD-LacCer, because of its ceramide backbone, to a more ordered environment. Indeed, a higher distribution to ordered domains was also observed in GPMVs (**Fig. 11B**).

Table 8: Fluorescence lifetimes of C6-NBD-PC and C6-NBD-LacCer in the plasma membrane of HeLa cells. Means \pm SD are presented. In the second row, lifetime values after M β CD treatment are indicated. In brackets, number of cells analyzed. ND: not detected. For statistical analysis, see text.

	NBD lifetime			
	25°C		10°C	
	τ_1 <i>ns</i>	τ_p <i>ns</i>	τ_1 <i>ns</i>	τ_p <i>ns</i>
C6-NBD-PC	3.3 \pm 0.6	11.7 \pm 0.3 (56)	3.2 \pm 0.3	12.7 \pm 0.1 (20)
C6-NBD-PC (M β CD)	3.2 \pm 0.4	11.3 \pm 0.2 (33)		ND
C6-NBD-LacCer	3.7 \pm 0.2	12.4 \pm 0.4 (43)		ND

As cholesterol content is a major determinant of lipid packing, we next monitored NBD lifetimes after depletion of cholesterol by M β CD-mediated extraction. This treatment induced a shift of the lifetime distribution of the long component towards lower values ($p < 0.0001$, unpaired two-tailed t test, **Table 8** and **Fig. 14**). In general, cell viability and morphology were not affected. Care was anyway taken to analyze cells that did not show altered morphology. Indeed, in those cells NBD lifetime was much shorter, indicating that major rearrangements of the plasma membrane structure occurred (not shown).

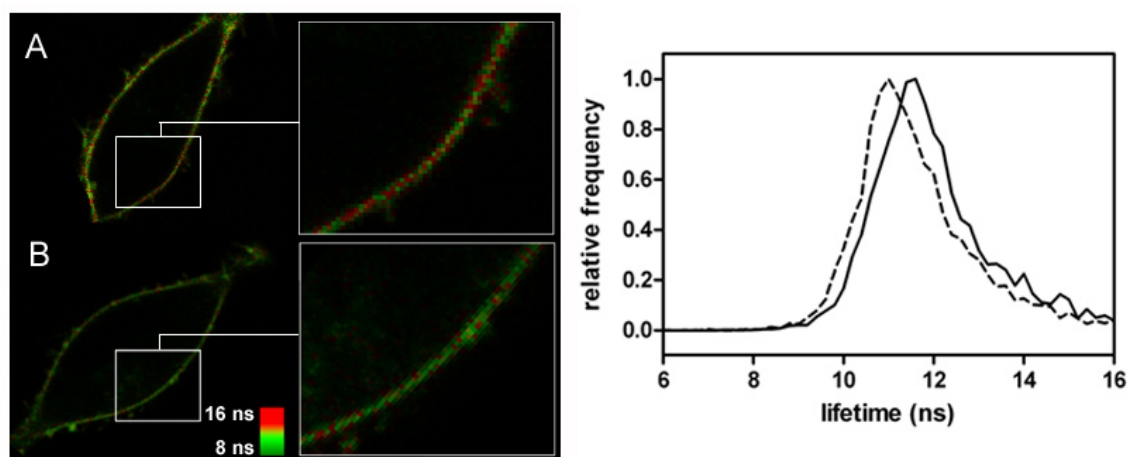


Fig. 14: Fluorescence lifetime of C6-NBD-PC in the plasma membrane of HeLa cells at 25°C. Left panel: average lifetime image of the plasma membrane before (A) and after (B) cholesterol depletion by M β CD-mediated extraction shown as pseudocolor image (see scale in B). Right panel: histogram of τ_p of C6-NBD-PC before (solid line) and after (dashed line) depletion of cholesterol. Histograms were normalized by setting the maximum to 1. Measurements were performed at 25°C.

It is important to mention that techniques based on fluorescence lifetimes are advantageous because, within a reasonable range, such values do not depend on the concentration of the fluorophore. For HeLa cells, we did not find a significant difference in the lifetimes when the starting labelling solution ranged from 0.25 μ M to 2 μ M (**Fig. 15**). However, when cells were labeled with a 2.5 μ M solution of C6-NBD-LacCer, a slight decrease in the lifetime values was observed. At a concentration of 10 μ M, spots of short lifetime probably corresponding to NBD-lipid analogue aggregates appeared at the plasma membrane (**Fig. 15D**). Again, the shorter component was not influenced. In the following chapters only the long component τ_p will be considered.

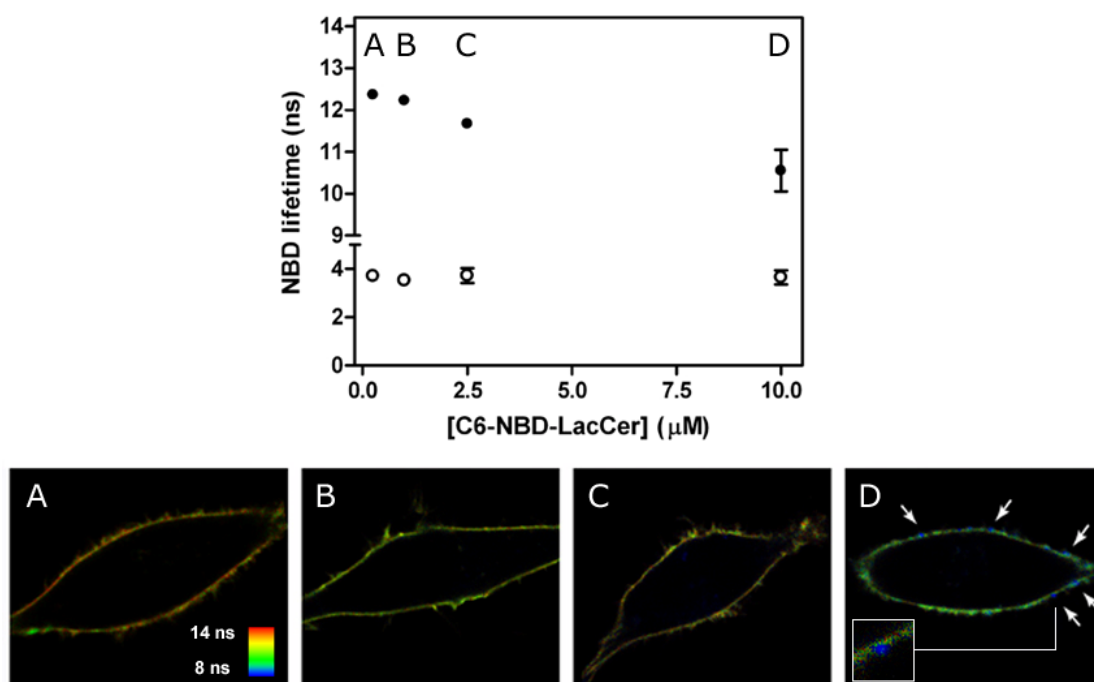


Fig. 15: Dependence of NBD lifetime on the concentration of the fluorophore. NBD lifetime did not substantially change when the solution to label the cells was ranging from 0.2 μM to 2 μM . At 10 μM , blue spots indicating regions of short fluorescent lifetime (see scale) appeared at the plasma membrane. Empty dots: τ_1 ; filled dots: τ_p . Values are shown as means \pm SEM of at least 10 cells.

4.1.4.3 Effect of ionomycin, cytochalasin D and sphingomyelinase on C6-NBD-PC lifetime

As a further approach, we investigated the sensitivity of the fluorescence lifetime of C6-NBD-PC to cell treatments known to interfere with the micro-organization of the plasma membrane, such as disruption of lipid asymmetry and of the cytoskeleton meshwork.

Energy-independent, bi-directional transbilayer movement of all major phospholipids, including PS, has been shown in the eukaryotic plasma membrane. This flip-flop, whose half time is in the order of one minute [224,225], is activated by cell stimulation and the subsequent increase in intracellular calcium and has been ascribed to the lipid scramblase protein (see introduction, section 1.1.4). Expression of many ABC transporters, including ABCA1, has also been associated with enhanced exposure of PS on the cell surface.

We triggered lipid scrambling in HeLa cells by enhancing intracellular calcium concentration via the calcium ionophore ionomycin, prior to C6-ND-PC labelling. Fluorescence lifetime analysis of the analogue in the plasma membrane revealed, upon ionomycin treatment, a shift of the lifetime to lower values with respect to control cells ($p < 0.005$, unpaired two-tailed t test) (**Fig. 16A**). Exposure of PS on the outer leaflet of the plasma membrane was confirmed by Annexin V binding (**Fig. 16B**), a well-established indicator of the effective randomization of phospholipids across the bilayer [226].

Cell treatment with 0.1 μM solution of ionomycin decreased the lifetime of ~ 1 ns. However, by using a 10-fold more concentrated solution, no further decrease in the NBD lifetime was observed, in spite of additional exposure of PS on the outer leaflet, assessed by the increase in FITC-Annexin V fluorescence. When cells were incubated with ionomycin in the absence of calcium, the decrease in the fluorescence lifetime was no longer observed. This indicates that the effect of ionomycin was indeed due to scrambling of lipids and not to its intercalation into the outer leaflet. Addition of EGTA, a calcium chelating agent, had similar effects.

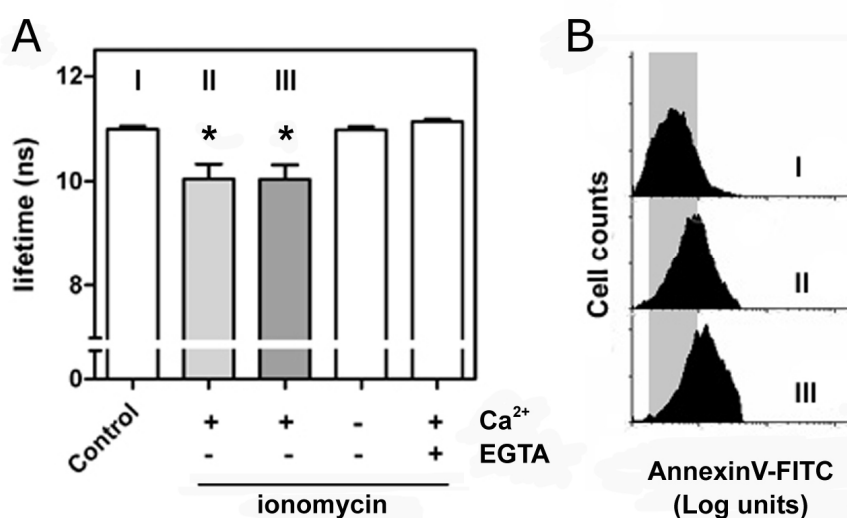


Fig. 16: Influence of lipid scrambling on the fluorescence lifetime of C6-NBD-PC. NBD lifetime was measured in the plasma membrane of HeLa cells at 25°C. (A) The average lifetime of τ_p in cells treated with 0.1 μM (II) or 1 μM (III) ionomycin solution in DMSO (final 0.1% v/v), in the presence of calcium, is shorter as compared to cells subjected to the same treatment but without ionomycin (control, I). Cells subjected to ionomycin treatment (1 μM) in the absence of calcium or in the presence of the calcium-chelating agent EGTA did not show any effect. Data are presented as mean \pm SEM ($n > 12$). (B) PS exposure on the outer leaflet of the plasma membrane as assessed by Annexin V binding. (I): control cells; (II): ionomycin, 0.1 μM ; (III): ionomycin, 1 μM .

The actin cytoskeleton meshwork acts as one of the major organizer of the plasma membrane compartmentalization. Therefore, we would expect that the disruption of the cytoskeleton would interfere with the organization of the plasma membrane, reflected in a change of the lifetime of C6-NBD-PC. To investigate the involvement of the cytoskeleton in the microdomain organization of plasma membrane, HeLa cells were treated with cytochalasin D (cyt D) before measuring lifetime of C6-NBD-PC. This drug is a mycotoxin that binds to actin microfilaments with high affinity and alters its polymerization [227]. The effect of actin depolymerization on the lateral properties of the cell membrane and on clustering of proteins has been well documented in literature (see [228] for a review).

In HeLa cells, a decrease in τ_p upon cytochalasin D treatment was measured ($p < 0.005$, unpaired two-tailed t test, **Fig. 17B**). Suitable experimental conditions were first set up to avoid changes in cell morphology and cell viability. HeLa cells appeared quite sensitive to cytochalasin D treatment: after 30 min of incubation at 37°C with low drug concentration (1 μM), the majority of cells appeared to be inviable under the microscope (not shown). Cell viability was maintained with a short treatment (10 min at 37°C) and a low drug concentration (0.4 μM). Rhodamine-conjugated phalloidin was used to visualize actin filaments within the cells [229], as shown in **Fig. 17A**. Under the conditions used, a rearrangement of the actin microfilaments could be observed.

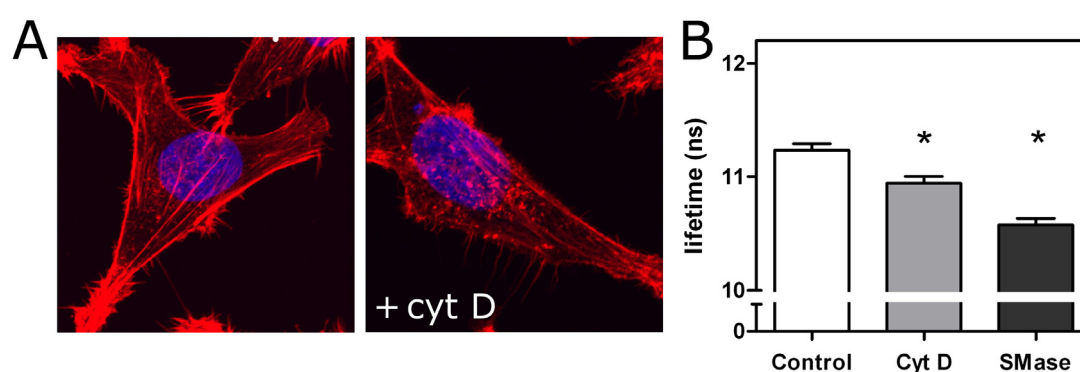


Fig. 17: Influence of cytochalasin D and sphingomyelinase treatment on C6-NBD-PC lifetime. (A) Staining of the actin microfilaments was performed with rhodamine phalloidin. After cytochalasin D (cyt D) treatment, disruption of actin filaments occurs. The cell nucleus is counterstained with DAPI (blue). (B) Effect of cytochalasin D and sphingomyelinase treatment on the fluorescence lifetime of C6-NBD-PC is depicted. Data are presented as mean \pm SEM (control and cytochalasin D: $n=12$, SMase: $n=23$). For p values (*), see text. Measurements were performed at 25°C.

A similar scenario appeared upon sphingomyelinase (SMase) treatment, which decreases the membrane content of sphingomyelin generating phosphocholine and ceramide. Ceramide has recently been shown to displace cholesterol from sphingomyelin-cholesterol domains as well as to induce strong alterations of the lateral organization in model [230] and cellular membranes [231]. Indeed, in comparison to control cells, a shorter lifetime was measured in the plasma membrane of SMase-treated cells ($p < 0.0001$, unpaired two-tailed t test, **Fig. 17B**).

4.2 Influence of ABCA1 on the lipid microenvironment at the plasma membrane

4.2.1 Impact of ABCA1 on the plasma membrane lateral organization

The ABCA1 transporter is a key controller of cellular lipid handling. The loss of its function in humans leads to the development of Tangier disease, a familial HDL deficiency [232]. ABCA1 is required for lipid effluxes from the cell membrane to plasmatic acceptors such as ApoA-I. This is the starting and rate-limiting step in the formation of HDL particles. However, how the ABCA1-dependent lipid loading takes place and how this is related to cholesterol removal is still unclear (see introduction, section 1.3).

Previous work has evidenced that the expression of ABCA1, or its loss, modifies the distribution of anionic phospholipids between the two leaflets of the plasma membrane [149,170,178,183]. These studies pointed out that lipidation of apolipoproteins requires not only the presence of ABCA1, but also specific ABCA1-dependent modifications of the lipid arrangement in the exoplasmic leaflet. Recently, several studies have investigated the relationship between ABCA1 and membrane microdomains, although controversies remain as to whether these structures are involved in lipid efflux to ApoA-I. It has been suggested that the ATPase activity of ABCA1 is responsible for the generation of loosely packed domains that facilitate ApoA-I-dependent cholesterol efflux [187]. Similar alterations were also observed in primary macrophages isolated from *abca1* transgenic mice [188].

In the attempt to further clarify the issue, we have used the sensitivity of fluorescence lifetime of NBD lipid analogues to assess the impact of ABCA1 on the lipid architecture at the plasma membrane. The data of the following sections are published in [233].

4.2.1.1 ABCA1 expression in HeLa cells

To characterize the influence of ABCA1 on the physicochemical properties of the plasma membrane, we made use of HeLa cells transiently or stably transfected with ABCA1 or ABCA1MM. These cells do not express endogenous ABCA1, as shown previously [149] and verified by immunoblotting. Mock-transfected cells were used as a control in each experiment. ABCA1MM is a non-functional mutant of ABCA1, which bears a methionine (M) substitution for lysine (K) in the Walker A motif of both nucleotide binding folds (K939M and K1952M). These mutations impair the function of the transporter by abolishing binding and hydrolysis of ATP, without altering its folding or its intracellular routing [128,149,178,234]. The wild type and mutant transporters were expressed as

chimeras with fluorescent proteins (EGFP, EYFP or ECFP) attached as a C-terminal tailpiece. This approach was shown not to interfere with the original activity of the protein [152,178].

In HeLa cells, ABCA1-EGFP localizes in the plasma membrane as well as in intracellular compartments corresponding to the Golgi apparatus and endolysosomal vesicles, as previously shown [149] (**Fig. 18A**). The mutations in ABCA1 Walker A motifs do not hamper its subcellular localization. Cells expressing either the wild type or mutant protein show comparable levels of protein expression at the plasma membrane, evaluated by the quantification of the EGFP fluorescence intensity (**Fig. 18B**).

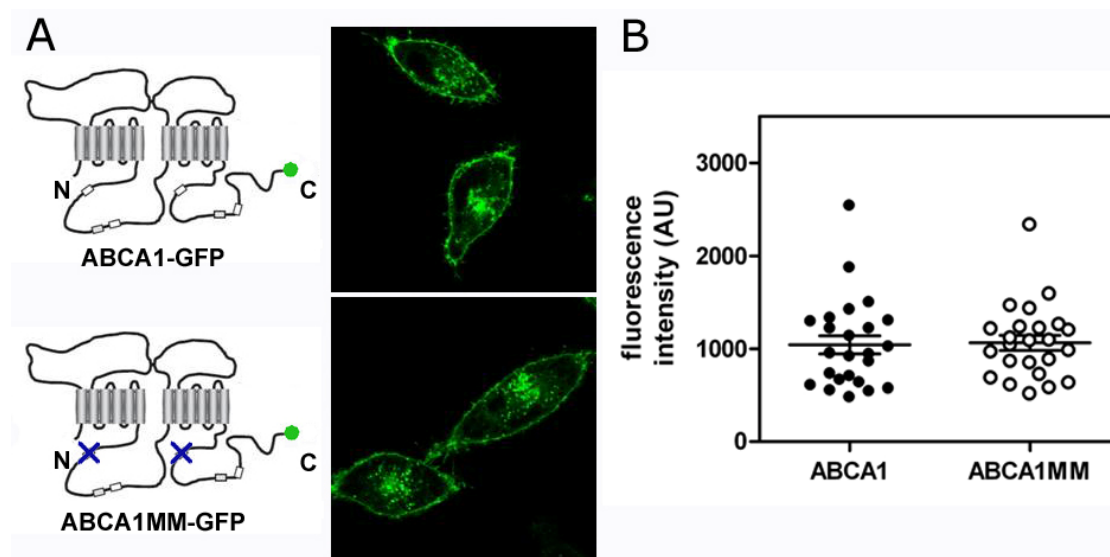


Fig. 18: Subcellular localization of ABCA1 and ABCA1MM in HeLa cells. Confocal microscopy images of cells expressing ABCA1-EGFP or ABCA1MM-EGFP chimera. ABCA1MM bears lysine/methionine substitutions in both nucleotide binding domains. Both proteins localize to the plasma membrane and intracellular compartments corresponding to the Golgi apparatus and endolysosomal vesicles [149] (A). Cells expressing either the wild type or mutant protein show comparable level of protein expression at the plasma membrane (B), assessed as EGFP fluorescence intensity. Bars indicate mean and SEM values of 24 cells.

4.2.1.2 ABCA1 activity affects the physicochemical properties of the cell surface

To analyze the impact of ABCA1 on the physical properties of the outer membrane leaflet, HeLa cells expressing an intact or mutant ABCA1 transporter were incubated with a C6-NBD-PC solution, as previously described. Subsequently, fluorescence decay curves of the analogues located in the plasma membrane were measured. Upon expression of ABCA1, a shift of τ_p towards longer values was measured in comparison to non-transfected HeLa cells or cells expressing ABCA1MM ($p < 0.0001$, unpaired two-tailed t test, **Fig. 19** and **Table 9**). In addition, an increase in the width of the distribution of NBD lifetimes was observed in ABCA1-containing plasma membrane, which

suggests a higher heterogeneity in the microenvironment of the probe (**Fig. 19**). A broader distribution was also assessed in the presence of ABCA1MM, which likely derives from overexpression of the protein itself. Indeed, the presence of membrane proteins in lipid bilayers was shown to broaden fluorescence lifetime distribution [235,236]. A similar scenario was found for C6-NBD-LacCer, with lifetimes shifted to longer values (**Table 9**).

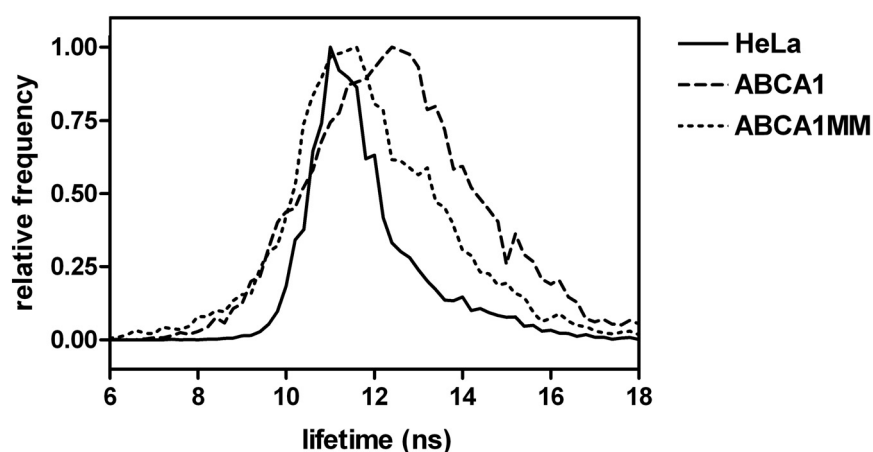


Fig. 19: ABCA1 influence on C6-NBD-PC fluorescence lifetime. Histograms of the lifetime component τ_p of C6-NBD-PC in the plasma membrane of untransfected HeLa cells and cells expressing the wild type ABCA1 or the non-functional mutant ABCA1MM. Histograms were normalized by setting the maximum to 1. Means \pm SD of the lifetimes calculated as described in the material and method section are reported in Table 9. Measurements were performed at 25°C.

It was previously described that cholesterol depletion from HeLa cells by M β CD caused a decrease in the lifetime of C6-NBD-PC. Similarly, also in cells expressing ABCA1 and ABCA1MM extraction of cholesterol led to a shift of the lifetime distribution towards lower values. In addition, this treatment abolished the difference detected before in the presence of the active transporter (**Table 9**).

Table 9: Fluorescence lifetime of C6-NBD-PC and C6-NBD-LacCer in the presence of ABCA1 or ABCA1MM. Upon expression of ABCA1, a shift of τ_p towards longer values was detected ($p < 0.0001$ for both lipid analogues, unpaired two-tailed t test). For completeness, the short component τ_1 is also shown. For values corresponding to the plasma membrane of untransfected HeLa cells, see Table 8. Untransfected cells and cells expressing ABCA1MM display similar values. Data are shown as mean \pm SD. In brackets, the number of cells analyzed is indicated. Measurements were performed at 25°C.

	NBD lifetime			
	ABCA1		ABCA1MM	
	τ_1 <i>ns</i>	τ_p <i>ns</i>	τ_1 <i>ns</i>	τ_p <i>ns</i>
C6-NBD-PC	2.9 \pm 0.3	12.4 \pm 0.3 (38)	2.7 \pm 0.2	11.5 \pm 0.3 (49)
C6-NBD-PC (M β CD)	2.9 \pm 0.4	11.6 \pm 0.2 (25)	2.7 \pm 0.2	11.6 \pm 0.2 (25)
C6-NBD-LacCer	3.0 \pm 0.3	12.9 \pm 0.2 (35)	3.1 \pm 0.3	12.2 \pm 0.2 (38)

Since the ABCA1-specific increase in the NBD lifetime was sensitive to depletion of cholesterol by M β CD treatment, we investigated whether removal of cholesterol by ApoA-I could, as well, influence the properties of the plasma membrane. To this aim, cells were incubated with 10 μ g/ml ApoA-I for 16 h prior to the labelling procedure. As illustrated in **Fig. 20**, this treatment did not influence the lifetime behavior of C6-NBD analogues. This could be due to the lower amount of cholesterol extracted by ApoA-I in comparison to the efflux to M β CD (see section 4.3.1.3). More likely, the long time-span of the experiment allows the cells to restore the initial conditions through the cellular processes involved in the transport of cholesterol to the plasma membrane. Experiments showing the extent of cholesterol efflux to ApoA-I are described in section 4.3.1.3.

To investigate the influence of the expression of a different transmembrane protein linked to the GFP to the physical properties of the plasma membrane, assessed by C6-NBD-PC, HeLa cells were transiently transfected with the influenza viral protein hemagglutinin tagged with the Cerulean fluorescent protein (HA-Cer). This protein localizes into lipid rafts at the plasma membrane (Engel *et al.*, unpublished data). No difference in NBD lifetime was observed in the plasma membrane of HA-Cer expressing cells and mock-transfected cells (**Fig. 20**, $p > 0.1$).

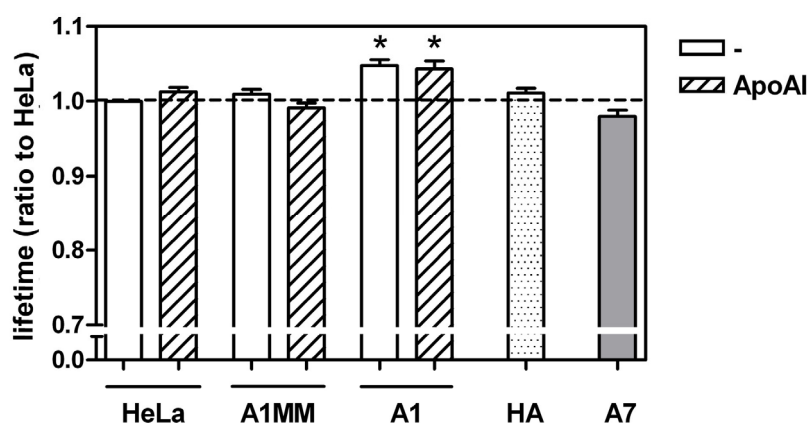


Fig. 20: Fluorescence lifetime of NBD in absence or presence of ApoA-I and upon expression of HA or ABCA7. Cells were labelled with C6-NBD-PC or C6-NBD-LacCer and lifetime values normalized to the value measured in the plasma membrane of HeLa cells. A1MM: ABCA1MM; A1: ABCA1, HA: hemagglutinin, A7: ABCA7. Data are normalized to NBD lifetime measured in the plasma membrane of untransfected HeLa cells and shown as mean \pm SEM ($n > 10$). *: $p < 0.05$, unpaired two-tailed t test. Measurements were performed at 25°C.

Among the different mechanisms proposed for the ABCA1-mediated lipid efflux to ApoA-I, it has been suggested that ApoA-I could either bind directly to ABCA1 or indirectly to a “lipid site” created by its activity (see introduction, chapter 1.3.3.2). ABCA7 was also shown to be able to bind ApoA-I and to mediate efflux of phospholipids to this acceptor, although efflux of cholesterol is still controversial. In contrast to ABCA1, ABCA7 does not mediate formation of HDL particles *in vivo*. As a relationship between formation of lipid domains and efflux of phospholipids and cholesterol to

ApoA-I has been suggested, it was of interest to investigate whether ABCA7 is also able to perturb the plasma membrane micro-organization. Therefore, cells were transfected with ABCA7-YFP and fluorescence lifetime of C6-NBD-PC was measured. As shown in **Fig. 20**, expression of ABCA7-YFP at the plasma membrane did not induce any significant change in the lifetime of NBD.

Taken together, these results prove the influence of ABCA1 on the micro-organization of the plasma membrane. Conversely, no effect was detected upon expression of the functional mutant ABCA1MM or of ABCA7. Based on the data obtained from GUVs and GPMVs, the longer lifetime measured at the plasma membrane in the presence of the wild type ABCA1 indicates that the C6-NBD probes are sensing a more packed lipid environment.

4.2.1.3 Efflux of cholesterol to M β CD and ApoA-I

In parallel to the FLIM measurements, cholesterol extractability by M β CD and by ApoA-I was measured after labelling of the cellular cholesterol pool with [3 H]-cholesterol.

Under the experimental conditions used (5 mM M β CD for 1 min on ice), M β CD extracted $19.8\% \pm 0.8$ (mean \pm SEM, n=3) of the total cell [3 H]-cholesterol from HeLa cells. This value may be overestimated due to the relative high signal background in the presence of M β CD; it was therefore decided to present the data as ratio to efflux in non-transfected HeLa cells. An increase in M β CD-extractable cholesterol was found for ABCA1 expressing cells (**Fig. 21A**). A higher amount of [3 H]-cholesterol in the medium was also measured from cells expressing ABCA1MM. This effect may be due to non-specific disturbances on the plasma membrane by overexpression of the protein, potentially related to the presence of its twelve transmembrane domains. In parallel, for each experiment the percentage of cells expressing the protein was analyzed at the cytofluorimeter, by monitoring GFP fluorescence intensity. This revealed that ABCA1-GFP expressing cells were $\sim 30\%$, whereas $\sim 54\%$ of the cells expressed ABCA1MM-GFP. When values were normalized to protein expression, a 5-fold increase in cholesterol efflux to M β CD could be measured in ABCA1-*versus* ABCA1MM- expressing cells.

Similarly, efflux of [3 H]-cholesterol to ApoA-I was analyzed (**Fig. 21B**). To this aim, cells were incubated with 10 μ g/ml of ApoA-I for 16 h. We found that ABCA1 expression induced more than 2-fold increase in cholesterol efflux compared to untransfected and ABCA1MM expressing HeLa cells ($2.5\% \pm 0.6$ and $2.2\% \pm 0.2$ of total [3 H]-cholesterol was extracted by ApoA-I from HeLa and ABCA1MM-expressing cells, respectively, and $6.2\% \pm 0.6$ from ABCA1-expressing cells).

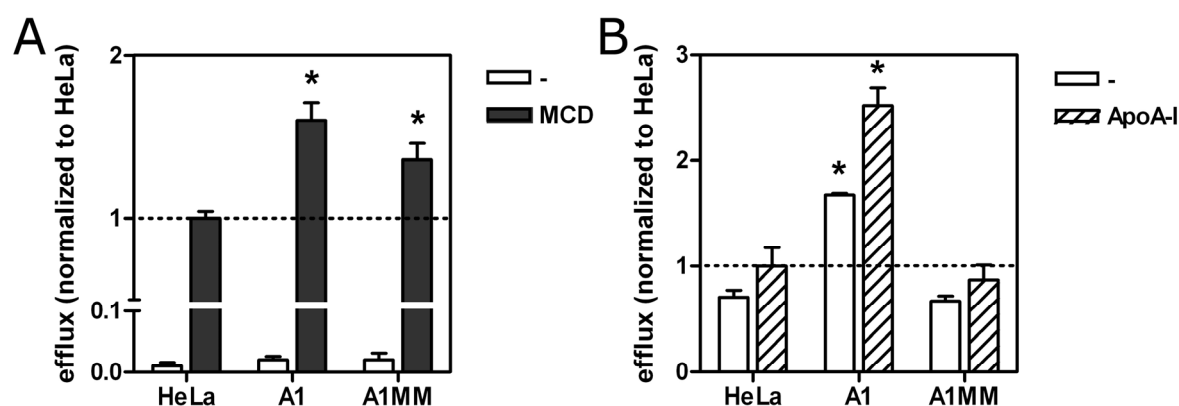


Fig. 21: Efflux of [³H]-cholesterol to MβCD (A) and ApoA-I (B). ABCA1 promotes cellular release of [³H]-cholesterol to both MβCD and ApoA-I. See text for detailed explanation. Data are presented as mean ± SEM of 3 (MβCD) and 2 (ApoA-I) independent experiments. Data are normalized to the efflux measured in HeLa cells incubated with the indicated acceptors. *: $p < 0.05$, unpaired two-tailed t test. A1: ABCA1; A1MM: ABCA1MM.

Interestingly, ABCA1 expression alone was sufficient to induce a larger cholesterol efflux over untransfected and ABCA1MM expressing cells in the absence of ApoA-I. This basal cholesterol efflux was approximately 30% of the total efflux when ApoA-I was present. Very recently, similar results were reported by Nandi *et al.* [191].

4.2.1.4 C6-NBD-PC lifetime in condensed membranes: activated Jurkat cells

To explore the possibility that enhanced lifetime measured in ABCA1-expressing plasma membranes was associated with formation of condensed, raft-like domains, we analyzed C6-NBD-PC lifetime in the plasma membrane of Jurkat cells after activation of the T cell receptor (TCR) via anti-CD3 antibodies. This treatment has been shown to trigger formation of condensed membrane domains at the activation sites, as assessed by the fluorescent probes Laurdan [237] and PMI-COOH [37]. Cells were incubated with OKT3 antibodies which were, in turn, cross-linked with a fluorescently labelled secondary antibody before staining with C6-NBD-PC. The analysis of fluorescence lifetime at the plasma membrane revealed a shortening of τ_p in activated Jurkat cells as compared to untreated cells (**Fig. 22**). In a second approach, Jurkat cells were incubated with sphingomyelinase to induce hydrolysis of SM and production of ceramide, a process also described to be involved in the natural activation sequence of these cells [238]. Again, a decreased NBD lifetime was observed for the longer component τ_p (**Fig. 22**). No visible domains were detected both upon OKT3 antibody activation or sphingomyelinase treatment. In some cells, regions in which the NBD probe became enriched were observed. However, lifetime analysis revealed that these regions were characterized by a shorter τ_p in comparison to the rest of the plasma membrane, probably due to self-quenching of

the probe, and were therefore excluded from the analysis. Experiments with Jurkat cells were performed in collaboration with Dr. Martin Stöckl.

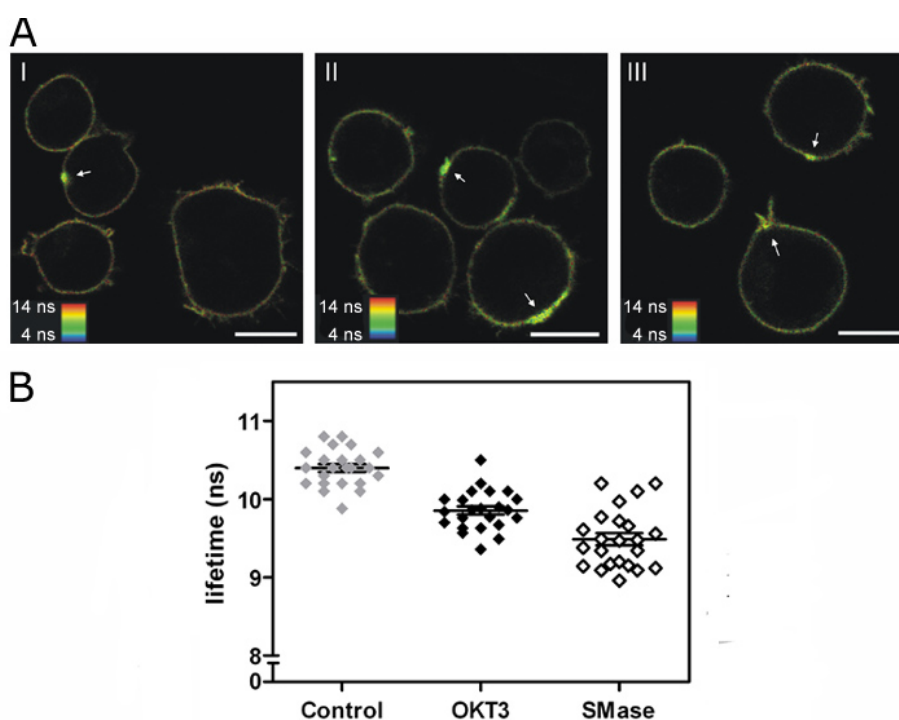


Fig. 22: Fluorescence lifetime of C6-NBD-PC in Jurkat cells. (A) Fluorescence lifetime images of Jurkat cells (2x2 pixels binned). The average lifetime is shown as pseudocolor, according to the scale. Bars correspond to 10 μm . Regions in which C6-NBD-PC is enriched (arrows) were excluded from the analysis (see text). (I): untreated cells (control); (II): activated cells; (III): cells after sphingomyelinase treatment. (B) Analysis of τ_p in the plasma membrane of Jurkat cells. Cells activated by treatment with OKT3 antibodies cross-linked by secondary antibodies display shorter lifetime as compared to non treated cells (control). Sphingomyelinase treatment (SMase) also induced a decrease in τ_p ($p < 0.0001$ for both treatments). Mean \pm SEM are indicated in the graph (23 cells per sample analyzed). Measurements were performed at 25°C.

It was previously concluded that, in the presence of ABCA1, the NBD lipid analogues sense a more packed lipid environment. However, based on the observation that condensation of lipid domains rather provokes a decrease in the lifetime, we could exclude that the increment in lifetime observed upon expression of ABCA1 originated from condensation of lipid domains.

Considering the correlation between lifetime and cholesterol content [209], this increment should reflect an increase in the cholesterol content in the compartments where the probes are enriched. Therefore, to gain further information about the spatial distribution of the C6-NBD-PC, its lateral mobility in the plasma membrane of HeLa cells was measured by Fluorescence Recovery After Photobleaching (FRAP).

4.2.1.5 Lateral mobility of C6-NBD-PC

FRAP is one of the non-invasive methods of choice to study lateral mobility and dynamics of lipids in living cells [239,240]. With this technique, fluorescent molecules in a small region of the cells are irreversibly photobleached using a high-powered laser beam. The subsequent movement of the surrounding non-bleached fluorescent molecules into the photobleached area is then recorded at low laser power. The diffusion mobility of lipids is recognized to be in close relationship with membrane viscosity and membrane cholesterol content [241]. Moreover, diffusion of membrane proteins and lipids is influenced by the lipid environment in which they are embedded. In model membranes, mobility of lipid analogues was shown to be reduced in the Lo phase in comparison to the Ld phase [7,242,243], reflecting the higher cholesterol content in the Lo phase.

In the previous chapter, it was proposed that C6-NBD-PC is embedded in a more viscous, cholesterol-enriched environment at the plasma membrane in the presence of ABCA1. In this case, a reduction in the mobility of the lipid analogue has to be expected. Therefore, the diffusion coefficient of C6-NBD-PC, under the same conditions used for FLIM experiments, was determined by FRAP.

Measurements were performed in the apical membrane of cells, to avoid the high background fluorescence present when focusing on the basal membrane. To minimize the influence of membrane trafficking events, experiments were performed at 25°C. Typical FRAP recovery curves for ABCA1- and ABCA1MM-expressing cells are shown in **Fig 23**. During the acquisition of the recovery signal, no decrease of the fluorescence intensity due to repeated bleaching occurred under the conditions used (**Fig. 23**, inset). From the recovery curves, the diffusion coefficient (D) and the mobile fraction (M_f) can be calculated as explained in section 3.2.3.6. D is a measure of the rate of movement of the fluorescent molecules, while M_f represents the fraction of fluorescent molecules that can diffuse into the bleached region during the time course of the experiment.

C6-NBD-PC in the plasma membrane of HeLa cells shows a D value in the order of $0.1 \mu\text{m}^2/\text{s}$. This value is in agreement with diffusion coefficients previously reported for NBD lipid analogues in the plasma membrane of mammalian cells [240,244,245]. In the presence of an active ABCA1, a slower diffusion was observed in comparison to both ABCA1MM-expressing cells and non-transfected HeLa cells ($p < 0.0001$, unpaired two-tailed t test; $D = 0.033 \pm 0.002 \mu\text{m}^2/\text{s}$ for ABCA1-expressing cells and $D = 0.080 \pm 0.007 \mu\text{m}^2/\text{s}$ for ABCA1MM-expressing cells, **Table 10**).

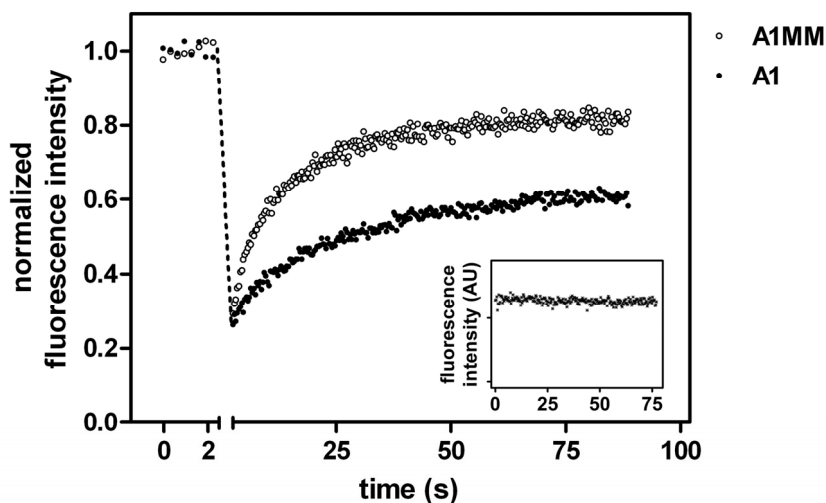


Fig. 23: Representative fluorescence recovery curves of C6-NBD-PC in the plasma membrane of HeLa cells transiently transfected with ABCA1 or ABCA1MM. Experimental conditions were optimized to ensure that no bleaching of the probe occurred during measurement of the fluorescence recovery (inset). The lipid analogue shows slower diffusion in the presence of an active ABCA1. Recovery curves from non-transfected HeLa cells were similar to those of cells expressing ABCA1MM (not shown, see Table 10 for diffusion coefficients and mobile fraction). Measurements were performed at 25°C.

Table 10: Diffusion parameters of C6-NBD-PC in the plasma membrane of HeLa cells expressing the indicated proteins. D: diffusion coefficient, M_f : mobile fraction. Mean values \pm SEM are indicated. Measurements were performed at 25°C. $p(\text{HeLa vs M}\beta\text{CD}) < 0.01$; $p(\text{ABCA1 vs ABCA1MM}) < 0.0001$; $p(\text{ABCA1 vs HeLa}) < 0.0001$; $p(\text{HeLa vs ABCA1MM}) > 0.05$, unpaired two-tailed t test. In brackets, number of cells analyzed.

Protein expressed	D	M_f
	$\mu\text{m}^2/\text{s}$	%
-	0.102 ± 0.009 (14)	85 ± 3
ABCA1	0.033 ± 0.002 (16)	57 ± 5
ABCA1MM	0.080 ± 0.007 (13)	83 ± 3
- (M β CD)	0.162 ± 0.018 (11)	77 ± 4

The slower diffusion in the presence of an active ABCA1 is consistent with the enhanced packing sensed by C6-NBD-PC, as assessed by FLIM. Indeed, depletion of about 20% of the total cell cholesterol with M β CD from the cells resulted in an increase of the diffusion coefficient of C6-NBD-PC of 1.6-fold (**Table 10**), [239,246] because of decreasing lipid packing order of the membrane [10].

In the presence of ABCA1, a lower mobile fraction of the fluorescent molecules was detected, indicating that a significant part of NBD molecules were essentially immobile in the cell membrane. This could indicate that a fraction of the fluorescence molecules could be bound to a fixed substrate.

Alternatively, discontinuities within the structures where the molecules localize may also be responsible for the reduced mobile fraction [247].

4.2.2 ABCA1 partitioning in GPMVs

GPMVs obtained by blebbing of the plasma membrane display large, visible Ld- and Lo-like domains at temperatures $\leq 25^{\circ}\text{C}$ and can be used to characterize the phase preference of lipids and proteins [17,18]. In these vesicles, protein partition can be studied in their natural lipid environment and can be directly visualized by optical microscopy, by analyzing those vesicles that show phase coexistence and that contain the protein of interest conveniently labelled.

GPMVs were generated from HeLa cells. First, to evaluate the phase preference of membrane proteins in general, cells were labelled with concanavalin A-Texas Red (ConA) prior to formation of blebs. This protein binds to α -methyl mannoside-containing glycoproteins and glycolipids on the cell surface (**Fig. 24**, image on the left).

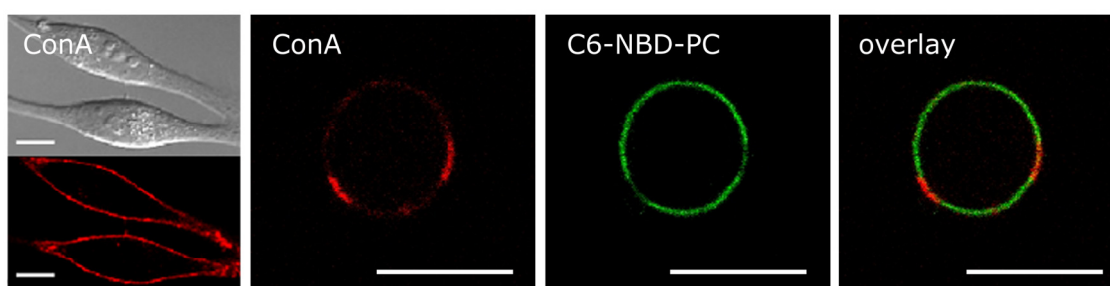


Fig. 24: Phase preference of concanavalin A-Texas Red labelled glycoproteins and glycolipids in GPMVs. Upon incubation of HeLa cells with concanavalin A-Texas Red as described in 2.2.4.2, mainly the plasma membrane is labelled. Concanavalin A-Texas Red labelled glycoproteins and glycolipids show enrichment in the Ld-like phase, as determined by complementary partitioning with C6-NBD-PC, previously shown to be slightly enriched in the Lo-like phase. Bars correspond to 10 μm . Imaging was performed at 25°C .

As shown in **Fig. 24**, at 25°C ConA-labelled glycoproteins and glycolipids show a marked enrichment in the Ld-like phase, as determined by complementary partitioning with C6-NBD-PC. ConA receptor proteins that segregate in the blebbing vesicles represent a substantial fraction of the ConA binding sites on the cell surface, as estimated by comparison of their fluorescence intensity in cell-attached GPMVs (not shown and [17]). Similar results were obtained at 10°C .

Unspecific labelling of different types of proteins can be also obtained with *N*-hydroxysuccinimide esters of biotin. These reagents react with primary amino groups of proteins and are commonly used for the labelling of the cell surface [248], in combination with fluorophore-conjugated streptavidin. However, we found that this treatment, although efficiently labelling the cell surface of cells (not

shown), dramatically decreased the yield of vesicles obtained, most likely because of the cross linking of proteins induced by streptavidin [249].

The approach of GPMVs was subsequently utilized to determine the phase preference of ABCA1 and ABCA1MM between coexisting membrane phases. Indeed, intensive investigations have been performed to study the relationship between ABCA1 and membrane lipid phases. In initial studies, Drobnik *et al.* showed that ABCA1 is partially localized in Lubrol WX but not in Triton-X 100 resistant membranes in monocyte-derived macrophages [250]. ABCA1 was also detected in Brij 98 resistant membranes (A. Zarubica, unpublished data) and in the light density fractions of membranes isolated with a detergent-free method (section 4.2.3.1, to follow). Comparison of the partitioning of the non-functional mutant ABCA1MM revealed that the latter is enriched in the low density fractions. However, until present no study in laterally intact cellular bilayer has been performed.

GPMVs were formed from HeLa cells expressing ABCA1 or ABCA1MM fused with the EGFP or ECFP at the C-terminal and from non-transfected cells. At 25°C, more than 50% of the vesicles exhibit phase separation as indicated by selective enrichment of R18. As shown in **Fig. 25A**, in vesicles with coexisting phases both ABCA1 and ABCA1MM were almost exclusively present in the Ld-like phase, colabelled with R18. This is in agreement with the partitioning of most transmembrane proteins, which are found to be preferentially excluded from Lo phases in model membranes [217,251].

Interestingly, a larger Ld-like phase at 25°C was observed in GPMVs prepared from ABCA1-expressing cells, in comparison with both non-transfected cells (HeLa) and ABCA1MM-expressing cells (**Fig. 25, A and B**). Typically, 1-3 domains per vesicles were found. The frequency distribution of the relative extent of the Ld-like phase calculated as described in 3.2.4.2 is shown in **B**.

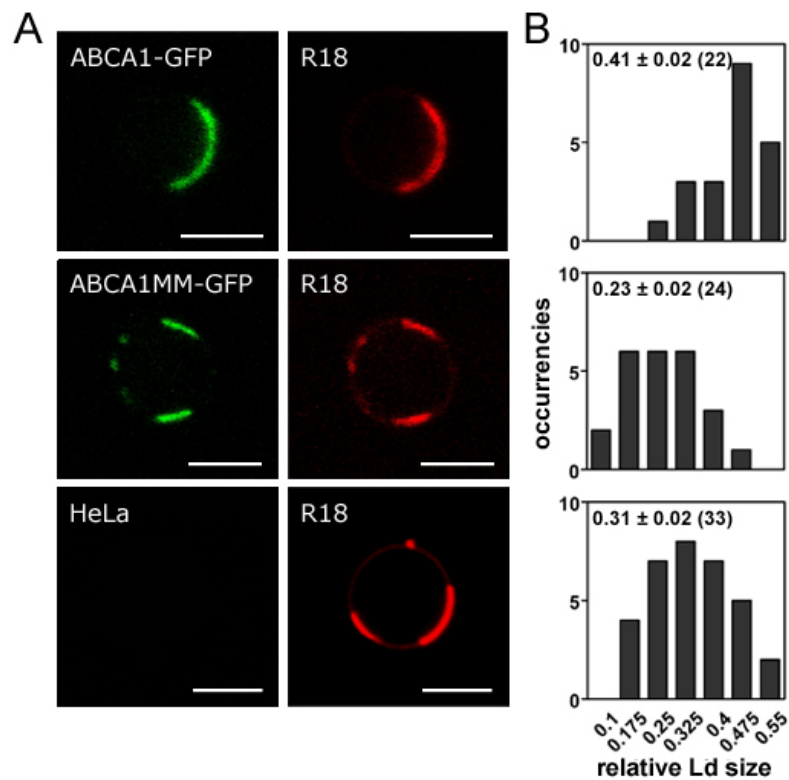


Fig. 25: ABCA1 partitions into the Ld-like phase in GPMVs and modulates its size. GPMVs were prepared from mock transfected HeLa cells (mock) and cells expressing ABCA1 and ABCA1MM tagged with EGFP (A). Both proteins are almost exclusively present in the Ld-like phase, identified by co-staining with R18. Images were taken at the equatorial plane of the vesicles at 25°C. Bars correspond to 5 μm . (B) Histograms showing the distribution of the relative size of the Ld-like phase in the corresponding samples. In the presence of ABCA1, a shift of the distribution to higher values was observed ($p < 0.001$, unpaired two-tailed t test). Means \pm SEM are indicated in the top left corner. In brackets: number of domains analyzed. Typically, 1-3 domains per vesicle were found.

4.2.3 Fractionation of the plasma membrane

4.2.3.1 Raft partitioning and ABCA1 activity

To complement and confirm the biophysical measurements with more widely used biochemical approaches, we analyzed the partitioning behavior of ABCA1 in membrane domains isolated according to the detergent-free method developed by Macdonald and Pike [197]. Traditional biochemical approaches to isolate lipid rafts made use of detergents, classically the non-ionic Triton X-100, to extract the whole cells followed by separation of the low-density, detergent resistant membrane fractions on density gradients. However, several observations pointed out that this procedure does not reflect the original situation in intact membranes [27,252]. A number of other methods that do not require the use of detergent have been developed [253,254]. The procedure we used is based on floatation on OptiPrep density gradients and allows obtaining good yield of a membrane fraction enriched in cholesterol and protein markers of lipid rafts.

The approach was first validated on non-transfected HeLa cells (**Fig. 26A**). Fractions corresponding to the plasma membrane (1 to 6) were defined based on the enrichment of plasma membrane marker proteins and devoid of contamination from the Golgi or ER compartments, indicated from β -COP and calnexin (CNX), respectively.

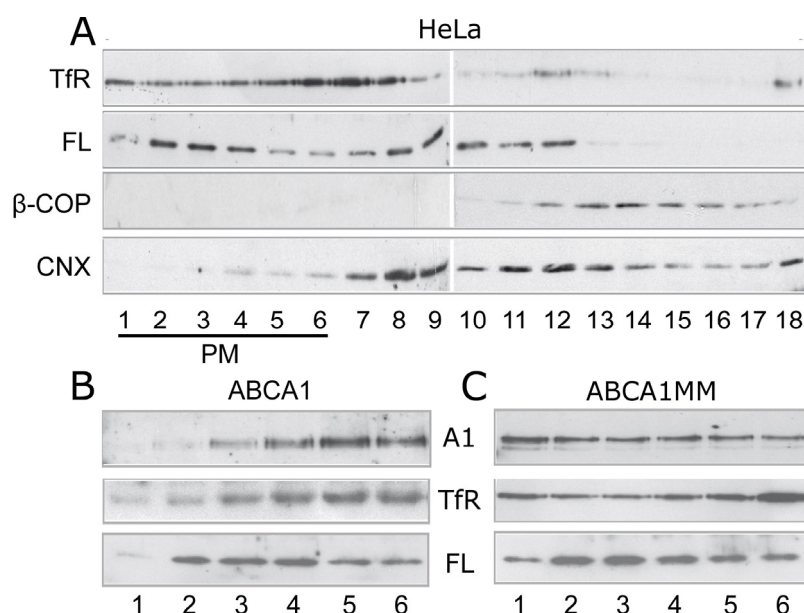


Fig. 26: Detergent-free membrane fractionation. Fractions are numbered from the top to the bottom of the gradient. Data shown in the panels are representative of at least three independent experiments. TfR: transferrin receptor, FL: flotillin; CNX: calnexin; PM: plasma membrane. Figures are kindly provided by Ana Zarubica, Marseille, France. B) and C). ABCA1MM is enriched in the first three fractions as compared with ABCA1 FL distribution was not influenced by the presence of either the wild type or the non-functional ABCA1, whereas an altered partitioning of TfR was evidenced in the presence of ABCA1.

Raft fractions were identified as the first three fractions, based on the enrichment of the transmembrane protein flotillin (FL) [197,255]. Non-raft fractions were identified by the enrichment of transferrin receptor (TfR), a marker for non-raft plasma membrane [197].

ABCA1 was recovered in fractions corresponding to the plasma membrane (**Fig. 26B**), Golgi apparatus and endo-lysosomal vesicles, witnessed by the enrichment in β -COP and LAMP 2, respectively (not shown). This distribution is in agreement with the subcellular localization of the protein in living cells (section 4.2.1.1). Interestingly, a minor but consistent fraction of the transporter partitioned in the lighter fractions of the plasma membrane.

As shown in **Fig. 26, B and C**, an altered partitioning of ABCA1MM *versus* the wild type protein was detected in the plasma membrane fractions. Quantitative assessment was performed by densitometry analysis of the hybridization signals in the first three fractions as compared to the total signal at the membrane. This revealed that while $32.5\% \pm 6.2$ (mean \pm SEM, $n=4$) of the total ABCA1 at the membrane partitions in fractions 1 to 3, $65.2\% \pm 5.1$ ($n=3$) of ABCA1MM showed similar floatation characteristics ($p<0.05$, unpaired two-tailed t test, **Table 11**). To assess whether the ABCA1-mediated modulation of the plasma membrane properties affected the organization of other membrane proteins, in the same preparation the partitioning of TfR and FL was analyzed. FL distribution was not influenced by the presence of either the wild type or the non-functional ABCA1, whereas an altered partitioning of TfR (**Fig. 26, B and C**) was evidenced in the presence of ABCA1 ($p<0.05$, unpaired two-tailed t test).

We then investigated the correlation between the partitioning in membrane domains and the surface phenotypes elicited by the expression of ABCA1, *i.e.* the binding of ApoA-I and Annexin V. These two events are both prerequisites for the efflux of cellular phospholipids and cholesterol to ApoA-I [178,183]. We took advantage of two ABCA1-related molecules, CED-7 and HA819, which show different patterns of phenotypes in comparison to ABCA1. CED-7 is an ABC transporter of the A class, functional ortholog of ABCA1 in *C. elegans* [168], whereas HA819 is a previously described gain-of-function variant of the transporter [183]. When expressed in HeLa cells, ABCA1, CED-7 and the HA819 variant elicited binding of Annexin V to similar values, while the binding of ApoA-I varied broadly (**Table 11**). CED-7 failed to elicit any binding or significant efflux of lipids while HA819 was more efficient than native ABCA1 in inducing both binding and efflux [183].

Table 11: Functional parameters of ABCA1 and related transporters in comparison to raft partitioning. The ability to bind ApoA-I or Annexin V and to efflux phospholipids (PL) was assessed on HeLa cells expressing ABCA1, ABCA1MM, HA 819 or CED-7 [183]. Values are expressed as percent of the binding/efflux observed upon expression of the active ABCA1 transporter. The percent of partitioning in raft was assessed by densitometry of gradient fractions resolved by SDS-PAGE and analyzed for the content of the transporters. Means \pm SEM are indicated. In brackets: number of individual experiments. These experiments were done in collaboration with A. Zarubica and Dr. G. Chimini, CIML, Marseille, France.

	Apo-AI binding	Annexin V binding	PL efflux	Raft partitioning
	<i>% of ABCA1</i>	<i>% of ABCA1</i>	<i>% of ABCA1</i>	<i>%</i>
ABCA1	100	100	100	32.5 \pm 6.3 (4)
ABCA1MM	13 \pm 5 (5)	10 \pm 2 (4)	10 \pm 3 (3)	65.2 \pm 5.1 (3)
HA 819	151 \pm 11 (7)	109 \pm 31 (4)	113 \pm 24 (4)	35.8 \pm 1.8 (2)
CED-7	20 \pm 3 (3)	102 \pm 14 (3)	31 \pm 7 (5)	33.9 \pm 1.2 (2)

The biochemical analysis of partitioning evidenced that the three molecules - ABCA1, CED-7 and the HA819 mutant - floated similarly (**Table 11**). This excludes a causal link between the induction of ApoA-I binding or cholesterol effluxes and membrane partitioning. Rather, the partitioning in lighter fractions correlates with the binding of Annexin V, indicative of the exposure of PS on the cell surface. Therefore, the destabilization of the membrane lipid microenvironment may be a direct consequence of the ABCA1-dependent PS redistribution, and upstream to the final efflux of membrane cholesterol.

4.2.3.2 Lipid composition of plasma membrane fractions

To ascertain more precisely the organization of membrane cholesterol under the influence of ABCA1, we analyzed the lipid composition of the membrane fractions isolated from cells expressing ABCA1 or ABCA1MM. Cholesterol content in the plasma membrane fractions was similar, in the presence of either the active or the non-functional mutant transporter (nmol cholesterol/mg of proteins loaded onto the gradient, mean \pm SEM: 5.1 ± 1.3 and 6.2 ± 2.3 for A1 and A1MM (n=3), respectively). Likewise, its distribution across the fractions corresponding to the plasma membrane was similar (**Fig. 27A**). As expected, cholesterol was more than ~ 3 -fold enriched in the raft fractions.

To exclude the possibility that cholesterol may be sequestered in some intracellular compartments in ABCA1-expressing cells, we performed cell fractionation to characterize its distribution after labelling the cellular pools with [3 H]-cholesterol, as described in 3.2.2.5 [187] (**Fig. 27B**). This procedure allows to separate cytosolic fractions, found at low density and witnessed by the presence of heat shock protein 70 (Hsp70), from fractions corresponding to the plasma membrane, that follow (indicated by enrichment of caveolin, here highlighted by the grey rectangle) and from the ER, witnessed by enrichment in calreticulin (not shown). No major differences in the three cell types were found. This supports the conclusion, previously drawn [177], that ABCA1, while not affecting the membrane cholesterol content, induces its redistribution into pools readily accessible to external acceptors.

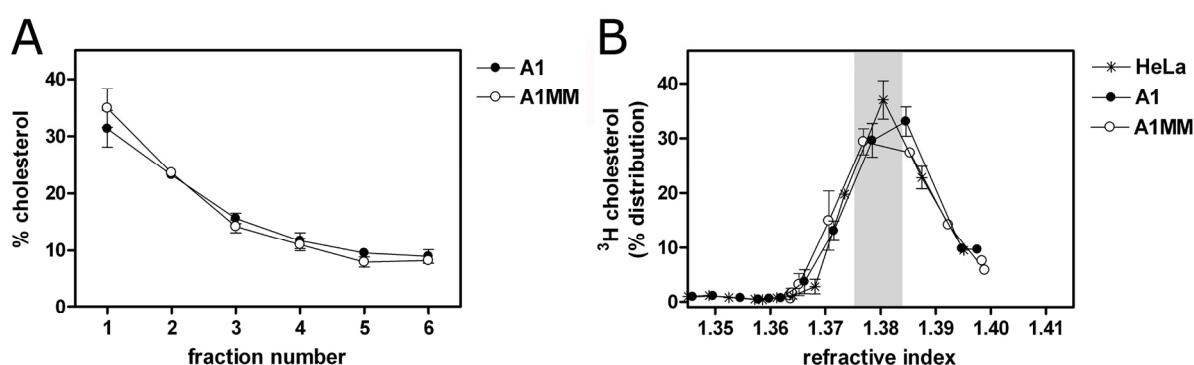


Fig. 27: Cholesterol distribution in fractions obtained after OptiPrep (A) and sucrose gradient (B) fractionation. (A) Percent distribution of cholesterol across fractions 1 to 6 (mean \pm SEM), corresponding to the plasma membrane, collected in 3 independent detergent-free gradients prepared from bulk cell cultures. (B) [3 H]-cholesterol subcellular distribution analyzed by cell fractionation. Each fraction (1 to 12, see 2.2.2.5 for further details) was analyzed for [3 H] counts and marker proteins for cytosol (Hsp70), plasma membrane (caveolin) and ER (calreticulin) (not shown). Data were normalized to the density of the fractions to correct for variations between gradients made in different experiments. The grey rectangle highlights the cholesterol peak corresponding to the plasma membrane fractions. Error bars are SEM of two independent experiments.

In the attempt to identify the differences between the isolated fractions and to find a rationale for the differential partitioning of ABCA1 and ABCA1MM, we have analyzed the fractions corresponding to the plasma membrane (1 to 6) with MALDI-TOF (matrix assisted laser desorption ionization - time of flight) mass spectrometry after extraction of the lipids. This technique has, among others, the advantage of giving excellent reproducibility because the analytes and the matrix compound, both readily soluble in organic solvents, can form high homogeneous crystals between them [256]. To meet the requirement of sufficient amount of lipids, bulk cultures of HeLa cells (25×10^6) were transfected with ABCA1 or ABCA1MM and subjected to membrane fractionation. The low amount of lipids present in the fractions (1-6 nmol) convinced us to avoid the use of an internal standard when analyzing the samples. This, although useful to quantify the absolute amount of the different lipids identified, would have increased the probability of suppressing signals originating from those lipid species present in low amounts.

In **Fig. 28** representative positive (pos) and negative (neg) ion MALDI-TOF mass spectra of fractions 1 to 6 of ABCA1 and ABCA1MM are presented. In the positive ion spectra (left side), the most abundant species, PC 16:0 18:1, is highlighted ($m/z = 760.6$ for the H^+ and 782.6 for the Na^+ adduct). This lipid species represents more than 50% of the total positive phospholipids. In the negative ion spectra, several peaks corresponding to negatively charged PL can be distinguished. Besides of the presence of the peaks associated with the DHB matrix ($m/z = 851$ and 857), indicated with an asterisk, the main lipid peaks correspond to PS 18:0 18:1 ($m/z = 788.5$), PI 18:0 18:1 ($m/z = 863.6$) and PI 18:0 20:4 ($m/z = 885.6$). The assignments of the most intense peaks are indicated in **Table 6** in section 3.2.4.6.

In the case of the fractions prepared from ABCA1-expressing cells, in the positive ion mode lipids are mainly found in the fractions 3 to 6, whereas negative lipids were mainly enriched in fractions 5 and 6. Conversely, in fractions isolated from ABCA1MM-expressing cells, lipids were similarly detected in raft (1 to 3) and non-raft (4 to 6) fractions. The presence of negatively charged lipids in lipid rafts was already reported by other groups [257,258].

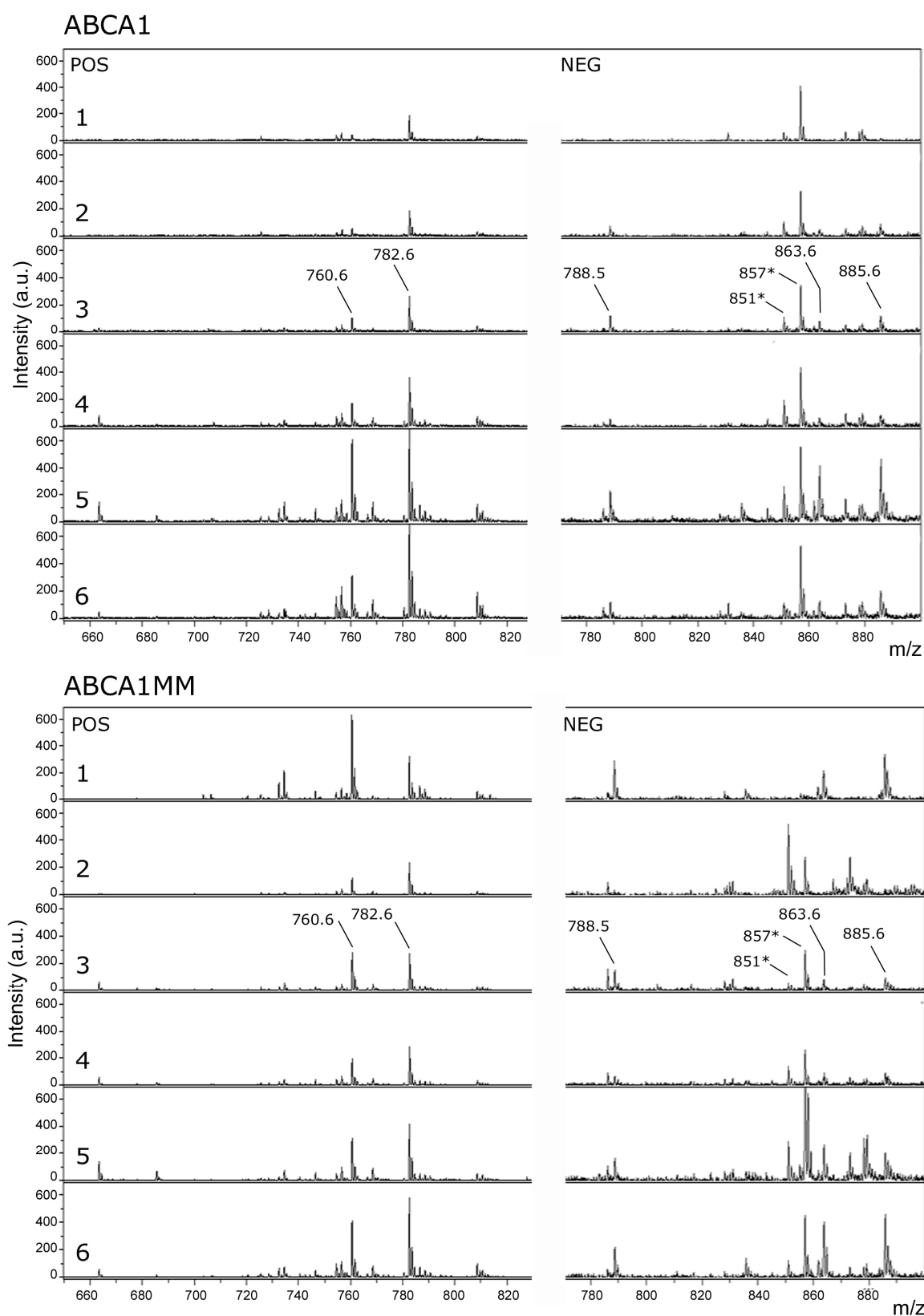


Fig. 28: Positive and negative ion MALDI-TOF mass spectra of plasma membrane fractions. Lipids in fractions 1 to 6, isolated with a subcellular membrane fractionation procedure and corresponding to the plasma membrane, were extracted and analyzed. All spectra were recorded using DHB as matrix. Assignments of the most intense peaks are indicated in Table 6.

In order to plot also the minor lipid species present in the samples and to compare the raft and non-raft fractions isolated from ABCA1- and ABCA1MM-expressing cells, the intensity signals of the peaks in fractions 1 to 3 and 4 to 6 were summed up. Data are presented in Fig. 29.

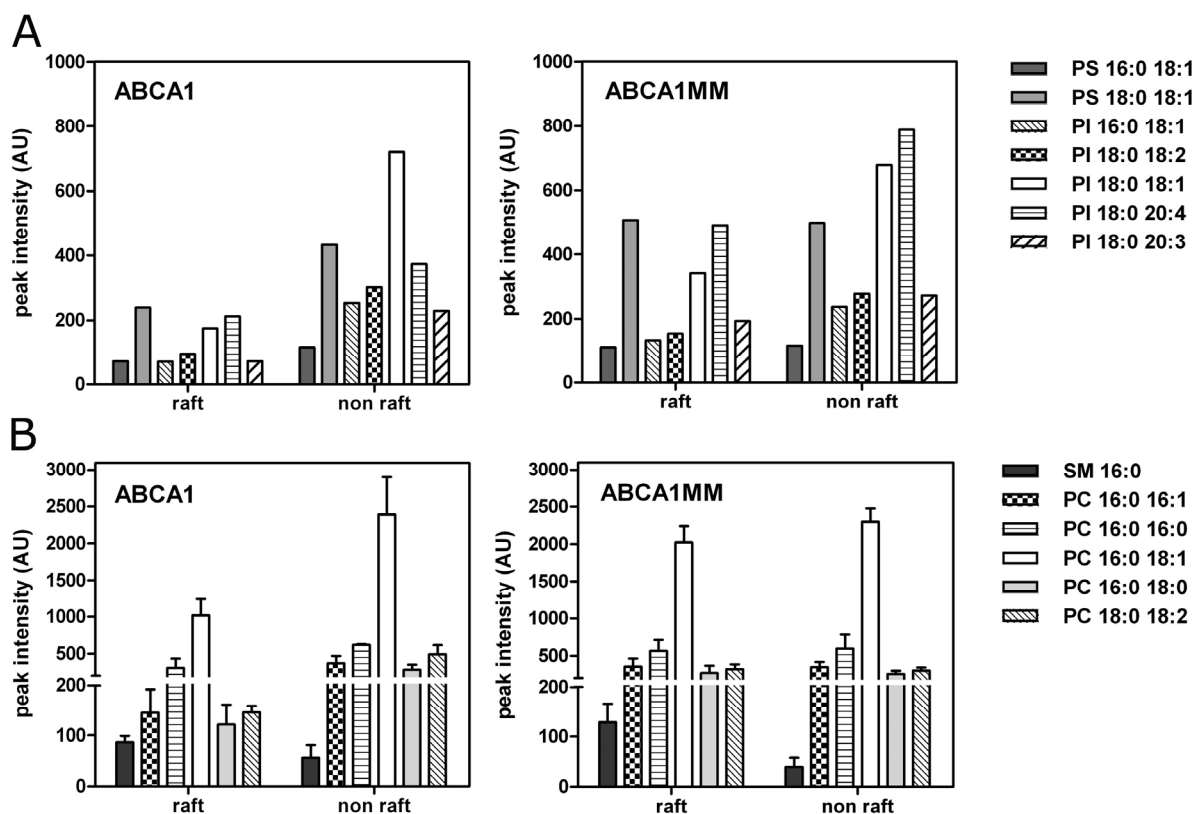


Fig. 29: Distribution of lipids in fractions 1-3 (raft) and 4-6 (non-raft). The intensities of the different lipid species shown in Fig. 28 were quantified and values in fractions 1-3 and 4-6 summed up. The major lipid species detected in the positive ion mode are shown in A, in the negative ion mode in B. In A, values are expressed as mean \pm SEM of two independent experiments.

As already suggested from the raw mass spectra, a \sim 2-fold depletion in both negative (**A**) and positive (**B**) lipids is detected in fractions 1-3 isolated from ABCA1-expressing cells. ABCA1MM presents, on the contrary, similar amounts of almost all lipid species in the raft and non-raft fractions. An exception is SM, being, as expected, enriched in the first fractions. Unfortunately, the spectra of negative lipids could not be recorded in an independent experiment, due to the massive amount of starting material required. It has to be mentioned that PE species are notoriously difficult to be detected by MALDI-TOF mass spectrometry, since this phospholipid is hardly detectable as negative ion [203] and is suppressed in the positive ion mode by lipids with quaternary ammonia groups, that are more sensibly detected [259]. Moreover, PE possesses an amino group with exchangeable protons; this gives rise to a complicated spectrum that presents peaks corresponding to the H^+ adducts, the Na^+ adducts, and to an exchange of one H^+ by Na^+ [202]. Thin layer chromatography

analysis of part of the fractions revealed that PE represented about 40% of the total lipids (not shown).

The larger amount of lipids in the non-raft fractions of ABCA1-containing membranes was not specific for any of the lipid species analyzed, but, rather, indicated a general enrichment of material in these fractions. This could suggest that the presence of ABCA1 alters the properties of the plasma membrane, such as density, which are likely to influence its overall floatation behavior in a density gradient. The reduction in the content of lipids in the raft fractions could be an indication of a general reduction of the surface area occupied by these lipid domains [260]. On the other hand, we found no differential distribution of any particular lipid species analyzed.

4.2.3.3 Lipid order of plasma membrane fractions

To gain further insights in the organization of the membranes in the different fractions and to assess whether the detected different floatation properties of ABCA1 and ABCA1MM plasma membrane could be related to differences in the lipid order of the fractions, we measured the Generalized Polarization (GP) of the lipid membranes using the fluorescent probe Laurdan. This molecule detects changes in membrane phase properties through its sensitivity to the polarity of the environment in the bilayer [206,261,262,263].

In artificial membranes, the coexistence of separate phase domains can be distinguished by Laurdan fluorescent properties. In **Fig. 30**, Laurdan steady state excitation and emission spectra at 25°C, measured in multilamellar vesicles composed of DOPC, with cholesterol concentrations varying from 0 to 40 mol %, are shown. In pure DOPC vesicles, Laurdan fluorescent spectra show a maximum at ~ 350 nm and ~ 490 nm for excitation and emission, respectively (**Fig. 30A**, a). These values are typical of the liquid crystalline phase [263]. Addition of cholesterol induces an increase in the red excitation band and a blue shift in the emission spectra, with concomitant decrease in the intensity at about 490 nm (**Fig. 30A**, from a to b). Similar results were obtained with POPC vesicles (not shown). The red excitation band derives from the stabilization of Laurdan ground state conformation $L\alpha$, which is stronger in the gel phase because of more favorable orientation of the solvent dipole molecules surrounding the probe dipole. The red shift of Laurdan emission spectra in the liquid crystalline phase (a) is due to the faster rate of dipolar relaxation processes that can occur in comparison to the gel phase.

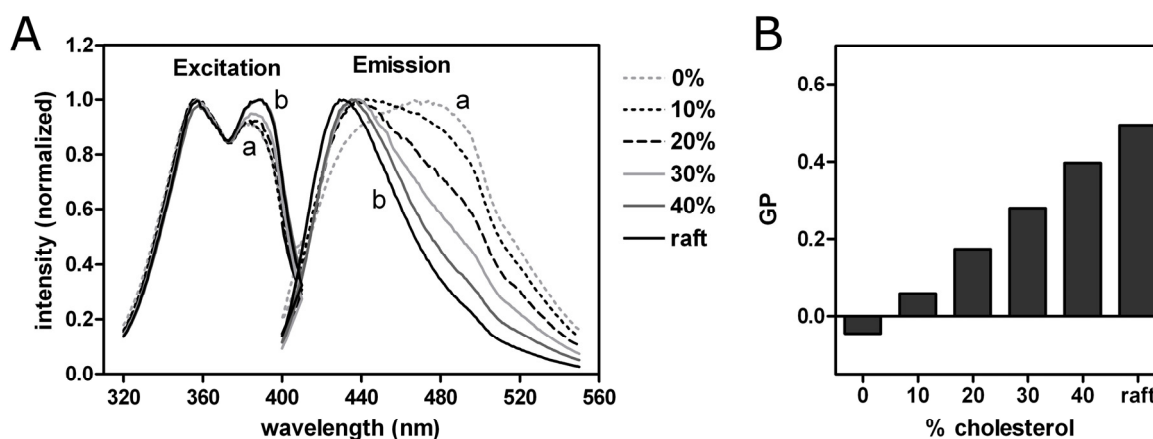


Fig. 30: Laurdan excitation, emission spectra and GP in lipid vesicles. (A) Normalized Laurdan excitation and emission spectra in DOPC vesicles at 25°C at different cholesterol concentrations. Cholesterol mol% with respect to DOPC is indicated in the legend; raft: DOPC/brain SM/cholesterol 1/1/1. Excitation and emission wavelengths were set at 360 nm and 428 nm, respectively. Addition of cholesterol (from a to b) induces an increase in the red excitation band and a blue shift in the emission spectra, with concomitant decrease in the intensity at 490 nm. (B) GP values of Laurdan calculated from the emission spectra as a function of cholesterol concentration.

The effect of cholesterol is to reduce the relaxation rate of the solvent molecules in the proximity of Laurdan dipole, resulting in the characteristic spectra. An additional shift towards shorter emission wavelengths is detected in MLVs composed of DOPC/brain SM/cholesterol 1/1/1 (raft), indicating a tighter molecular packing. This lipid mixture is known to form coexisting Ld and Lo domains at 25°C [264]. The shift in the Laurdan emission spectra can be quantified by calculating the GP value, according to the formula $GP = (I_{437} - I_{482}) / (I_{437} + I_{482})$. This value theoretically ranges from -1 to +1, where -1 indicates a more fluid and +1 a more condensed membrane. The increase of the GP value with increasing cholesterol concentration is shown in **Fig. 30B**.

Fluorescence excitation and emission spectra of Laurdan in the plasma membrane fractions isolated with the detergent-free method from HeLa cells are shown in **Fig. 31A**. These spectra, with an excitation maximum at ~ 390 nm and emission maximum at ~ 440 nm, resemble those of MLVs with a raft mixture (**Fig. 30A**) and are typical of membranes containing high concentration of cholesterol [265]. GP values in the plasma membrane fractions were above 0.4, in agreement with values previously described in isolated membranes [266]. Though very small differences were observed among the different fractions, a flattening of the GP profile can be noticed in ABCA1-expressing membranes in comparison to those expressing the mutant transporter (**Fig. 31B**). As lipid packing is tightly related to cholesterol content, these data may substantiate the assumption that ABCA1 influences the distribution of cholesterol within the plasma membrane. On the other hand, it is also possible that the method utilized is not sensitive enough for the detection of this fine modulated process.

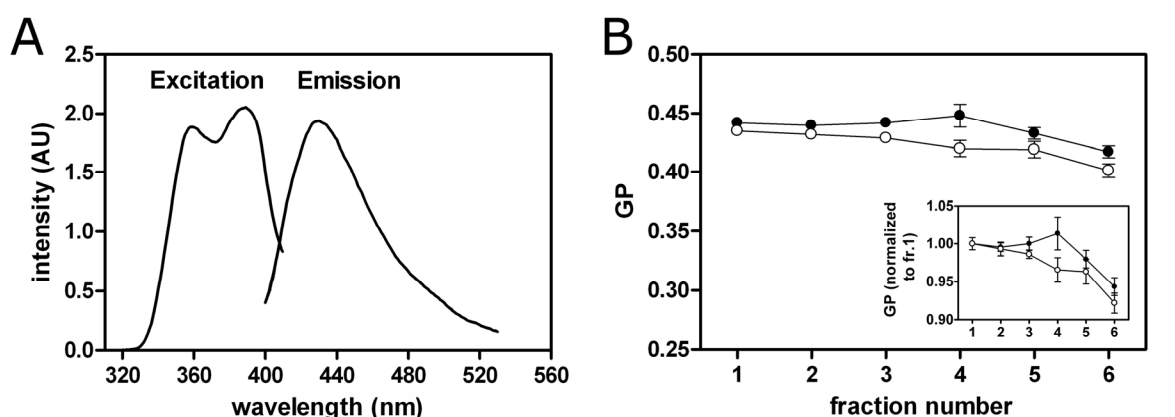


Fig. 31: Laurdan excitation and emission spectra and GP values in plasma membrane fractions. (A) Laurdan fluorescence spectra in membranes isolated from HeLa cells with the detergent-free method. Here, spectra measured in fraction 1 at 25°C are shown. Excitation and emission wavelengths were set at 360 nm and 428 nm, respectively. In (B), GP values calculated from the intensities at 437 nm and 482 nm (see formula in the text) of the emission spectra in ABCA1- (closed circles) and ABCA1MM-containing membranes (open circles) are plotted (mean \pm SEM of two independent experiments in duplicates). In the inset, values normalized to fraction 1 are shown.

4.2.4 ABCA1 and ABCA7: similarities and differences

Among the A subfamily of ABC transporters, ABCA7 shares the highest amino acid sequence homology with ABCA1. Based on this structural homology and on the fact that many ABC proteins are linked with the transport of lipids across cellular membranes, the study of ABCA7 function has focused on lipid metabolism (see introduction, section 1.2.4.2). To shortly summarize, ABCA7 transfected in several cell lines was shown to stimulate efflux of phospholipids to ApoA-I [99,102,104], although efflux of cholesterol is still controversial. Some groups reported no cholesterol efflux to ApoA-I, [102,103], whereas others showed low but positive cholesterol release [99,104,105]. Moreover, studies on *abca1* knock-out mice and Tangier disease patients showed that ABCA1, but not ABCA7, is essential to maintain the plasma HDL concentration [101], but further investigations are required to establish the function of this protein *in vivo*. Up to now, the studies on ABCA7 have been concentrated on efflux of lipids to lipoproteins, while no study on ABCA7-dependent lipid exposure has been performed.

We have investigated the exposure of endogenous PS and of fluorescent lipid analogues in the plasma membrane of MDCKII and HeLa cells expressing ABCA7. A comparative study between ABCA7 and ABCA1 was performed, focusing on the influence of the protein on the lateral and transbilayer lipid distribution.

ABCA7-YFP was expressed in HeLa and MDCKII cells. Tagging of the protein at the C-terminal does not affect phospholipid and cholesterol release to ApoA-I with respect to the wild type

transporter [99,104]. ABCA7-YFP was localized at the plasma membrane and intracellularly both in HeLa and in non polarized MDCKII cells (**Fig. 33**), similarly to ABCA1-GFP.

To confirm that ABCA7-YFP was active in our expression system, lipid efflux to ApoA-I was analyzed. To this aim, cellular phospholipids were labelled with [32 P]-orthophosphate and cells were subsequently incubated with 10 μ g/ml of ApoA-I for 16 h at 37°C. Lipids in the medium and in the cells were extracted and analyzed after separation by two-dimensional TLC. The percentage of efflux was calculated as the radioactivity in the medium relative to the total radioactivity in cells and medium. In **Fig. 32**, the data normalized to efflux in the absence of ApoA-I are presented. In the presence of ABCA7-YFP, ApoA-I extracted about 3.9 % \pm 0.6 of the total PC detected in the medium and cells. We found that ABCA7-YFP promoted efflux of PC and SM to ApoA-I at similar levels to cells expressing ABCA1, as previously reported after labelling of phospholipids with [3 H]-choline [103]. No efflux was measured in non transfected HeLa cells subjected to the same treatment (C) and in ABCA7-YFP expressing cells in the absence of ApoA-I. This confirmed that ABCA7-YFP was functional in our expression system.

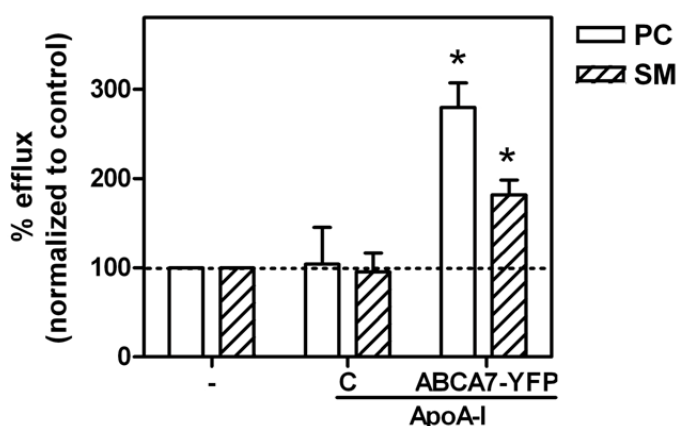


Fig. 32: Efflux of [32 P]-containing phospholipids from non-transfected and ABCA7-YFP-expressing cells to ApoA-I. HeLa cells were labelled with [32 P]-phosphate and efflux to ApoA-I (10 μ g/ml) was performed for 16 h at 37°C. The results are expressed as the amount of radioactivity corresponding to the indicated phospholipids found in the medium divided by the total radioactivity in the medium and cells. Results are normalized to the control efflux in the absence of ApoA-I. C: non-transfected HeLa cells. Mean \pm SEM of 3 independent experiments in duplicates are plotted.

ABCA1-expressing cells expose a higher amount of PS on the outer leaflet of the plasma membrane, as detected by prothrombinase activity and binding of Annexin V [149,170,178]. Moreover, by using C6-NBD-labelled phospholipid analogues, redistribution of PS- but not of PC-analogues from the cytoplasmic to the exoplasmic leaflet of the plasma membrane was observed in ABCA1-expressing cells [170]. However, whether ABCA7 also promotes exposure/efflux of phospholipid (analogues) is unknown.

Exposure of endogenous PS on the exoplasmic plasma membrane leaflet of HeLa and MDCKII cells was assessed by APC-Annexin V binding quantified by flow cytometry. Regions were set to exclude subcellular particles and damaged cells, the latter identified by co-labelling with propidium iodide. Expressing and non-expressing cells (A7 pos and A7 neg, respectively) in the same sample were distinguished by gating on the YFP fluorescent signal. As can be seen in **Fig. 33**, APC-Annexin V binding was enhanced in ABCA7-YFP expressing cells, in comparison to non expressing cells, in both HeLa (**A**) and MDCKII cells (**B**). This effect was not observed in HeLa cells transiently transfected with a mutant ABCA7-YFP with impaired ATPase activity (data not shown).

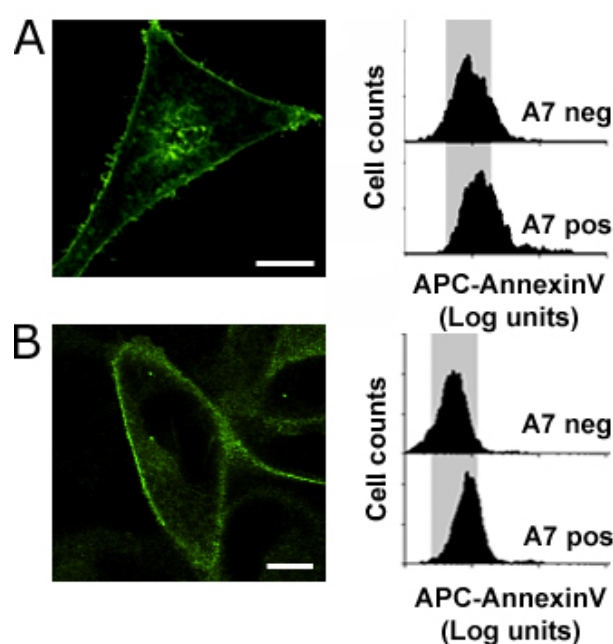


Fig. 33: Subcellular localization of ABCA7-YFP and exposure of endogenous PS in ABCA7-YFP-expressing cells. (A) Subcellular localization of ABCA7-YFP and flow cytometric analysis of APC-Annexin V binding to the cell surface of HeLa cells (A) and MDCKII cells (B). ABCA7-YFP localizes to the plasma membrane and to intracellular compartments in both cell lines. After appropriate gating to exclude damaged cells and debris, cells expressing (A7 pos) and non-expressing (A7 neg) ABCA7-YFP were identified by gating on the YFP fluorescent signal. Cells expressing the transporter show enhanced exposure of endogenous PS, assessed by APC-Annexin V binding. Bars correspond to 10 μm .

To study the outward redistribution of C6-NBD-PS from the inner to the outer leaflet of the plasma membrane, MDCKII cells and ABCA7-YFP expressing cells were incubated at 20°C for 30 min with C6-NBD-PS. This step allows the inward movement of the lipid analogues by an aminophospholipid translocase activity present in the plasma membrane of the cells [207]. Analogues remaining in the exoplasmic leaflet were removed by repeated washing with BSA. To follow the redistribution of the lipid analogues to the outer leaflet, cells were incubated at 37°C in BSA-containing medium in order to extract any analogue that reached the cell surface during the time course of the experiment. The kinetics of the outward redistribution in MDCKII cells are shown in **Fig. 34**.

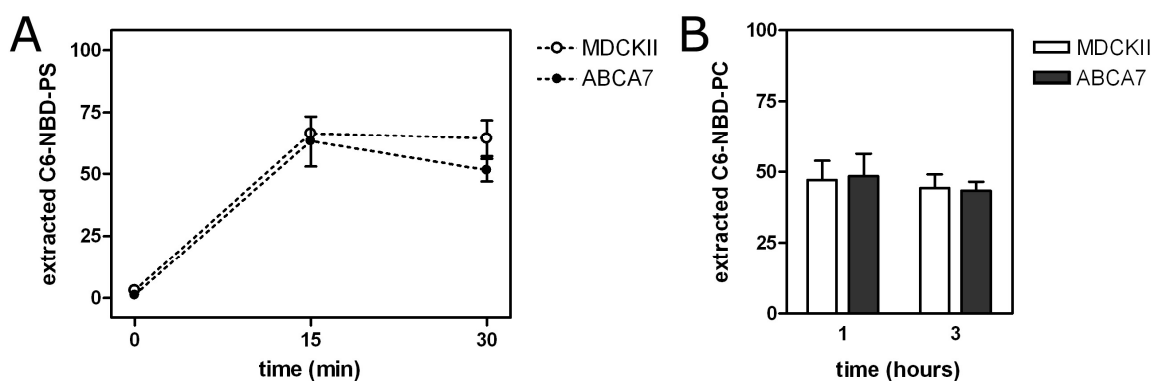


Fig. 34: Outward redistribution of C6-NBD-PS (A) and C6-NBD-PC (B) in ABCA7-YFP-expressing MDCKII cells. (A) Kinetics of outward redistribution in non transfected MDCKII cells and cells expressing ABCA7-YFP at 37°C. Data are shown as mean \pm SEM of at least two independent experiments.

About 60% of the analogues distributed in the inner leaflet became accessible to BSA within 15 min of incubation in BSA-containing medium. No difference between non transfected MDCKII cells and ABCA7-YFP expressing cells was detected. Similar results were obtained for HeLa cells (not shown). These results indicate that ABCA7, differently from ABCA1, does not redistribute PS analogues to the outer leaflet of the plasma membrane. However, it remains possible that this fluorescent analogue of PS is not recognized by the transporter.

As a next step, the outward redistribution of C6-NBD-PC was examined. To this aim, cells were incubated with C6-NBD-PA as a complex with 1% BSA for 1 h or 3 h at 15°C. This lipid analogue is partially converted to C6-NBD-diacylglycerol, which can translocate across the plasma membrane and become available for intracellular synthesis of C6-NBD-PC [58]. After the incubation, the medium was collected and cells were washed with DPBS containing 1% BSA. Washes and media were pooled and lipids extracted from the media and cells were analyzed after two-dimensional separation (as explained in 3.2.4.9). After 1 h or 3 h of incubation at 15°C in the presence of BSA, the amount of C6-NBD-PC extracted was in the order of \sim 50% of the total C6-NBD-PC present in the medium and cells. No difference between non transfected and ABCA7-YFP-expressing cells was detected (**Fig. 34B**).

To gain further insight into the differences and similarities between ABCA7 and ABCA1, GPMVs were prepared from HeLa cells expressing ABCA7-YFP as described in 3.2.4.2. The preferential partitioning of the protein in these vesicles was determined by comparison to the distribution of the marker of the Ld-like phase R18. Similarly to ABCA1-GFP and ABCA1MM-GFP, ABCA7-YFP was enriched in the Ld-like phase (**Fig. 35**).

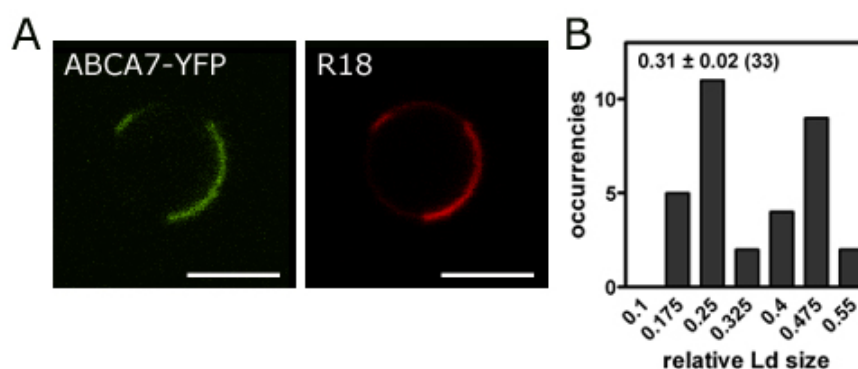


Fig. 35: Partitioning of ABCA7-YFP in GPMVs. GPMVs were prepared from HeLa cells expressing ABCA7-YFP. At 25°C, the majority of the vesicles show coexisting lipid phases. (A) ABCA7-YFP preferentially partitions in the Ld-like phase identified by co-staining with R18. Images were taken at the equatorial plane of the vesicles. Bars correspond to 5 μm . The histograms showing the distribution of the relative size of the Ld-like phase in these vesicles are shown in (B). Mean \pm SEM is indicated in the top left corner. In brackets: number of domains analyzed. Typically, 1-3 domains per vesicle were found.

As previously described, the extent of the Ld-like phase in the presence of the protein was quantified. This revealed that blebs prepared from cells expressing ABCA7-YFP share a similar morphology to those originating from HeLa cells and ABCA1MM-GFP expressing cells (compare paragraph 4.2.2). In line with this result, the lifetime of C6-NBD-PC was also not modified in ABCA7-containing membranes (section 4.2.1.2, **Fig. 20**).

In summary, these results indicate that ABCA7 shares with ABCA1 some functional features: they both show enhanced binding of Annexin V, which suggests an enhanced exposure of endogenous PS on the cell surface, and both promote efflux of phospholipids to ApoA-I *in vitro*. However, differently from ABCA1, ABCA7 does not mediate outward redistribution of C6-NBD-PS. In addition, the analysis of C6-NBD-PC fluorescence lifetime and the study of the influence of ABCA7 on the lipid domain organization in laterally intact cellular bilayer membranes suggest that ABCA7 has no influence on the lateral organization of the plasma membrane.

5 Discussion

5.1 FLIM of C6-NBD lipid analogues: a tool to study the lateral heterogeneity of membranes

The plasma membrane is currently considered to be a complex and heterogeneous composite in which transient and short lived domains may form. However, the properties of such domains and even their existence has divided discussions, in particular because of the lack of proper tools capable of resolving such nanoscaled and short lived heterogeneities.

In the last couple of years, new approaches towards studying such domains have emerged. Among them, are specific fluorophores sensitive to the environment in which they are embedded. These have been employed to study the lateral organization of model and cellular membranes. In contrast to steady-state fluorescence techniques, which are dependent on the resolution limit, fluorescence lifetime can show the characteristic components of the lipid environment surrounding the fluorophores, even if they are localized in the same focal spot [35]. To resolve two distinct lipid environments by FLIM, lipid analogues must not interchange between them during emission. Thus, domains should be stable for at least three times the fluorescence lifetime of the fluorophore, *e.g.* for about 30 ns in the case of C6-NBD-PC. In this time period, assuming a lateral lipid diffusion of $10 \mu\text{m}^2/\text{s}$, an analogue would diffuse ~ 2 nm. Therefore, lipid domains as small as $\sim 10 \text{ nm}^2$ should be detectable by FLIM. As in the plasma membrane of HeLa cells, the lateral diffusion of C6-NBD-PC was $0.1 \mu\text{m}^2/\text{s}$, in agreement with diffusion coefficients measured in fibroblasts [240] and red blood cells [267], domains resolvable by FLIM could be even smaller.

We applied this approach first to GUVs, a well controlled and simple system, to characterize the dependence of the lifetime on the lipid environment. Subsequently, GPMVs were studied to investigate the influence of a highly heterogeneous lipid and protein composition. This allowed a direct comparison to the data obtained in cellular membranes. Finally, this technique was applied to study the influence of ABCA1 on the physicochemical properties of the plasma membrane.

5.1.1 Visualization of lipid domains by fluorescence lifetime of C6-NBD-PC in GUVs

The sensitivity of the fluorescence lifetime of the NBD group to the phase state of lipid membranes was first employed to study the lateral organization of lipids in model membranes. The NBD group of different NBD-labeled lipids localizes at a distance of 18.8 - 20.8 Å from the center of the bilayer, which suggests the preferential localization of the fluorophore in the vicinity of the glycerol backbone and the carbonyl region of adjacent lipid molecules [268]. Similar results were reported by

Huster *et al.*, using NMR cross-relaxation rate measurements [269], and by Loura and Ramalho, by molecular dynamics simulations [270]. This localization places the fluorophore in a suitable position to detect changes in the viscosity of its environment and in the acyl chain packing of the surrounding lipids.

In DOPC/SSM/cholesterol GUVs, forming visible phase separation at 25°C, the long component of NBD fluorescence lifetime τ_2 was shown to be sensitive to the lipid phase in which the lipid analogues were embedded. In Ld domains, the lifetime τ_{2Ld} was about 7 ns, whereas it was shifted to about 11 to 12 ns in Lo domains (τ_{2Lo}). The longer values assessed in the Lo phases, enriched in cholesterol and saturated lipids, can be attributed to slower rate of emission of the excited state due to the higher degree of order in this phase. An alternative explanation is suggested from recent findings, which indicate that the NBD group of acyl chain-labelled lipids resides in a more hydrophobic region in gel phase membranes [271]. Therefore, the longer lifetime in the Lo phase may be due to a relocation of the NBD group from the membrane interface to more hydrophobic membrane interior.

Besides τ_2 , a second component τ_1 of low amplitude was also detected. This component may derive from the NBD groups exposed to the aqueous environment [272]. Alternatively, it may originate from the red edge excitation shift of NBD in membranes, as in our experimental setup the excitation wavelength of the NBD fluorescence was 468 nm, about 3 nm above the excitation maximum. As a consequence, photons emitted early with a small Stokes shift are preselected and give rise to the faster decay component [273]. In addition, it was suggested that this fast component may reflect rotational motion involving the NBD fluorophore [270].

Measurements performed on GUVs prepared from POPC/PSM/cholesterol, which do not form visible domains at 25°C [6], demonstrated that domains of submicroscopic size were formed [209], as already suggested by previous studies via fluorescence energy transfer [274,275]. In fact, in these vesicles, two lifetime components similar to τ_{2Ld} and τ_{2Lo} were found. This indicates that measuring the lifetime of the NBD group is a suitable approach to detect the presence of lipid domains even below the resolution limit of the microscope.

5.1.2 Fluorescence lifetime of C6-NBD-PC in GPMVs

To characterize the properties of the NBD lifetime in membrane bilayers with biological lipid composition, GPMVs were prepared from HeLa cells. These vesicles were recently shown to undergo domain formation at temperatures below $\leq 25^\circ\text{C}$ [17]. Interestingly, in these vesicles C6-NBD-PC was either almost homogeneously distributed between the Ld and the Lo phase, or displayed even a slight preference for the Lo phase. In the first case, the effective formation of

domains was confirmed by the heterogeneous distribution of other probes, such as Rho-DOPE or R18. Such partitioning is in contrast to the preferential localization of the lipid analogue in the Ld phase in GUV [209,211]. This indicates that the preferential enrichment of C6-NBD-PC depends not only on the nature of the lipid phase, but also on its direct lipid environment. Indeed, in GUVs in which a large difference in physical properties exist between the two phases (*e.g.* DOPC/SSM/cholesterol, which display phase separation at 25°C), C6-NBD-PC was clearly enriched in the Ld domain (**Fig. 36A**). On the contrary, GUVs made from POPC/PSM/cholesterol do not show phase coexistence at 25°C, but domain formation can be seen at temperatures $\leq 10^\circ\text{C}$. In such vesicles, in which the difference of enthalpy between the phases is smaller, the preference for the Ld domain was much weaker (**Fig. 36B**). In GPMVs, which consist of different lipid species and proteins, the transition between the different membrane states should be more easily achievable. Indeed, in these vesicles C6-NBD-PC displayed no phase enrichment or even a slight preference for the Lo phase (**Fig. 36C**). These results indicate that C6-NBD-PC is excluded from tightly packed but can penetrate less compact Lo phases, such those of GPMVs. They also show that the assignment of fluorescent lipid probes as specific for distinct lipid domains has to be verified for each membrane system.

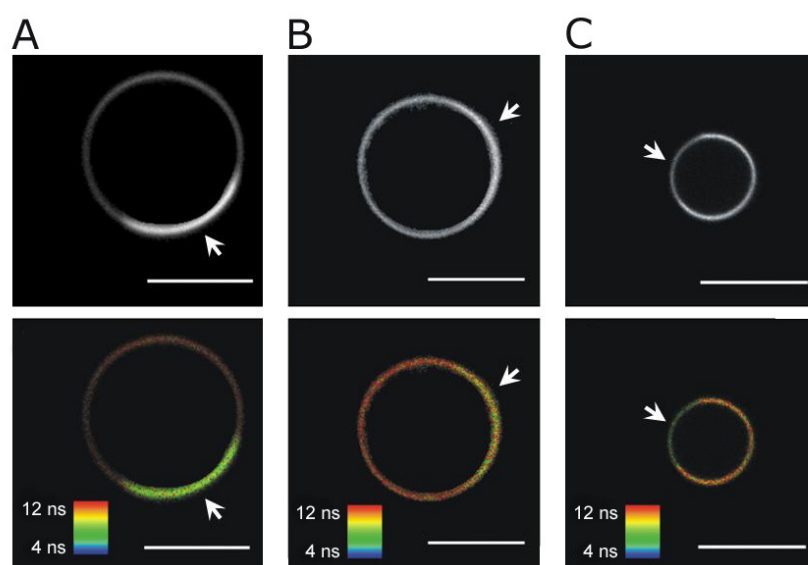


Fig. 36: Phase partition and fluorescence lifetime of C6-NBD-PC in GUVs and GPMVs at 10°C. C6-NBD-PC strongly partition in the Ld phase in GUVs prepared from DOPC/SM/cholesterol 1/1/1 (A), whereas its phase preference is weaker in POPC/SM/cholesterol 1/1/1 GUVs (B). In GPMVs prepared from HeLa cells, C6-NBD-PC even displays a preference for the Lo phase (C). Top row: fluorescence intensity images of C6-NBD-PC; bottom row: average fluorescence lifetime images, pseudocolored according to the scale. The Ld phase is indicated by the arrow. Bars correspond to 10 μm . Images of GUVs (A and B) were kindly provided by Dr. Martin Stöckl.

Notably, despite the differential phase preference, the typical NBD lifetime pattern in the Ld and the Lo phase was preserved. However, in GPMVs, the difference between the lifetimes in the two phases was less pronounced, with values centered around 6.7 ns and 9.6 ns. This can be due to the fact that in these vesicles Lo phases are likely less condensed than those of GUVs. In addition, partial loss of lipid asymmetry may also account for the decrease in the lifetime of the Lo phase, as the presence of PS was shown to shorten lifetime values in GUVs [209] and in the plasma membrane of HeLa cells (section 4.1.4.3). Moreover, this can be concluded from the fact that the envelope of the two lifetime distributions of domain-forming GPMVs gives rise to a continuous and not to a bimodal lifetime distribution as found for GUVs. Remarkably, the envelope histograms of domain-forming GPMVs and of vesicles showing no phase separation were strikingly similar. This may indicate that, in the latter case, large domains disintegrated into smaller ones below the microscopic resolution, while the essential physical properties, *e.g.* lipid packing, were preserved. Being aware of the limitation of GPMVs, a similar situation may be applied to the plasma membrane of cells (see chapter to follow).

5.1.3 Fluorescence lifetime of C6-NBD-PC in cellular membranes

In all the cell lines tested - HeLa, HepG2 and Jurkat - a bimodal distribution of the fluorescence lifetime τ_2 of C6-NBD-PC, C6-NBD-LacCer or C6-NBD-PS was observed. Based on the analysis of the FLIM images, the short component τ_i was associated to intracellular membranes, whereas the long component τ_p to the plasma membrane. Support for this conclusion was given by the fact that, when cells were labeled with C6-NBD-PS, an increase in the amplitude of the short component was detected. It is known that PS, as well as its analogue C6-NBD-PS, is transported from the exoplasmic to the cytoplasmic leaflet of the plasma membrane of HepG2 and HeLa cells by an aminophospholipid translocase activity [170,221] and is then redistributed to intracellular membranes. The plasma membrane-associated lifetime of C6-NBD-PS was found to be slightly shorter than that of C6-NBD-PC. This can be explained by the presence of a higher fraction of the PS analogue in the cytoplasmic leaflet. Indeed, it was previously concluded that the inner leaflet has reduced lipid packing with respect to the exoplasmic leaflet [240,267]. Conversely, the lifetime of the plasma membrane-associated C6-NBD-LacCer was shifted to higher values, in agreement with the preferential localization of ceramide-based lipids to a more ordered environment.

The difference in lifetime between the plasma membrane and intracellular membranes can be explained by the higher cholesterol content of the plasma membrane. Indeed, cholesterol depletion by M β CD induced a shift of the lifetime distribution towards shorter values. The lifetime distribution of the C6-NBD-analogues in the plasma membrane was centered at about 11.5 ns, values typically found for Lo phases of GUVs. These results highlight the sensitivity of this approach to the local

lipid composition of membranes and would agree with the hypothesis, previously drawn, that the plasma membrane may consist of a continuous Lo-like phase with embedded possible small Ld domains [276]. Moreover, the lifetime distribution in the plasma membrane was rather broad as compared to GUVs and GPMVs, even though no separated components were observed. This continuous distribution supports the existence of a large variety of domains varying in size, composition and stability. Previous work has already discussed the presence of an array of domains of different sizes, compositions and fluctuating in time [5,277].

The lifetime of NBD-lipid analogues was demonstrated to be sensitive to cell treatments known to interfere with the lateral and transbilayer organization of membranes. Scrambling of phospholipids between the two leaflets of the plasma membrane via the calcium ionophore ionomycin induced a decrease in the lifetime of NBD. As previously mentioned, this is likely due to the creation of a less ordered environment upon exposure of PS to the outer leaflet of the plasma membrane. A similar effect was observed after disruption of the cytoskeleton by cytochalasin D, confirming that the cytoskeleton meshwork may also contribute to the micro-organization of the plasma membrane. Indeed, in the absence of cytoskeletal constraint, GPMVs blebbed from the plasma membrane of cells can undergo phase separation.

In conclusion, our study suggests the existence of a variety of short-lived submicroscopic domains in the plasma membrane of cells. This view is consistent with the complex network of connections driving the organization and dynamics of the plasma membrane, in which, besides lipid-lipid interactions, protein-lipid and protein-protein interactions also play a fundamental role. The cytoskeleton meshwork and the presence of vesicles continuously fusing and budding to and from the membrane likely also contribute to its dynamics. Finally, also membrane proteins, either by their mere presence or by their influence on the lipid distribution between the two leaflets (section 1.1.4), may contribute to the modulation of the physical properties of the plasma membrane. Indeed, FLIM allowed detecting and characterizing the effect of ABCA1 on the physicochemical properties of the plasma membrane (see chapter to follow).

5.2 Influence of ABCA1 on the lipid microenvironment at the plasma membrane

The described approach based on FLIM of C6-NBD-lipid analogues was employed to assess the influence of ABCA1 on the physicochemical properties of the plasma membrane.

Soon after the identification of ABCA1, it was proposed based on large experimental evidence that its lipid translocase activity can modify the lipid distribution at the plasma membrane, creating a site required for the docking of ApoA-I and the subsequent formation of HDL particles (section 1.3.3). Moreover, a redistribution of cholesterol between different pools at the plasma membrane was hypothesized to explain the increased sensitivity of ABCA1-expressing cells to cholesterol oxidase [177], as this enzyme is believed to be sensitive to the physical properties of the membrane in which cholesterol is embedded [186]. Recently, the influence of the transporter on the overall lipid packing at the plasma membrane has been reported, although this conclusion was mainly supported using detergent-based methods [187,188]. Indeed, the limitations of these approaches have lately emerged [27].

5.2.1 ABCA1 affects the lateral organization of the plasma membrane

We present here for the first time a study of the influence of ABCA1 on the plasma membrane micro-organization by a biophysical approach applied on living cells. Using this technique, the influence of the transporter on the lipid packing at the plasma membrane was demonstrated. In the presence of the wild type transporter, but not of its non-functional mutant, an increase in the fluorescence lifetime of C6-NBD-PC was detected. Considering the correlation between lifetime and cholesterol content, this increment indicated that, in the presence of ABCA1, the NBD probes were embedded in a cholesterol-enriched environment. Support to this conclusion was provided by the decreased mobility of C6-NBD-PC measured, under the same conditions, by FRAP analysis. Indeed, a reduced diffusion mobility of lipids is recognized to be correlated with a higher membrane viscosity and cholesterol content [241]. In line with this assumption, cholesterol depletion induced both a decrease in the lifetime and an increase in the mobility of C6-NBD-PC. Similarly, an ABCA1-dependent increment in lifetime was detected for C6-NBD-LacCer, indicating that the effect observed was not due to preferential interactions between ABCA1 and C6-NBD-PC.

To explore the possibility that the enhanced lifetime measured was associated with formation of condensed, raft-like domains, C6-NBD-PC lifetime was analyzed in the plasma membrane of Jurkat cells after activation of the TCR via an anti-CD3 antibody. This treatment was demonstrated to

trigger formation of condensed membrane domains at the activation sites [37,237]. Similarly, generation of ceramide by sphingomyelinase treatment was also shown to be involved in the natural activation sequence of these cells [238]. After both procedures, a decrease in the fluorescence lifetime was detected. This result may, at a first glance, be in contradiction with the effective formation of condensed domains. However, we have previously highlighted that C6-NBD-PC is excluded from strongly ordered lipid domains, whereas it is able to penetrate the less compact Lo domains of GPMVs (**Fig. 36**). Hence, we conclude that the induction of strongly ordered domain compartments after cell activation or sphingomyelinase treatment leads to an enrichment of the probe in the surrounding disordered environment, causing the observed decrease of the fluorescence lifetime.

We surmise from this data that ABCA1 destabilizes raft domains, resulting either in an enhanced partitioning of the NBD analogues to these domains, or in a redistribution of cholesterol outside rafts enhancing lipid packing in the non-raft domains. This membrane reorganization was dependent on a functional nucleotide binding fold, suggesting the involvement of ATPase-related functions. Alternatively, it could be argued that ABCA1-containing plasma membrane has a higher amount of cholesterol. However, as the plasma membrane cholesterol content between cells expressing the wild type and the non-functional mutant protein was similar (section 4.2.3.2), in agreement with previous results [187], a redistribution of cholesterol between different plasma membrane pools is more likely.

This hypothesis was confirmed by the analysis of ABCA1 partitioning with a detergent-free biochemical approach, described in the chapter to follow.

5.2.2 Mechanism of ABCA1-dependent destabilization of raft domains

The analysis of plasma membrane fractions isolated via density fractionation revealed a differential partitioning between the wild type ABCA1 and its non-functional mutant ABCA1MM (section 4.2.3), as previously shown based on detergent solubility [278]. A higher recovery of ABCA1 in the non-raft fractions of the plasma membrane was detected in comparison to ABCA1MM, which is consistent with an alteration of the physicochemical properties of the plasma membrane apt to influence its overall flotation behavior in a density gradient. Corroborated by the higher recovery of lipids in the non-raft fractions in the presence of ABCA1, this is in agreement with the generation of a more loosely packed fraction of the plasma membrane.

Interestingly, the differential partitioning of ABCA1 did not correlate with the binding or with the efflux of phospholipids to ApoA-I (section 4.2.3.1). Conversely, a dependence on the extent of

binding of Annexin V, a well-established indicator of PS exposure on the cell surface [226], was evidenced.

At this point, no conclusions can be drawn as to whether PS is actively translocated by ABCA1. Nevertheless, we speculate that outward exposure of PS, a polar phospholipid bearing unsaturated acyl chains, would justify the changes in the plasma membrane lipid microenvironment exerted by ABCA1. In synthetic phospholipid mixtures, PS can enhance the miscibility of cholesterol and phospholipids leading to a lateral redistribution of cholesterol [279]. Moreover, chemical treatments able to generate outward movement of PS, such as scrambling of phospholipids, were shown to lead to an increase in the M β CD-extractability of cholesterol and in its susceptibility to cholesterol oxidase [280,281,282]. In line with this hypothesis, in ABCA1-expressing cells a larger efflux of cholesterol to M β CD (section 4.2.1.3) [171,187] and a higher sensitivity to cholesterol oxidase [177] was detected in comparison with ABCA1MM-expressing cells. It was recently proposed that the movement of inner-leaflet phospholipids, which have reduced avidity for sterol complexation, to the outer leaflet of the plasma membrane may increase the chemical activity of cholesterol (defined as its escape tendency) [281,283]. Similarly, the sensitivity to cholesterol oxidase is also considered an indicator of cholesterol activity [283]. Moreover, it was demonstrated that lowering the abundance of plasma membrane sphingomyelin, which also increases the chemical activity of cholesterol [284], promoted cholesterol export by ABCA1 [285]. However, it has to be underlined that the order of magnitude of these two events *i.e.* the exposure of PS on the outer leaflet measured upon activation of lipid scrambling and in the presence of ABCA1 is considerably different.

One of the models proposed for the mechanism of ABCA1 function suggests that the lipid translocase activity of ABCA1 can modify the lipid distribution at the plasma membrane creating a site required for the docking of ApoA-I and subsequent formation of HDL particles (see introduction, section 1.3.3.2). However, from our and other studies, it emerges that exposure of PS alone cannot account for the ABCA1-dependent modification on the lipid microenvironment at the plasma membrane. In fact, expression of ABCA7, which is also associated with enhanced exposure of PS on the cell surface, has no influence on the plasma membrane micro-organization, assessed by the lifetime of C6-NBD-PC (section 4.2.1.2). In addition, it was previously shown that neither apoptotic cells are able to efflux cholesterol to ApoA-I, nor Annexin V to impair cholesterol efflux or ApoA-I binding [286].

Indeed, the deficiency of ABCA7 does not alter ApoA-I-stimulated cholesterol and phospholipid efflux *in vivo* [100]. Despite the fact that in transfected cells ABCA7 is able to promote efflux of PC and SM to ApoA-I (section 4.2.4), it has to be underlined that, under physiological condition, the contact between ABCA7 and ApoA-I may be limited. In fact, immunofluorescence microscopy of

endogenous ABCA7 in macrophages revealed a predominantly intracellular localization of this protein [102]. Moreover, the tissue distribution of ABCA1 and ABCA7 is considerably different, as the former is especially abundant in the liver, the major site of HDL production, whereas the latter is mainly localized in the brain, lung, spleen and adrenal gland and does not show induction by LXR activation [103]. It is possible that, *in vitro*, the observed efflux of lipids to ApoA-I is triggered by a small pool of apolipoprotein binding to ABCA7.

Based on our data and on the findings described in literature we propose the following model (**Fig. 37**).

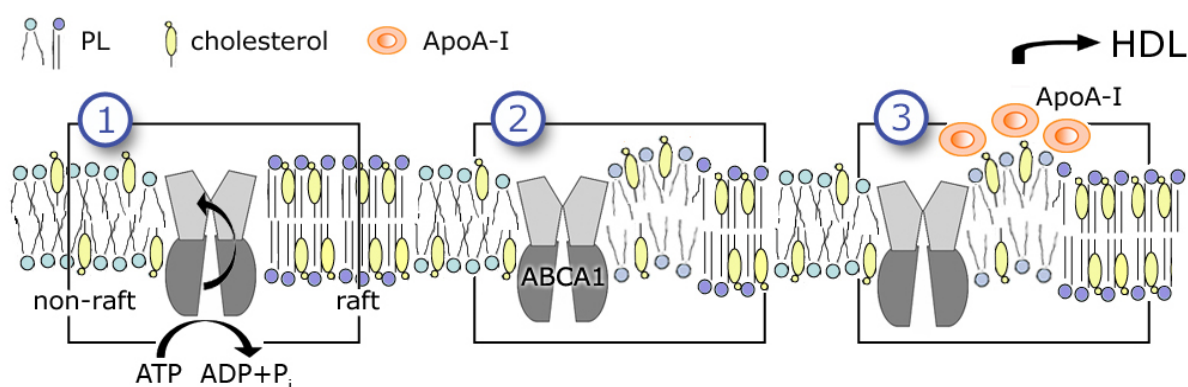


Fig. 37: Model for ABCA1 function. ABCA1 actively translocates phospholipids to the outer leaflet of the plasma membrane (1), leading to the creation of less packed membrane domains (2) in which cholesterol redistributes and becomes available for extraction by ApoA-I (3). For more details, see text.

We hypothesize that ABCA1 actively translocates phospholipids (and/or cholesterol) to the outer leaflet of the plasma membrane (**Fig. 37, 1**). Given the fact that the ATP-binding domain and the putative substrate entry site of the protein are oriented toward the cytoplasmic leaflet, it is expected that a cytoplasmic phospholipid would be preferentially transported. Alternatively, cholesterol could also be translocated to the outer leaflet, although controversy is present whether energy-dependent transport proteins are indeed required for its transbilayer movement, based on the fact that cholesterol can rapidly diffuse across the bilayer (see [287] for a review). On the other hand, the transbilayer dynamics of cholesterol may be restricted by specific interactions with lipids and proteins. Previous studies reported an influence of lipid composition on cholesterol translocation [288,289]. Moreover, simulation models suggest that cholesterol molecules confined to lipid domains, such as Lo domains, may not easily flip-flop between the two leaflets of the bilayer [290].

The ABCA1-mediated translocation event leads to a local increase in the fluidity of the membrane, causing the redistribution of cholesterol from tightly packed to more fluid domains (**Fig. 37, 2**). This is consistent with the higher lifetime measured in the plasma membrane upon expression of ABCA1, as the NBD-labelled probes can now penetrate into these less condensed membrane portions. The

generation of loosely packed membrane microdomains in ABCA1-expressing cells was previously reported by biochemical methods [187,188]. Furthermore, this would imply the localization of ABCA1 in disordered regions of the membrane (sections 4.2.2 and 4.2.3.1) at the boundary between raft and non-raft domains. Indeed, in detergent resistant membranes, ABCA1 was partially detected in fractions insoluble to the mild detergents Lubrol WX and Brij 98, but was excluded from Triton X-100 insoluble membranes (A. Zarubica, unpublished data).

The transfer of molecules from the inner to the outer leaflet and the increased membrane fluidity facilitates the generation of curved structures, as bending the phospholipid bilayer toward the extracellular space would relieve the lateral stress in the membrane [179,291]. At the same time, in these regions, the chemical activity of cholesterol increases, as uncomplexed, high-activity cholesterol resides in disordered regions [283]. In agreement with this hypothesis, it was recently shown that ABCA1-expressing cells produce cholesterol/phospholipid microparticles even in the absence of ApoA-I and that this process could be prevented by rigidifying the plasma membrane [191].

Finally, cholesterol molecules localized in these regions would be more accessible to extracellular acceptors, such as ApoA-I (**Fig. 37, 3**). In addition, ApoA-I may be preferentially recruited to these domains [179]. The increased accessibility of cholesterol to M β CD extraction in the presence of ABCA1 that we and others reported [171,187], as well as its enhanced susceptibility to cholesterol oxidase [177], would also be a consequence of its higher chemical activity.

It was already suggested for ABC proteins, in particular for ABCA5/G8, to stimulate the exposure of cholesterol molecules out of the membrane surface, presenting them to external acceptors (in this case mixed bile salt-phospholipid micelles or vesicles) [74]. According to our data, we surmise that this “liftase” or “exponase” function is indirectly achieved in the case of ABCA1.

In conclusion, the ability of ABCA1 to promote cholesterol efflux seems to be independent and to precede its binding to plasmatic acceptors such as ApoA-I. We propose that the ABCA1-induced plasma membrane modifications are necessary for lipidation of ApoA-I and generation of HDL particles. Moreover, the effect of ABCA1 on the lateral lipid distribution is also a determinant for other receptors, as shown for the case of the TfR. A redistribution of this receptor in different domains at the membrane (section 4.2.3.1) could be the underlying cause of its reduced mobility [233] and of the reduced receptor-mediated endocytosis [169,170] in ABCA1-expressing cells.

By analogy with other ABC transporters and from several experimental hints, it is possible that this is achieved by the floppase activity of ABCA1. However, the lipids that may be the substrate for ABCA1 transport have not been unequivocally identified. Therefore, despite the intense studies being carried out in this area, the story of this protein still has to be fully written.

Bibliography

- [1] Sud, M.; Fahy, E.; Cotter, D.; Brown, A.; Dennis, E. A.; Glass, C. K.; Merrill, A. H., Jr.; Murphy, R. C.; Raetz, C. R.; Russell, D. W. and Subramaniam, S. (2007): LMSD: LIPID MAPS structure database, *Nucleic Acids Res* 35 [Database issue], pp. D527-32.
- [2] van Meer, G.; Voelker, D. R. and Feigenson, G. W. (2008): Membrane lipids: where they are and how they behave, *Nat Rev Mol Cell Biol* 9 [2], pp. 112-24.
- [3] Smaby, J. M.; Momsen, M.; Kulkarni, V. S. and Brown, R. E. (1996): Cholesterol-induced interfacial area condensations of galactosylceramides and sphingomyelins with identical acyl chains, *Biochemistry* 35 [18], pp. 5696-704.
- [4] Hung, W. C.; Lee, M. T.; Chen, F. Y. and Huang, H. W. (2007): The condensing effect of cholesterol in lipid bilayers, *Biophys J* 92 [11], pp. 3960-7.
- [5] Hancock, J. F. (2006): Lipid rafts: contentious only from simplistic standpoints, *Nat Rev Mol Cell Biol* 7 [6], pp. 456-62.
- [6] de Almeida, R. F.; Fedorov, A. and Prieto, M. (2003): Sphingomyelin/phosphatidylcholine/cholesterol phase diagram: boundaries and composition of lipid rafts, *Biophys J* 85 [4], pp. 2406-16.
- [7] Korlach, J.; Schwille, P.; Webb, W. W. and Feigenson, G. W. (1999): Characterization of lipid bilayer phases by confocal microscopy and fluorescence correlation spectroscopy, *Proc Natl Acad Sci U S A* 96 [15], pp. 8461-6.
- [8] Veatch, S. L. and Keller, S. L. (2005): Seeing spots: complex phase behavior in simple membranes, *Biochim Biophys Acta* 1746 [3], pp. 172-85.
- [9] Elliott, R.; Szleifer, I. and Schick, M. (2006): Phase diagram of a ternary mixture of cholesterol and saturated and unsaturated lipids calculated from a microscopic model, *Phys Rev Lett* 96 [9], p. 098101.
- [10] Brown, D. A. and London, E. (2000): Structure and function of sphingolipid- and cholesterol-rich membrane rafts, *J Biol Chem* 275 [23], pp. 17221-4.
- [11] Silvius, J. R. (2003): Role of cholesterol in lipid raft formation: lessons from lipid model systems, *Biochim Biophys Acta* 1610 [2], pp. 174-83.
- [12] Simons, K. and Ikonen, E. (1997): Functional rafts in cell membranes, *Nature* 387 [6633], pp. 569-72.
- [13] Huang, J. and Feigenson, G. W. (1999): A microscopic interaction model of maximum solubility of cholesterol in lipid bilayers, *Biophys J* 76 [4], pp. 2142-57.
- [14] McConnell, H. M. and Radhakrishnan, A. (2003): Condensed complexes of cholesterol and phospholipids, *Biochim Biophys Acta* 1610 [2], pp. 159-73.
- [15] McConnell, H. M. and Vrljic, M. (2003): Liquid-liquid immiscibility in membranes, *Annu Rev Biophys Biomol Struct* 32, pp. 469-92.
- [16] Pandit, S. A.; Jakobsson, E. and Scott, H. L. (2004): Simulation of the early stages of nano-domain formation in mixed bilayers of sphingomyelin, cholesterol, and dioleoylphosphatidylcholine, *Biophys J* 87 [5], pp. 3312-22.
- [17] Baumgart, T.; Hammond, A. T.; Sengupta, P.; Hess, S. T.; Holowka, D. A.; Baird, B. A. and Webb, W. W. (2007): Large-scale fluid/fluid phase separation of proteins and lipids in giant plasma membrane vesicles, *Proc Natl Acad Sci U S A* 104 [9], pp. 3165-70.
- [18] Sengupta, P.; Hammond, A.; Holowka, D. and Baird, B. (2008): Structural determinants for partitioning of lipids and proteins between coexisting fluid phases in giant plasma membrane vesicles, *Biochim Biophys Acta* 1778 [1], pp. 20-32.
- [19] Bacia, K.; Scherfeld, D.; Kahya, N. and Schwille, P. (2004): Fluorescence correlation spectroscopy relates rafts in model and native membranes, *Biophys J* 87 [2], pp. 1034-43.
- [20] Lingwood, D.; Ries, J.; Schwille, P. and Simons, K. (2008): Plasma membranes are poised for activation of raft phase coalescence at physiological temperature, *Proc Natl Acad Sci U S A* 105 [29], pp. 10005-10.
- [21] Sengupta, P.; Baird, B. and Holowka, D. (2007): Lipid rafts, fluid/fluid phase separation, and their relevance to plasma membrane structure and function, *Semin Cell Dev Biol* 18 [5], pp. 583-90.

- [22] Singer, S. J. and Nicolson, G. L. (1972): The fluid mosaic model of the structure of cell membranes, *Science* 175 [23], pp. 720-31.
- [23] van Meer, G.; Stelzer, E. H.; Wijnaendts-van-Resandt, R. W. and Simons, K. (1987): Sorting of sphingolipids in epithelial (Madin-Darby canine kidney) cells, *J Cell Biol* 105 [4], pp. 1623-35.
- [24] Simons, K. and van Meer, G. (1988): Lipid sorting in epithelial cells, *Biochemistry* 27 [17], pp. 6197-202.
- [25] Brown, D. A. and Rose, J. K. (1992): Sorting of GPI-anchored proteins to glycolipid-enriched membrane subdomains during transport to the apical cell surface, *Cell* 68 [3], pp. 533-44.
- [26] Brown, D. A. and London, E. (1998): Structure and origin of ordered lipid domains in biological membranes, *J Membr Biol* 164 [2], pp. 103-14.
- [27] Munro, S. (2003): Lipid rafts: elusive or illusive? *Cell* 115 [4], pp. 377-88.
- [28] Heerklotz, H. (2002): Triton promotes domain formation in lipid raft mixtures, *Biophys J* 83 [5], pp. 2693-701.
- [29] Ayuyan, A. G. and Cohen, F. S. (2008): Raft composition at physiological temperature and pH in the absence of detergents, *Biophys J* 94 [7], pp. 2654-66.
- [30] Sharma, P.; Varma, R.; Sarasij, R. C.; Ira; Gousset, K.; Krishnamoorthy, G.; Rao, M. and Mayor, S. (2004): Nanoscale organization of multiple GPI-anchored proteins in living cell membranes, *Cell* 116 [4], pp. 577-89.
- [31] Prior, I. A.; Muncke, C.; Parton, R. G. and Hancock, J. F. (2003): Direct visualization of Ras proteins in spatially distinct cell surface microdomains, *J Cell Biol* 160 [2], pp. 165-70.
- [32] Plowman, S. J.; Muncke, C.; Parton, R. G. and Hancock, J. F. (2005): H-ras, K-ras, and inner plasma membrane raft proteins operate in nanoclusters with differential dependence on the actin cytoskeleton, *Proc Natl Acad Sci U S A* 102 [43], pp. 15500-5.
- [33] Swamy, M. J.; Ciani, L.; Ge, M.; Smith, A. K.; Holowka, D.; Baird, B. and Freed, J. H. (2006): Coexisting domains in the plasma membranes of live cells characterized by spin-label ESR spectroscopy, *Biophys J* 90 [12], pp. 4452-65.
- [34] Sengupta, P.; Holowka, D. and Baird, B. (2007): Fluorescence resonance energy transfer between lipid probes detects nanoscopic heterogeneity in the plasma membrane of live cells, *Biophys J* 92 [10], pp. 3564-74.
- [35] de Almeida, R. F.; Borst, J.; Fedorov, A.; Prieto, M. and Visser, A. J. (2007): Complexity of lipid domains and rafts in giant unilamellar vesicles revealed by combining imaging and microscopic and macroscopic time-resolved fluorescence, *Biophys J* 93 [2], pp. 539-53.
- [36] Owen, D. M.; Lanigan, P. M.; Dunsby, C.; Munro, I.; Grant, D.; Neil, M. A.; French, P. M. and Magee, A. I. (2006): Fluorescence lifetime imaging provides enhanced contrast when imaging the phase-sensitive dye di-4-ANEPPDHQ in model membranes and live cells, *Biophys J* 90 [11], pp. L80-2.
- [37] Margineanu, A.; Hotta, J.; Vallee, R. A.; Van der Auweraer, M.; Ameloot, M.; Stefan, A.; Beljonne, D.; Engelborghs, Y.; Herrmann, A.; Mullen, K.; De Schryver, F. C. and Hofkens, J. (2007): Visualization of membrane rafts using a perylene monoimide derivative and fluorescence lifetime imaging, *Biophys J* 93 [8], pp. 2877-91.
- [38] Eggeling, C.; Ringemann, C.; Medda, R.; Schwarzmann, G.; Sandhoff, K.; Polyakova, S.; Belov, V. N.; Hein, B.; von Middendorff, C.; Schonle, A. and Hell, S. W. (2008): Direct observation of the nanoscale dynamics of membrane lipids in a living cell, *Nature*.
- [39] Takamori, S.; Holt, M.; Stenius, K.; Lemke, E. A.; Gronborg, M.; Riedel, D.; Urlaub, H.; Schenck, S.; Brugger, B.; Ringler, P.; Muller, S. A.; Rammner, B.; Grater, F.; Hub, J. S.; De Groot, B. L.; Mieskes, G.; Moriyama, Y.; Klingauf, J.; Grubmuller, H.; Heuser, J.; Wieland, F. and Jahn, R. (2006): Molecular anatomy of a trafficking organelle, *Cell* 127 [4], pp. 831-46.
- [40] Marsh, D. (2008): Protein modulation of lipids, and vice-versa, in membranes, *Biochim Biophys Acta* 1778 [7-8], pp. 1545-75.
- [41] Sprong, H.; van der Sluijs, P. and van Meer, G. (2001): How proteins move lipids and lipids move proteins, *Nat Rev Mol Cell Biol* 2 [7], pp. 504-13.
- [42] Zachowski, A. (1993): Phospholipids in animal eukaryotic membranes: transverse asymmetry and movement, *Biochem J* 294 (Pt 1), pp. 1-14.

- [43] Blau, L. and Bittman, R. (1978): Cholesterol distribution between the two halves of the lipid bilayer of human erythrocyte ghost membranes, *J Biol Chem* 253 [23], pp. 8366-8.
- [44] Lange, Y. and Slayton, J. M. (1982): Interaction of cholesterol and lysophosphatidylcholine in determining red cell shape, *J Lipid Res* 23 [8], pp. 1121-7.
- [45] Schroeder, F.; Nemezc, G.; Wood, W. G.; Joiner, C.; Morrot, G.; Ayrault-Jarrier, M. and Devaux, P. F. (1991): Transmembrane distribution of sterol in the human erythrocyte, *Biochim Biophys Acta* 1066 [2], pp. 183-92.
- [46] Pomorski, T.; Holthuis, J. C.; Herrmann, A. and van Meer, G. (2004): Tracking down lipid flippases and their biological functions, *J Cell Sci* 117 [Pt 6], pp. 805-13.
- [47] Sims, P. J. and Wiedmer, T. (2001): Unraveling the mysteries of phospholipid scrambling, *Thromb Haemost* 86 [1], pp. 266-75.
- [48] Sahu, S. K.; Gummadi, S. N.; Manoj, N. and Aradhyam, G. K. (2007): Phospholipid scramblases: an overview, *Arch Biochem Biophys* 462 [1], pp. 103-14.
- [49] Dean, M.; Rzhetsky, A. and Allikmets, R. (2001): The human ATP-binding cassette (ABC) transporter superfamily, *Genome Res* 11 [7], pp. 1156-66.
- [50] Pohl, A.; Devaux, P. F. and Herrmann, A. (2005): Function of prokaryotic and eukaryotic ABC proteins in lipid transport, *Biochim Biophys Acta* 1733 [1], pp. 29-52.
- [51] Klein, I.; Sarkadi, B. and Varadi, A. (1999): An inventory of the human ABC proteins, *Biochim Biophys Acta* 1461 [2], pp. 237-62.
- [52] Biemans-Oldehinkel, E.; Doeven, M. K. and Poolman, B. (2006): ABC transporter architecture and regulatory roles of accessory domains, *FEBS Lett* 580 [4], pp. 1023-35.
- [53] Higgins, C. F. and Linton, K. J. (2004): The ATP switch model for ABC transporters, *Nat Struct Mol Biol* 11 [10], pp. 918-26.
- [54] Linton, K. J. (2007): Structure and function of ABC transporters, *Physiology (Bethesda)* 22, pp. 122-30.
- [55] Higgins, C. F. and Gottesman, M. M. (1992): Is the multidrug transporter a flippase? *Trends Biochem Sci* 17 [1], pp. 18-21.
- [56] Pohl, A.; Lage, H.; Muller, P.; Pomorski, T. and Herrmann, A. (2002): Transport of phosphatidylserine via MDR1 (multidrug resistance 1)P-glycoprotein in a human gastric carcinoma cell line, *Biochem J* 365 [Pt 1], pp. 259-68.
- [57] Raggars, R. J.; Pomorski, T.; Holthuis, J. C.; Kalin, N. and van Meer, G. (2000): Lipid traffic: the ABC of transbilayer movement, *Traffic* 1 [3], pp. 226-34.
- [58] van Helvoort, A.; Smith, A. J.; Sprong, H.; Fritzsche, I.; Schinkel, A. H.; Borst, P. and van Meer, G. (1996): MDR1 P-glycoprotein is a lipid translocase of broad specificity, while MDR3 P-glycoprotein specifically translocates phosphatidylcholine, *Cell* 87 [3], pp. 507-17.
- [59] Ernest, S. and Bello-Reuss, E. (1999): Secretion of platelet-activating factor is mediated by MDR1 P-glycoprotein in cultured human mesangial cells, *J Am Soc Nephrol* 10 [11], pp. 2306-13.
- [60] Smit, J. J.; Schinkel, A. H.; Oude Elferink, R. P.; Groen, A. K.; Wagenaar, E.; van Deemter, L.; Mol, C. A.; Ottenhoff, R.; van der Lugt, N. M.; van Roon, M. A. and et al. (1993): Homozygous disruption of the murine *mdr2* P-glycoprotein gene leads to a complete absence of phospholipid from bile and to liver disease, *Cell* 75 [3], pp. 451-62.
- [61] Davit-Spraul, A.; Gonzales, E.; Baussan, C. and Jacquemin, E. (2009): Progressive familial intrahepatic cholestasis, *Orphanet J Rare Dis* 4 [1], p. 1.
- [62] Wanders, R. J.; Visser, W. F.; van Roermund, C. W.; Kemp, S. and Waterham, H. R. (2007): The peroxisomal ABC transporter family, *Pflugers Arch* 453 [5], pp. 719-34.
- [63] Savary, S.; Troffer-Charlier, N.; Gyapay, G.; Mattei, M. G. and Chimini, G. (1997): Chromosomal localization of the adrenoleukodystrophy-related gene in man and mice, *Eur J Hum Genet* 5 [2], pp. 99-101.
- [64] Theodoulou, F. L.; Holdsworth, M. and Baker, A. (2006): Peroxisomal ABC transporters, *FEBS Lett* 580 [4], pp. 1139-55.
- [65] Mosser, J.; Douar, A. M.; Sarde, C. O.; Kioschis, P.; Feil, R.; Moser, H.; Poustka, A. M.; Mandel, J. L. and Aubourg, P. (1993): Putative X-linked adrenoleukodystrophy gene shares unexpected homology with ABC transporters, *Nature* 361 [6414], pp. 726-30.

- [66] McGuinness, M. C.; Zhang, H. P. and Smith, K. D. (2001): Evaluation of pharmacological induction of fatty acid beta-oxidation in X-linked adrenoleukodystrophy, *Mol Genet Metab* 74 [1-2], pp. 256-63.
- [67] Klucken, J.; Buchler, C.; Orso, E.; Kaminski, W. E.; Porsch-Ozcuremez, M.; Liebisch, G.; Kapinsky, M.; Diederich, W.; Drobnik, W.; Dean, M.; Allikmets, R. and Schmitz, G. (2000): ABCG1 (ABC8), the human homolog of the *Drosophila* white gene, is a regulator of macrophage cholesterol and phospholipid transport, *Proc Natl Acad Sci U S A* 97 [2], pp. 817-22.
- [68] Vaughan, A. M. and Oram, J. F. (2006): ABCA1 and ABCG1 or ABCG4 act sequentially to remove cellular cholesterol and generate cholesterol-rich HDL, *J Lipid Res* 47 [11], pp. 2433-43.
- [69] Berge, K. E.; Tian, H.; Graf, G. A.; Yu, L.; Grishin, N. V.; Schultz, J.; Kwiterovich, P.; Shan, B.; Barnes, R. and Hobbs, H. H. (2000): Accumulation of dietary cholesterol in sitosterolemia caused by mutations in adjacent ABC transporters, *Science* 290 [5497], pp. 1771-5.
- [70] Lee, M. H.; Lu, K.; Hazard, S.; Yu, H.; Shulenin, S.; Hidaka, H.; Kojima, H.; Allikmets, R.; Sakuma, N.; Pegoraro, R.; Srivastava, A. K.; Salen, G.; Dean, M. and Patel, S. B. (2001): Identification of a gene, ABCG5, important in the regulation of dietary cholesterol absorption, *Nat Genet* 27 [1], pp. 79-83.
- [71] Graf, G. A.; Li, W. P.; Gerard, R. D.; Gelissen, I.; White, A.; Cohen, J. C. and Hobbs, H. H. (2002): Coexpression of ATP-binding cassette proteins ABCG5 and ABCG8 permits their transport to the apical surface, *J Clin Invest* 110 [5], pp. 659-69.
- [72] Graf, G. A.; Yu, L.; Li, W. P.; Gerard, R.; Tuma, P. L.; Cohen, J. C. and Hobbs, H. H. (2003): ABCG5 and ABCG8 are obligate heterodimers for protein trafficking and biliary cholesterol excretion, *J Biol Chem* 278 [48], pp. 48275-82.
- [73] Yu, L.; Hammer, R. E.; Li-Hawkins, J.; Von Bergmann, K.; Lutjohann, D.; Cohen, J. C. and Hobbs, H. H. (2002): Disruption of *Abcg5* and *Abcg8* in mice reveals their crucial role in biliary cholesterol secretion, *Proc Natl Acad Sci U S A* 99 [25], pp. 16237-42.
- [74] Small, D. M. (2003): Role of ABC transporters in secretion of cholesterol from liver into bile, *Proc Natl Acad Sci U S A* 100 [1], pp. 4-6.
- [75] Wang, J.; Zhang, D. W.; Lei, Y.; Xu, F.; Cohen, J. C.; Hobbs, H. H. and Xie, X. S. (2008): Purification and reconstitution of sterol transfer by native mouse ABCG5 and ABCG8, *Biochemistry* 47 [18], pp. 5194-204.
- [76] Luciani, M. F.; Denizot, F.; Savary, S.; Mattei, M. G. and Chimini, G. (1994): Cloning of two novel ABC transporters mapping on human chromosome 9, *Genomics* 21 [1], pp. 150-9.
- [77] Klugbauer, N. and Hofmann, F. (1996): Primary structure of a novel ABC transporter with a chromosomal localization on the band encoding the multidrug resistance-associated protein, *FEBS Lett* 391 [1-2], pp. 61-5.
- [78] Connors, T. D.; Van Raay, T. J.; Petry, L. R.; Klinger, K. W.; Landes, G. M. and Burn, T. C. (1997): The cloning of a human ABC gene (ABC3) mapping to chromosome 16p13.3, *Genomics* 39 [2], pp. 231-4.
- [79] Allikmets, R. (1997): A photoreceptor cell-specific ATP-binding transporter gene (ABCR) is mutated in recessive Stargardt macular dystrophy, *Nat Genet* 17 [1], p. 122.
- [80] Albrecht, C. and Viturro, E. (2007): The ABCA subfamily--gene and protein structures, functions and associated hereditary diseases, *Pflugers Arch* 453 [5], pp. 581-9.
- [81] Vulevic, B.; Chen, Z.; Boyd, J. T.; Davis, W., Jr.; Walsh, E. S.; Belinsky, M. G. and Tew, K. D. (2001): Cloning and characterization of human adenosine 5'-triphosphate-binding cassette, sub-family A, transporter 2 (ABCA2), *Cancer Res* 61 [8], pp. 3339-47.
- [82] Tanaka, Y.; Yamada, K.; Zhou, C. J.; Ban, N.; Shioda, S. and Inagaki, N. (2003): Temporal and spatial profiles of ABCA2-expressing oligodendrocytes in the developing rat brain, *J Comp Neurol* 455 [3], pp. 353-67.
- [83] Zhou, C.; Zhao, L.; Inagaki, N.; Guan, J.; Nakajo, S.; Hirabayashi, T.; Kikuyama, S. and Shioda, S. (2001): Atp-binding cassette transporter ABC2/ABCA2 in the rat brain: a novel mammalian lysosome-associated membrane protein and a specific marker for oligodendrocytes but not for myelin sheaths, *J Neurosci* 21 [3], pp. 849-57.

- [84] Chen, Z. J.; Vulevic, B.; Ile, K. E.; Soulika, A.; Davis, W., Jr.; Reiner, P. B.; Connop, B. P.; Nathwani, P.; Trojanowski, J. Q. and Tew, K. D. (2004): Association of ABCA2 expression with determinants of Alzheimer's disease, *Faseb J* 18 [10], pp. 1129-31.
- [85] Yamano, G.; Funahashi, H.; Kawanami, O.; Zhao, L. X.; Ban, N.; Uchida, Y.; Morohoshi, T.; Ogawa, J.; Shioda, S. and Inagaki, N. (2001): ABCA3 is a lamellar body membrane protein in human lung alveolar type II cells, *FEBS Lett* 508 [2], pp. 221-5.
- [86] Cheong, N.; Madesh, M.; Gonzales, L. W.; Zhao, M.; Yu, K.; Ballard, P. L. and Shuman, H. (2006): Functional and trafficking defects in ATP binding cassette A3 mutants associated with respiratory distress syndrome, *J Biol Chem* 281 [14], pp. 9791-800.
- [87] Cheong, N.; Zhang, H.; Madesh, M.; Zhao, M.; Yu, K.; Dodia, C.; Fisher, A. B.; Savani, R. C. and Shuman, H. (2007): ABCA3 is critical for lamellar body biogenesis in vivo, *J Biol Chem* 282 [33], pp. 23811-7.
- [88] Ahn, J.; Wong, J. T. and Molday, R. S. (2000): The effect of lipid environment and retinoids on the ATPase activity of ABCR, the photoreceptor ABC transporter responsible for Stargardt macular dystrophy, *J Biol Chem* 275 [27], pp. 20399-405.
- [89] Kubo, Y.; Sekiya, S.; Ohigashi, M.; Takenaka, C.; Tamura, K.; Nada, S.; Nishi, T.; Yamamoto, A. and Yamaguchi, A. (2005): ABCA5 resides in lysosomes, and ABCA5 knockout mice develop lysosomal disease-like symptoms, *Mol Cell Biol* 25 [10], pp. 4138-49.
- [90] Wenzel, J. J.; Kaminski, W. E.; Piehler, A.; Heimerl, S.; Langmann, T. and Schmitz, G. (2003): ABCA10, a novel cholesterol-regulated ABCA6-like ABC transporter, *Biochem Biophys Res Commun* 306 [4], pp. 1089-98.
- [91] Kaminski, W. E.; Wenzel, J. J.; Piehler, A.; Langmann, T. and Schmitz, G. (2001): ABCA6, a novel a subclass ABC transporter, *Biochem Biophys Res Commun* 285 [5], pp. 1295-301.
- [92] Piehler, A.; Kaminski, W. E.; Wenzel, J. J.; Langmann, T. and Schmitz, G. (2002): Molecular structure of a novel cholesterol-responsive A subclass ABC transporter, ABCA9, *Biochem Biophys Res Commun* 295 [2], pp. 408-16.
- [93] Abe-Dohmae, S.; Ueda, K. and Yokoyama, S. (2006): ABCA7, a molecule with unknown function, *FEBS Lett* 580 [4], pp. 1178-82.
- [94] Zuo, Y.; Zhuang, D. Z.; Han, R.; Isaac, G.; Tobin, J. J.; McKee, M.; Welti, R.; Brissette, J. L.; Fitzgerald, M. L. and Freeman, M. W. (2008): ABCA12 maintains the epidermal lipid permeability barrier by facilitating formation of ceramide linoleic esters, *J Biol Chem* 283 [52], pp. 36624-35.
- [95] Prades, C.; Arnould, I.; Annilo, T.; Shulenin, S.; Chen, Z. Q.; Orosco, L.; Triunfol, M.; Devaud, C.; Maintoux-Larois, C.; Lafargue, C.; Lemoine, C.; Deneffe, P.; Rosier, M. and Dean, M. (2002): The human ATP binding cassette gene ABCA13, located on chromosome 7p12.3, encodes a 5058 amino acid protein with an extracellular domain encoded in part by a 4.8-kb conserved exon, *Cytogenet Genome Res* 98 [2-3], pp. 160-8.
- [96] Ban, N.; Sasaki, M.; Sakai, H.; Ueda, K. and Inagaki, N. (2005): Cloning of ABCA17, a novel rodent sperm-specific ABC (ATP-binding cassette) transporter that regulates intracellular lipid metabolism, *Biochem J* 389 [Pt 2], pp. 577-85.
- [97] Piehler, A. P.; Wenzel, J. J.; Olstad, O. K.; Haug, K. B.; Kierulf, P. and Kaminski, W. E. (2006): The human ortholog of the rodent testis-specific ABC transporter Abca17 is a ubiquitously expressed pseudogene (ABCA17P) and shares a common 5' end with ABCA3, *BMC Mol Biol* 7, p. 28.
- [98] Kaminski, W. E.; Orso, E.; Diederich, W.; Klucken, J.; Drobnik, W. and Schmitz, G. (2000): Identification of a novel human sterol-sensitive ATP-binding cassette transporter (ABCA7), *Biochem Biophys Res Commun* 273 [2], pp. 532-8.
- [99] Ikeda, Y.; Abe-Dohmae, S.; Munehira, Y.; Aoki, R.; Kawamoto, S.; Furuya, A.; Shitara, K.; Amachi, T.; Kioka, N.; Matsuo, M.; Yokoyama, S. and Ueda, K. (2003): Posttranscriptional regulation of human ABCA7 and its function for the apoA-I-dependent lipid release, *Biochem Biophys Res Commun* 311 [2], pp. 313-8.
- [100] Kim, W. S.; Fitzgerald, M. L.; Kang, K.; Okuhira, K.; Bell, S. A.; Manning, J. J.; Koehn, S. L.; Lu, N.; Moore, K. J. and Freeman, M. W. (2005): Abca7 null mice retain normal macrophage phosphatidylcholine and cholesterol efflux activity despite alterations in adipose mass and serum cholesterol levels, *J Biol Chem* 280 [5], pp. 3989-95.

- [101] Oram, J. F. and Heinecke, J. W. (2005): ATP-binding cassette transporter A1: a cell cholesterol exporter that protects against cardiovascular disease, *Physiol Rev* 85 [4], pp. 1343-72.
- [102] Linsel-Nitschke, P.; Jehle, A. W.; Shan, J.; Cao, G.; Bacic, D.; Lan, D.; Wang, N. and Tall, A. R. (2005): Potential role of ABCA7 in cellular lipid efflux to apoA-I, *J Lipid Res* 46 [1], pp. 86-92.
- [103] Wang, N.; Lan, D.; Gerbod-Giannone, M.; Linsel-Nitschke, P.; Jehle, A. W.; Chen, W.; Martinez, L. O. and Tall, A. R. (2003): ATP-binding cassette transporter A7 (ABCA7) binds apolipoprotein A-I and mediates cellular phospholipid but not cholesterol efflux, *J Biol Chem* 278 [44], pp. 42906-12.
- [104] Abe-Dohmae, S.; Ikeda, Y.; Matsuo, M.; Hayashi, M.; Okuhira, K.; Ueda, K. and Yokoyama, S. (2004): Human ABCA7 supports apolipoprotein-mediated release of cellular cholesterol and phospholipid to generate high density lipoprotein, *J Biol Chem* 279 [1], pp. 604-11.
- [105] Hayashi, M.; Abe-Dohmae, S.; Okazaki, M.; Ueda, K. and Yokoyama, S. (2005): Heterogeneity of high density lipoprotein generated by ABCA1 and ABCA7, *J Lipid Res* 46 [8], pp. 1703-11.
- [106] Sasaki, M.; Shoji, A.; Kubo, Y.; Nada, S. and Yamaguchi, A. (2003): Cloning of rat ABCA7 and its preferential expression in platelets, *Biochem Biophys Res Commun* 304 [4], pp. 777-82.
- [107] Kielar, D.; Kaminski, W. E.; Liebisch, G.; Piehler, A.; Wenzel, J. J.; Mohle, C.; Heimerl, S.; Langmann, T.; Friedrich, S. O.; Bottcher, A.; Barlage, S.; Drobnik, W. and Schmitz, G. (2003): Adenosine triphosphate binding cassette (ABC) transporters are expressed and regulated during terminal keratinocyte differentiation: a potential role for ABCA7 in epidermal lipid reorganization, *J Invest Dermatol* 121 [3], pp. 465-74.
- [108] Chan, S. L.; Kim, W. S.; Kwok, J. B.; Hill, A. F.; Cappai, R.; Rye, K. A. and Garner, B. (2008): ATP-binding cassette transporter A7 regulates processing of amyloid precursor protein in vitro, *J Neurochem* 106 [2], pp. 793-804.
- [109] Brown, M. S. and Goldstein, J. L. (1976): Familial hypercholesterolemia: A genetic defect in the low-density lipoprotein receptor, *N Engl J Med* 294 [25], pp. 1386-90.
- [110] Gordon, T.; Castelli, W. P.; Hjortland, M. C.; Kannel, W. B. and Dawber, T. R. (1977): High density lipoprotein as a protective factor against coronary heart disease. The Framingham Study, *Am J Med* 62 [5], pp. 707-14.
- [111] Glomset, J. A. (1968): The plasma lecithins:cholesterol acyltransferase reaction, *J Lipid Res* 9 [2], pp. 155-67.
- [112] Biesbroeck, R.; Oram, J. F.; Albers, J. J. and Bierman, E. L. (1983): Specific high-affinity binding of high density lipoproteins to cultured human skin fibroblasts and arterial smooth muscle cells, *J Clin Invest* 71 [3], pp. 525-39.
- [113] Oram, J. F.; Brinton, E. A. and Bierman, E. L. (1983): Regulation of high density lipoprotein receptor activity in cultured human skin fibroblasts and human arterial smooth muscle cells, *J Clin Invest* 72 [5], pp. 1611-21.
- [114] Acton, S.; Rigotti, A.; Landschulz, K. T.; Xu, S.; Hobbs, H. H. and Krieger, M. (1996): Identification of scavenger receptor SR-BI as a high density lipoprotein receptor, *Science* 271 [5248], pp. 518-20.
- [115] Chiu, D. S.; Oram, J. F.; LeBoeuf, R. C.; Alpers, C. E. and O'Brien, K. D. (1997): High-density lipoprotein-binding protein (HBP)/vigilin is expressed in human atherosclerotic lesions and colocalizes with apolipoprotein E, *Arterioscler Thromb Vasc Biol* 17 [11], pp. 2350-8.
- [116] Matsumoto, A.; Mitchell, A.; Kurata, H.; Pyle, L.; Kondo, K.; Itakura, H. and Fidge, N. (1997): Cloning and characterization of HB2, a candidate high density lipoprotein receptor. Sequence homology with members of the immunoglobulin superfamily of membrane proteins, *J Biol Chem* 272 [27], pp. 16778-82.
- [117] Francis, G. A.; Knopp, R. H. and Oram, J. F. (1995): Defective removal of cellular cholesterol and phospholipids by apolipoprotein A-I in Tangier Disease, *J Clin Invest* 96 [1], pp. 78-87.
- [118] Remaley, A. T.; Schumacher, U. K.; Stonik, J. A.; Farsi, B. D.; Nazih, H. and Brewer, H. B., Jr. (1997): Decreased reverse cholesterol transport from Tangier disease fibroblasts. Acceptor specificity and effect of brefeldin on lipid efflux, *Arterioscler Thromb Vasc Biol* 17 [9], pp. 1813-21.
- [119] Rogler, G.; Trumbach, B.; Klima, B.; Lackner, K. J. and Schmitz, G. (1995): HDL-mediated efflux of intracellular cholesterol is impaired in fibroblasts from Tangier disease patients, *Arterioscler Thromb Vasc Biol* 15 [5], pp. 683-90.

- [120] Walter, M.; Gerdes, U.; Seedorf, U. and Assmann, G. (1994): The high density lipoprotein- and apolipoprotein A-I-induced mobilization of cellular cholesterol is impaired in fibroblasts from Tangier disease subjects, *Biochem Biophys Res Commun* 205 [1], pp. 850-6.
- [121] Rust, S.; Rosier, M.; Funke, H.; Real, J.; Amoura, Z.; Piette, J. C.; Deleuze, J. F.; Brewer, H. B.; Duverger, N.; Deneffe, P. and Assmann, G. (1999): Tangier disease is caused by mutations in the gene encoding ATP-binding cassette transporter 1, *Nat Genet* 22 [4], pp. 352-5.
- [122] Bodzioch, M.; Orso, E.; Klucken, J.; Langmann, T.; Bottcher, A.; Diederich, W.; Drobnik, W.; Barlage, S.; Buchler, C.; Porsch-Ozcurumez, M.; Kaminski, W. E.; Hahmann, H. W.; Oette, K.; Rothe, G.; Aslanidis, C.; Lackner, K. J. and Schmitz, G. (1999): The gene encoding ATP-binding cassette transporter 1 is mutated in Tangier disease, *Nat Genet* 22 [4], pp. 347-51.
- [123] Brooks-Wilson, A.; Marcil, M.; Clee, S. M.; Zhang, L. H.; Roomp, K.; van Dam, M.; Yu, L.; Brewer, C.; Collins, J. A.; Molhuizen, H. O.; Loubser, O.; Ouelette, B. F.; Fichter, K.; Ashbourne-Excoffon, K. J.; Sensen, C. W.; Scherer, S.; Mott, S.; Denis, M.; Martindale, D.; Frohlich, J.; Morgan, K.; Koop, B.; Pimstone, S.; Kastelein, J. J.; Genest, J., Jr. and Hayden, M. R. (1999): Mutations in ABC1 in Tangier disease and familial high-density lipoprotein deficiency, *Nat Genet* 22 [4], pp. 336-45.
- [124] Kolovou, G. D.; Mikhailidis, D. P.; Anagnostopoulou, K. K.; Daskalopoulou, S. S. and Cokkinos, D. V. (2006): Tangier disease four decades of research: a reflection of the importance of HDL, *Curr Med Chem* 13 [7], pp. 771-82.
- [125] Bungert, S.; Molday, L. L. and Molday, R. S. (2001): Membrane topology of the ATP binding cassette transporter ABCR and its relationship to ABC1 and related ABCA transporters: identification of N-linked glycosylation sites, *J Biol Chem* 276 [26], pp. 23539-46.
- [126] Dean, M.; Hamon, Y. and Chimini, G. (2001): The human ATP-binding cassette (ABC) transporter superfamily, *J Lipid Res* 42 [7], pp. 1007-17.
- [127] Fitzgerald, M. L.; Mendez, A. J.; Moore, K. J.; Andersson, L. P.; Panjeton, H. A. and Freeman, M. W. (2001): ATP-binding cassette transporter A1 contains an NH₂-terminal signal anchor sequence that translocates the protein's first hydrophilic domain to the exoplasmic space, *J Biol Chem* 276 [18], pp. 15137-45.
- [128] Trompier, D.; Alibert, M.; Davanture, S.; Hamon, Y.; Pierres, M. and Chimini, G. (2006): Transition from dimers to higher oligomeric forms occurs during the ATPase cycle of the ABCA1 transporter, *J Biol Chem* 281 [29], pp. 20283-90.
- [129] Zarubica, A.; Trompier, D. and Chimini, G. (2007): ABCA1, from pathology to membrane function, *Pflugers Arch* 453 [5], pp. 569-79.
- [130] Li, A. C. and Glass, C. K. (2004): PPAR- and LXR-dependent pathways controlling lipid metabolism and the development of atherosclerosis, *J Lipid Res* 45 [12], pp. 2161-73.
- [131] Chawla, A.; Repa, J. J.; Evans, R. M. and Mangelsdorf, D. J. (2001): Nuclear receptors and lipid physiology: opening the X-files, *Science* 294 [5548], pp. 1866-70.
- [132] Yang, C.; McDonald, J. G.; Patel, A.; Zhang, Y.; Umetani, M.; Xu, F.; Westover, E. J.; Covey, D. F.; Mangelsdorf, D. J.; Cohen, J. C. and Hobbs, H. H. (2006): Sterol intermediates from cholesterol biosynthetic pathway as liver X receptor ligands, *J Biol Chem* 281 [38], pp. 27816-26.
- [133] Desvergne, B. (2007): RXR: from partnership to leadership in metabolic regulations, *Vitam Horm* 75, pp. 1-32.
- [134] Chinetti, G.; Lestavel, S.; Bocher, V.; Remaley, A. T.; Neve, B.; Torra, I. P.; Teissier, E.; Minnich, A.; Jaye, M.; Duverger, N.; Brewer, H. B.; Fruchart, J. C.; Clavey, V. and Staels, B. (2001): PPAR-alpha and PPAR-gamma activators induce cholesterol removal from human macrophage foam cells through stimulation of the ABCA1 pathway, *Nat Med* 7 [1], pp. 53-8.
- [135] Schmitz, G. and Langmann, T. (2005): Transcriptional regulatory networks in lipid metabolism control ABCA1 expression, *Biochim Biophys Acta* 1735 [1], pp. 1-19.
- [136] Gan, X.; Kaplan, R.; Menke, J. G.; MacNaul, K.; Chen, Y.; Sparrow, C. P.; Zhou, G.; Wright, S. D. and Cai, T. Q. (2001): Dual mechanisms of ABCA1 regulation by geranylgeranyl pyrophosphate, *J Biol Chem* 276 [52], pp. 48702-8.
- [137] Oram, J. F.; Lawn, R. M.; Garvin, M. R. and Wade, D. P. (2000): ABCA1 is the cAMP-inducible apolipoprotein receptor that mediates cholesterol secretion from macrophages, *J Biol Chem* 275 [44], pp. 34508-11.

- [138] Le Goff, W.; Zheng, P.; Brubaker, G. and Smith, J. D. (2006): Identification of the cAMP-responsive enhancer of the murine ABCA1 gene: requirement for CREB1 and STAT3/4 elements, *Arterioscler Thromb Vasc Biol* 26 [3], pp. 527-33.
- [139] Cavelier, C.; Lorenzi, I.; Rohrer, L. and von Eckardstein, A. (2006): Lipid efflux by the ATP-binding cassette transporters ABCA1 and ABCG1, *Biochim Biophys Acta* 1761 [7], pp. 655-66.
- [140] Lusis, A. J. (2000): Atherosclerosis, *Nature* 407 [6801], pp. 233-41.
- [141] Panousis, C. G.; Evans, G. and Zuckerman, S. H. (2001): TGF-beta increases cholesterol efflux and ABC-1 expression in macrophage-derived foam cells: opposing the effects of IFN-gamma, *J Lipid Res* 42 [5], pp. 856-63.
- [142] Wang, T. Y. and Silvius, J. R. (2003): Sphingolipid partitioning into ordered domains in cholesterol-free and cholesterol-containing lipid bilayers, *Biophys J* 84 [1], pp. 367-78.
- [143] Wang, Y. and Oram, J. F. (2002): Unsaturated fatty acids inhibit cholesterol efflux from macrophages by increasing degradation of ATP-binding cassette transporter A1, *J Biol Chem* 277 [7], pp. 5692-7.
- [144] Okuhira, K.; Fitzgerald, M. L.; Sarracino, D. A.; Manning, J. J.; Bell, S. A.; Goss, J. L. and Freeman, M. W. (2005): Purification of ATP-binding cassette transporter A1 and associated binding proteins reveals the importance of beta1-syntrophin in cholesterol efflux, *J Biol Chem* 280 [47], pp. 39653-64.
- [145] Tamehiro, N.; Zhou, S.; Okuhira, K.; Benita, Y.; Brown, C. E.; Zhuang, D. Z.; Latz, E.; Hornemann, T.; von Eckardstein, A.; Xavier, R. J.; Freeman, M. W. and Fitzgerald, M. L. (2008): SPTLC1 binds ABCA1 to negatively regulate trafficking and cholesterol efflux activity of the transporter, *Biochemistry* 47 [23], pp. 6138-47.
- [146] Langmann, T.; Mauerer, R.; Zahn, A.; Moehle, C.; Probst, M.; Stremmel, W. and Schmitz, G. (2003): Real-time reverse transcription-PCR expression profiling of the complete human ATP-binding cassette transporter superfamily in various tissues, *Clin Chem* 49 [2], pp. 230-8.
- [147] Denis, M.; Bissonnette, R.; Haidar, B.; Krimbou, L.; Bouvier, M. and Genest, J. (2003): Expression, regulation, and activity of ABCA1 in human cell lines, *Mol Genet Metab* 78 [4], pp. 265-74.
- [148] Attie, A. D. (2007): ABCA1: at the nexus of cholesterol, HDL and atherosclerosis, *Trends Biochem Sci* 32 [4], pp. 172-9.
- [149] Hamon, Y.; Broccardo, C.; Chambenoit, O.; Luciani, M. F.; Toti, F.; Chaslin, S.; Freyssinet, J. M.; Devaux, P. F.; McNeish, J.; Marguet, D. and Chimini, G. (2000): ABC1 promotes engulfment of apoptotic cells and transbilayer redistribution of phosphatidylserine, *Nat Cell Biol* 2 [7], pp. 399-406.
- [150] Tall, A. R.; Costet, P. and Wang, N. (2002): Regulation and mechanisms of macrophage cholesterol efflux, *J Clin Invest* 110 [7], pp. 899-904.
- [151] Neufeld, E. B.; Demosky, S. J., Jr.; Stonik, J. A.; Combs, C.; Remaley, A. T.; Duverger, N.; Santamarina-Fojo, S. and Brewer, H. B., Jr. (2002): The ABCA1 transporter functions on the basolateral surface of hepatocytes, *Biochem Biophys Res Commun* 297 [4], pp. 974-9.
- [152] Neufeld, E. B.; Remaley, A. T.; Demosky, S. J.; Stonik, J. A.; Cooney, A. M.; Comly, M.; Dwyer, N. K.; Zhang, M.; Blanchette-Mackie, J.; Santamarina-Fojo, S. and Brewer, H. B., Jr. (2001): Cellular localization and trafficking of the human ABCA1 transporter, *J Biol Chem* 276 [29], pp. 27584-90.
- [153] Takahashi, Y. and Smith, J. D. (1999): Cholesterol efflux to apolipoprotein AI involves endocytosis and resecretion in a calcium-dependent pathway, *Proc Natl Acad Sci U S A* 96 [20], pp. 11358-63.
- [154] Azuma, Y.; Takada, M.; Shin, H. W.; Kioka, N.; Nakayama, K. and Ueda, K. (2009): Retroendocytosis pathway of ABCA1/apoA-I contributes to HDL formation, *Genes Cells* 14 [2], pp. 191-204.
- [155] Luciani, M. F. and Chimini, G. (1996): The ATP binding cassette transporter ABC1, is required for the engulfment of corpses generated by apoptotic cell death, *Embo J* 15 [2], pp. 226-35.
- [156] Singaraja, R. R.; Visscher, H.; James, E. R.; Chroni, A.; Coutinho, J. M.; Brunham, L. R.; Kang, M. H.; Zannis, V. I.; Chimini, G. and Hayden, M. R. (2006): Specific mutations in ABCA1 have discrete effects on ABCA1 function and lipid phenotypes both in vivo and in vitro, *Circ Res* 99 [4], pp. 389-97.
- [157] Brunham, L. R.; Singaraja, R. R. and Hayden, M. R. (2006): Variations on a gene: rare and common variants in ABCA1 and their impact on HDL cholesterol levels and atherosclerosis, *Annu Rev Nutr* 26, pp. 105-29.

- [158] Christiansen-Weber, T. A.; Volland, J. R.; Wu, Y.; Ngo, K.; Roland, B. L.; Nguyen, S.; Peterson, P. A. and Fung-Leung, W. P. (2000): Functional loss of ABCA1 in mice causes severe placental malformation, aberrant lipid distribution, and kidney glomerulonephritis as well as high-density lipoprotein cholesterol deficiency, *Am J Pathol* 157 [3], pp. 1017-29.
- [159] Basso, F.; Freeman, L.; Knapper, C. L.; Remaley, A.; Stonik, J.; Neufeld, E. B.; Tansey, T.; Amar, M. J.; Fruchart-Najib, J.; Duverger, N.; Santamarina-Fojo, S. and Brewer, H. B., Jr. (2003): Role of the hepatic ABCA1 transporter in modulating intrahepatic cholesterol and plasma HDL cholesterol concentrations, *J Lipid Res* 44 [2], pp. 296-302.
- [160] Wellington, C. L.; Brunham, L. R.; Zhou, S.; Singaraja, R. R.; Visscher, H.; Gelfer, A.; Ross, C.; James, E.; Liu, G.; Huber, M. T.; Yang, Y. Z.; Parks, R. J.; Groen, A.; Fruchart-Najib, J. and Hayden, M. R. (2003): Alterations of plasma lipids in mice via adenoviral-mediated hepatic overexpression of human ABCA1, *J Lipid Res* 44 [8], pp. 1470-80.
- [161] Mulligan, J. D.; Flowers, M. T.; Tebon, A.; Bitgood, J. J.; Wellington, C.; Hayden, M. R. and Attie, A. D. (2003): ABCA1 is essential for efficient basolateral cholesterol efflux during the absorption of dietary cholesterol in chickens, *J Biol Chem* 278 [15], pp. 13356-66.
- [162] Timmins, J. M.; Lee, J. Y.; Boudyguina, E.; Kluckman, K. D.; Brunham, L. R.; Mulya, A.; Gebre, A. K.; Coutinho, J. M.; Colvin, P. L.; Smith, T. L.; Hayden, M. R.; Maeda, N. and Parks, J. S. (2005): Targeted inactivation of hepatic *Abca1* causes profound hypoalphalipoproteinemia and kidney hypercatabolism of apoA-I, *J Clin Invest* 115 [5], pp. 1333-42.
- [163] Greaves, D. R.; Gough, P. J. and Gordon, S. (1998): Recent progress in defining the role of scavenger receptors in lipid transport, atherosclerosis and host defence, *Curr Opin Lipidol* 9 [5], pp. 425-32.
- [164] Tall, A. R. (2008): Cholesterol efflux pathways and other potential mechanisms involved in the athero-protective effect of high density lipoproteins, *J Intern Med* 263 [3], pp. 256-73.
- [165] van Eck, M.; Bos, I. S.; Kaminski, W. E.; Orso, E.; Rothe, G.; Twisk, J.; Bottcher, A.; Van Amersfoort, E. S.; Christiansen-Weber, T. A.; Fung-Leung, W. P.; Van Berkel, T. J. and Schmitz, G. (2002): Leukocyte ABCA1 controls susceptibility to atherosclerosis and macrophage recruitment into tissues, *Proc Natl Acad Sci U S A* 99 [9], pp. 6298-303.
- [166] Van Eck, M.; Singaraja, R. R.; Ye, D.; Hildebrand, R. B.; James, E. R.; Hayden, M. R. and Van Berkel, T. J. (2006): Macrophage ATP-binding cassette transporter A1 overexpression inhibits atherosclerotic lesion progression in low-density lipoprotein receptor knockout mice, *Arterioscler Thromb Vasc Biol* 26 [4], pp. 929-34.
- [167] Ravichandran, K. S. and Lorenz, U. (2007): Engulfment of apoptotic cells: signals for a good meal, *Nat Rev Immunol* 7 [12], pp. 964-74.
- [168] Wu, Y. C. and Horvitz, H. R. (1998): The *C. elegans* cell corpse engulfment gene *ced-7* encodes a protein similar to ABC transporters, *Cell* 93 [6], pp. 951-60.
- [169] Zha, X.; Genest, J., Jr. and McPherson, R. (2001): Endocytosis is enhanced in Tangier fibroblasts: possible role of ATP-binding cassette protein A1 in endosomal vesicular transport, *J Biol Chem* 276 [42], pp. 39476-83.
- [170] Alder-Baerens, N.; Muller, P.; Pohl, A.; Korte, T.; Hamon, Y.; Chimini, G.; Pomorski, T. and Herrmann, A. (2005): Headgroup-specific exposure of phospholipids in ABCA1-expressing cells, *J Biol Chem* 280 [28], pp. 26321-9.
- [171] Smith, J. D.; Le Goff, W.; Settle, M.; Brubaker, G.; Waelde, C.; Horwitz, A. and Oda, M. N. (2004): ABCA1 mediates concurrent cholesterol and phospholipid efflux to apolipoprotein A-I, *J Lipid Res* 45 [4], pp. 635-44.
- [172] Gillotte, K. L.; Zaiou, M.; Lund-Katz, S.; Anantharamaiah, G. M.; Holvoet, P.; Dhoest, A.; Palgunachari, M. N.; Segrest, J. P.; Weisgraber, K. H.; Rothblat, G. H. and Phillips, M. C. (1999): Apolipoprotein-mediated plasma membrane microsolvubilization. Role of lipid affinity and membrane penetration in the efflux of cellular cholesterol and phospholipid, *J Biol Chem* 274 [4], pp. 2021-8.
- [173] Lin, G. and Oram, J. F. (2000): Apolipoprotein binding to protruding membrane domains during removal of excess cellular cholesterol, *Atherosclerosis* 149 [2], pp. 359-70.
- [174] Fielding, P. E.; Nagao, K.; Hakamata, H.; Chimini, G. and Fielding, C. J. (2000): A two-step mechanism for free cholesterol and phospholipid efflux from human vascular cells to apolipoprotein A-1, *Biochemistry* 39 [46], pp. 14113-20.

- [175] Kiss, R. S.; Maric, J. and Marcel, Y. L. (2005): Lipid efflux in human and mouse macrophagic cells: evidence for differential regulation of phospholipid and cholesterol efflux, *J Lipid Res* 46 [9], pp. 1877-87.
- [176] Wang, N.; Silver, D. L.; Thiele, C. and Tall, A. R. (2001): ATP-binding cassette transporter A1 (ABCA1) functions as a cholesterol efflux regulatory protein, *J Biol Chem* 276 [26], pp. 23742-7.
- [177] Vaughan, A. M. and Oram, J. F. (2003): ABCA1 redistributes membrane cholesterol independent of apolipoprotein interactions, *J Lipid Res* 44 [7], pp. 1373-80.
- [178] Chambenoit, O.; Hamon, Y.; Marguet, D.; Rigneault, H.; Rosseneu, M. and Chimini, G. (2001): Specific docking of apolipoprotein A-I at the cell surface requires a functional ABCA1 transporter, *J Biol Chem* 276 [13], pp. 9955-60.
- [179] Vedhachalam, C.; Duong, P. T.; Nickel, M.; Nguyen, D.; Dhanasekaran, P.; Saito, H.; Rothblat, G. H.; Lund-Katz, S. and Phillips, M. C. (2007): Mechanism of ATP-binding cassette transporter A1-mediated cellular lipid efflux to apolipoprotein A-I and formation of high density lipoprotein particles, *J Biol Chem* 282 [34], pp. 25123-30.
- [180] Hauser, H. and Phillips, M. C. (1973): Structures of aqueous dispersions of phosphatidylserine, *J Biol Chem* 248 [24], pp. 8585-91.
- [181] Remaley, A. T.; Thomas, F.; Stonik, J. A.; Demosky, S. J.; Bark, S. E.; Neufeld, E. B.; Bocharov, A. V.; Vishnyakova, T. G.; Patterson, A. P.; Eggerman, T. L.; Santamarina-Fojo, S. and Brewer, H. B. (2003): Synthetic amphipathic helical peptides promote lipid efflux from cells by an ABCA1-dependent and an ABCA1-independent pathway, *J Lipid Res* 44 [4], pp. 828-36.
- [182] Fitzgerald, M. L.; Morris, A. L.; Chroni, A.; Mendez, A. J.; Zannis, V. I. and Freeman, M. W. (2004): ABCA1 and amphipathic apolipoproteins form high-affinity molecular complexes required for cholesterol efflux, *J Lipid Res* 45 [2], pp. 287-94.
- [183] Rigot, V.; Hamon, Y.; Chambenoit, O.; Alibert, M.; Duverger, N. and Chimini, G. (2002): Distinct sites on ABCA1 control distinct steps required for cellular release of phospholipids, *J Lipid Res* 43 [12], pp. 2077-86.
- [184] Hassan, H. H.; Denis, M.; Lee, D. Y.; Iatan, I.; Nyholt, D.; Ruel, I.; Krimbou, L. and Genest, J. (2007): Identification of an ABCA1-dependent phospholipid-rich plasma membrane apolipoprotein A-I binding site for nascent HDL formation: implications for current models of HDL biogenesis, *J Lipid Res* 48 [11], pp. 2428-42.
- [185] Vedhachalam, C.; Ghering, A. B.; Davidson, W. S.; Lund-Katz, S.; Rothblat, G. H. and Phillips, M. C. (2007): ABCA1-induced cell surface binding sites for ApoA-I, *Arterioscler Thromb Vasc Biol* 27 [7], pp. 1603-9.
- [186] Ahn, K. W. and Sampson, N. S. (2004): Cholesterol oxidase senses subtle changes in lipid bilayer structure, *Biochemistry* 43 [3], pp. 827-36.
- [187] Landry, Y. D.; Denis, M.; Nandi, S.; Bell, S.; Vaughan, A. M. and Zha, X. (2006): ATP-binding cassette transporter A1 expression disrupts raft membrane microdomains through its ATPase-related functions, *J Biol Chem* 281 [47], pp. 36091-101.
- [188] Koseki, M.; Hirano, K.; Masuda, D.; Ikegami, C.; Tanaka, M.; Ota, A.; Sandoval, J. C.; Nakagawa-Toyama, Y.; Sato, S. B.; Kobayashi, T.; Shimada, Y.; Ohno-Iwashita, Y.; Matsuura, F.; Shimomura, I. and Yamashita, S. (2007): Increased lipid rafts and accelerated lipopolysaccharide-induced tumor necrosis factor- α secretion in Abca1-deficient macrophages, *J Lipid Res* 48 [2], pp. 299-306.
- [189] Waheed, A. A.; Shimada, Y.; Heijnen, H. F.; Nakamura, M.; Inomata, M.; Hayashi, M.; Iwashita, S.; Slot, J. W. and Ohno-Iwashita, Y. (2001): Selective binding of perfringolysin O derivative to cholesterol-rich membrane microdomains (rafts), *Proc Natl Acad Sci U S A* 98 [9], pp. 4926-31.
- [190] Sato, S. B.; Ishii, K.; Makino, A.; Iwabuchi, K.; Yamaji-Hasegawa, A.; Senoh, Y.; Nagaoka, I.; Sakuraba, H. and Kobayashi, T. (2004): Distribution and transport of cholesterol-rich membrane domains monitored by a membrane-impermeant fluorescent polyethylene glycol-derivatized cholesterol, *J Biol Chem* 279 [22], pp. 23790-6.
- [191] Nandi, S.; Ma, L.; Denis, M.; Karwatsky, J.; Li, Z.; Jiang, X. C. and Zha, X. (2008): ABCA1-mediated cholesterol efflux generates microparticles in addition to HDL through processes governed by membrane rigidity, *J Lipid Res*.
- [192] Yguerabide, J.; Schmidt, J. A. and Yguerabide, E. E. (1982): Lateral mobility in membranes as detected by fluorescence recovery after photobleaching, *Biophys J* 40 [1], pp. 69-75.

- [193] Reits, E. A. and Neefjes, J. J. (2001): From fixed to FRAP: measuring protein mobility and activity in living cells, *Nat Cell Biol* 3 [6], pp. E145-7.
- [194] Angelova, M. I. and Dimitrov, D. S. (1986): Liposome Electroformation, *Faraday Discussions* [81], pp. 303-+.
- [195] Angelova, M. I.; Soleau, S.; Meleard, P.; Faucon, J. F. and Bothorel, P. (1992): Preparation of Giant Vesicles by External Ac Electric-Fields - Kinetics and Applications, *Trends in Colloid and Interface Science* Vi 89, pp. 127-131.
- [196] Ayuyan, A. G. and Cohen, F. S. (2006): Lipid peroxides promote large rafts: effects of excitation of probes in fluorescence microscopy and electrochemical reactions during vesicle formation, *Biophys J* 91 [6], pp. 2172-83.
- [197] Macdonald, J. L. and Pike, L. J. (2005): A simplified method for the preparation of detergent-free lipid rafts, *J Lipid Res* 46 [5], pp. 1061-7.
- [198] Maniatis, T.; Sambrook, J. and Fritsch, E.F. (1989): *Molecular cloning: a laboratory manual*, Cold Spring Harbor Laboratory Press 1.
- [199] Bligh, E. G. and Dyer, W. J. (1959): A rapid method of total lipid extraction and purification, *Can J Biochem Physiol* 37 [8], pp. 911-7.
- [200] Hess, H. H. and Derr, J. E. (1975): Assay of inorganic and organic phosphorus in the 0.1-5 nanomole range, *Anal Biochem* 63 [2], pp. 607-13.
- [201] Chalvardjian, A. and Rudnicki, E. (1970): Determination of lipid phosphorus in the nanomolar range, *Anal Biochem* 36 [1], pp. 225-6.
- [202] Schiller, J.; Suss, R.; Arnhold, J.; Fuchs, B.; Lessig, J.; Muller, M.; Petkovic, M.; Spalteholz, H.; Zschornig, O. and Arnold, K. (2004): Matrix-assisted laser desorption and ionization time-of-flight (MALDI-TOF) mass spectrometry in lipid and phospholipid research, *Prog Lipid Res* 43 [5], pp. 449-88.
- [203] Fuchs, B.; Schober, C.; Richter, G.; Suss, R. and Schiller, J. (2007): MALDI-TOF MS of phosphatidylethanolamines: different adducts cause different post source decay (PSD) fragment ion spectra, *J Biochem Biophys Methods* 70 [4], pp. 689-92.
- [204] Schiller, J.; Suss, R.; Fuchs, B.; Muller, M.; Petkovic, M.; Zschornig, O. and Waschipky, H. (2007): The suitability of different DHB isomers as matrices for the MALDI-TOF MS analysis of phospholipids: which isomer for what purpose? *Eur Biophys J* 36 [4-5], pp. 517-27.
- [205] Huster, D.; Scheidt, H. A.; Arnold, K.; Herrmann, A. and Muller, P. (2005): Desmosterol may replace cholesterol in lipid membranes, *Biophys J* 88 [3], pp. 1838-44.
- [206] Parasassi, T.; De Stasio, G.; Ravagnan, G.; Rusch, R. M. and Gratton, E. (1991): Quantitation of lipid phases in phospholipid vesicles by the generalized polarization of Laurdan fluorescence, *Biophys J* 60 [1], pp. 179-89.
- [207] Pomorski, T.; Muller, P.; Zimmermann, B.; Burger, K.; Devaux, P. F. and Herrmann, A. (1996): Transbilayer movement of fluorescent and spin-labeled phospholipids in the plasma membrane of human fibroblasts: a quantitative approach, *J Cell Sci* 109 (Pt 3), pp. 687-98.
- [208] Colleau, M.; Herve, P.; Fellmann, P. and Devaux, P. F. (1991): Transmembrane diffusion of fluorescent phospholipids in human erythrocytes, *Chem Phys Lipids* 57 [1], pp. 29-37.
- [209] Stöckl, M.; Plazzo, A. P.; Korte, T. and Herrmann, A. (2008): Detection of lipid domains in model and cell membranes by fluorescence lifetime imaging microscopy of fluorescent lipid analogues, *J Biol Chem* 283 [45], pp. 30828-37.
- [210] Bagatolli, L. A. (2006): To see or not to see: lateral organization of biological membranes and fluorescence microscopy, *Biochim Biophys Acta* 1758 [10], pp. 1541-56.
- [211] Shaw, J. E.; Epan, R. F.; Epan, R. M.; Li, Z.; Bittman, R. and Yip, C. M. (2006): Correlated fluorescence-atomic force microscopy of membrane domains: structure of fluorescence probes determines lipid localization, *Biophys J* 90 [6], pp. 2170-8.
- [212] Yetukuri, L.; Ekroos, K.; Vidal-Puig, A. and Oresic, M. (2008): Informatics and computational strategies for the study of lipids, *Mol Biosyst* 4 [2], pp. 121-7.
- [213] Fridriksson, E. K.; Shipkova, P. A.; Sheets, E. D.; Holowka, D.; Baird, B. and McLafferty, F. W. (1999): Quantitative analysis of phospholipids in functionally important membrane domains from

- RBL-2H3 mast cells using tandem high-resolution mass spectrometry, *Biochemistry* 38 [25], pp. 8056-63.
- [214] Gidwani, A.; Holowka, D. and Baird, B. (2001): Fluorescence anisotropy measurements of lipid order in plasma membranes and lipid rafts from RBL-2H3 mast cells, *Biochemistry* 40 [41], pp. 12422-9.
- [215] Baumgart, T.; Hunt, G.; Farkas, E. R.; Webb, W. W. and Feigenson, G. W. (2007): Fluorescence probe partitioning between Lo/Ld phases in lipid membranes, *Biochim Biophys Acta* 1768 [9], pp. 2182-94.
- [216] Sheets, E. D.; Holowka, D. and Baird, B. (1999): Critical role for cholesterol in Lyn-mediated tyrosine phosphorylation of FcεRI and their association with detergent-resistant membranes, *J Cell Biol* 145 [4], pp. 877-87.
- [217] Dietrich, C.; Bagatolli, L. A.; Volovyk, Z. N.; Thompson, N. L.; Levi, M.; Jacobson, K. and Gratton, E. (2001): Lipid rafts reconstituted in model membranes, *Biophys J* 80 [3], pp. 1417-28.
- [218] Keller, P. and Simons, K. (1998): Cholesterol is required for surface transport of influenza virus hemagglutinin, *J Cell Biol* 140 [6], pp. 1357-67.
- [219] Maxfield, F. R. (2002): Plasma membrane microdomains, *Curr Opin Cell Biol* 14 [4], pp. 483-7.
- [220] Wustner, D.; Mukherjee, S.; Maxfield, F. R.; Muller, P. and Herrmann, A. (2001): Vesicular and nonvesicular transport of phosphatidylcholine in polarized HepG2 cells, *Traffic* 2 [4], pp. 277-96.
- [221] Müller, P.; Pomorski, T.; Porwoli, S.; Tauber, R. and Herrmann, A. (1996): Transverse movement of spin-labeled phospholipids in the plasma membrane of a hepatocytic cell line (HepG2): implications for biliary lipid secretion, *Hepatology* 24 [6], pp. 1497-503.
- [222] Tannert, A.; Wustner, D.; Bechstein, J.; Muller, P.; Devaux, P. F. and Herrmann, A. (2003): Aminophospholipids have no access to the luminal side of the biliary canaliculus: implications for the specific lipid composition of the bile fluid, *J Biol Chem* 278 [42], pp. 40631-9.
- [223] Ritchie, K.; Iino, R.; Fujiwara, T.; Murase, K. and Kusumi, A. (2003): The fence and picket structure of the plasma membrane of live cells as revealed by single molecule techniques (Review), *Mol Membr Biol* 20 [1], pp. 13-8.
- [224] Smeets, E. F.; Comfurius, P.; Bevers, E. M. and Zwaal, R. F. (1994): Calcium-induced transbilayer scrambling of fluorescent phospholipid analogs in platelets and erythrocytes, *Biochim Biophys Acta* 1195 [2], pp. 281-6.
- [225] Williamson, P.; Bevers, E. M.; Smeets, E. F.; Comfurius, P.; Schlegel, R. A. and Zwaal, R. F. (1995): Continuous analysis of the mechanism of activated transbilayer lipid movement in platelets, *Biochemistry* 34 [33], pp. 10448-55.
- [226] Zwaal, R. F.; Comfurius, P. and Bevers, E. M. (2005): Surface exposure of phosphatidylserine in pathological cells, *Cell Mol Life Sci* 62 [9], pp. 971-88.
- [227] Cooper, J. A. (1987): Effects of cytochalasin and phalloidin on actin, *J Cell Biol* 105 [4], pp. 1473-8.
- [228] Kusumi, A.; Nakada, C.; Ritchie, K.; Murase, K.; Suzuki, K.; Murakoshi, H.; Kasai, R. S.; Kondo, J. and Fujiwara, T. (2005): Paradigm shift of the plasma membrane concept from the two-dimensional continuum fluid to the partitioned fluid: high-speed single-molecule tracking of membrane molecules, *Annu Rev Biophys Biomol Struct* 34, pp. 351-78.
- [229] Wulf, E.; Deboben, A.; Bautz, F. A.; Faulstich, H. and Wieland, T. (1979): Fluorescent phalloidin, a tool for the visualization of cellular actin, *Proc Natl Acad Sci U S A* 76 [9], pp. 4498-502.
- [230] Megha and London, E. (2004): Ceramide selectively displaces cholesterol from ordered lipid domains (rafts): implications for lipid raft structure and function, *J Biol Chem* 279 [11], pp. 9997-10004.
- [231] Tepper, A. D.; Ruurs, P.; Wiedmer, T.; Sims, P. J.; Borst, J. and van Blitterswijk, W. J. (2000): Sphingomyelin hydrolysis to ceramide during the execution phase of apoptosis results from phospholipid scrambling and alters cell-surface morphology, *J Cell Biol* 150 [1], pp. 155-64.
- [232] Young, S. G. and Fielding, C. J. (1999): The ABCs of cholesterol efflux, *Nat Genet* 22 [4], pp. 316-8.
- [233] Zarubica, A.; Plazzo, A. P.; Stöckl, M.; Trombik, T.; Hamon, Y.; Müller, P.; Pomorski, T.; Herrmann, A. and Chimini, G. (2009): Functional implications of the influence of ABCA1 on lipid microenvironment at the plasma membrane: a biophysical study, *Faseb J*.
- [234] Tam, S. P.; Mok, L.; Chimini, G.; Vasa, M. and Deeley, R. G. (2006): ABCA1 mediates high-affinity uptake of 25-hydroxycholesterol by membrane vesicles and rapid efflux of oxysterol by intact cells, *Am J Physiol Cell Physiol* 291 [3], pp. C490-502.

- [235] Ho, C.; Kelly, M. B. and Stubbs, C. D. (1994): The effects of phospholipid unsaturation and alcohol perturbation at the protein/lipid interface probed using fluorophore lifetime heterogeneity, *Biochim Biophys Acta* 1193 [2], pp. 307-15.
- [236] Ho, C.; Williams, B. W. and Stubbs, C. D. (1992): Analysis of cell membrane micro-heterogeneity using the fluorescence lifetime of DPH-type fluorophores, *Biochim Biophys Acta* 1104 [2], pp. 273-82.
- [237] Gaus, K.; Chklovskaya, E.; Fazekas de St Groth, B.; Jessup, W. and Harder, T. (2005): Condensation of the plasma membrane at the site of T lymphocyte activation, *J Cell Biol* 171 [1], pp. 121-31.
- [238] Grassme, H.; Jekle, A.; Riehle, A.; Schwarz, H.; Berger, J.; Sandhoff, K.; Kolesnick, R. and Gulbins, E. (2001): CD95 signaling via ceramide-rich membrane rafts, *J Biol Chem* 276 [23], pp. 20589-96.
- [239] Pucadyil, T. J. and Chattopadhyay, A. (2006): Effect of cholesterol on lateral diffusion of fluorescent lipid probes in native hippocampal membranes, *Chem Phys Lipids* 143 [1-2], pp. 11-21.
- [240] el Hage Chahine, J. M.; Cribier, S. and Devaux, P. F. (1993): Phospholipid transmembrane domains and lateral diffusion in fibroblasts, *Proc Natl Acad Sci U S A* 90 [2], pp. 447-51.
- [241] Searls, D. B. and Edidin, M. (1981): Lipid composition and lateral diffusion in plasma membranes of teratocarcinoma-derived cell lines, *Cell* 24 [2], pp. 511-7.
- [242] Kahya, N.; Scherfeld, D.; Bacia, K.; Poolman, B. and Schwille, P. (2003): Probing lipid mobility of raft-exhibiting model membranes by fluorescence correlation spectroscopy, *J Biol Chem* 278 [30], pp. 28109-15.
- [243] Scherfeld, D.; Kahya, N. and Schwille, P. (2003): Lipid dynamics and domain formation in model membranes composed of ternary mixtures of unsaturated and saturated phosphatidylcholines and cholesterol, *Biophys J* 85 [6], pp. 3758-68.
- [244] Murase, K.; Fujiwara, T.; Umemura, Y.; Suzuki, K.; Iino, R.; Yamashita, H.; Saito, M.; Murakoshi, H.; Ritchie, K. and Kusumi, A. (2004): Ultrafine membrane compartments for molecular diffusion as revealed by single molecule techniques, *Biophys J* 86 [6], pp. 4075-93.
- [245] Millot, C.; Le Berre-Anton, V.; Tocanne, J. F. and Tournier, J. F. (2000): Plasma membrane coating with cationic silica particles and osmotic shock alters the morphology of bovine aortic endothelial cells, *Biochim Biophys Acta* 1467 [1], pp. 85-90.
- [246] Ramprasad, O. G.; Rangaraj, N.; Srinivas, G.; Thiery, J. P.; Dufour, S. and Pande, G. (2008): Differential regulation of the lateral mobility of plasma membrane phospholipids by the extracellular matrix and cholesterol, *J Cell Physiol* 215 [2], pp. 550-61.
- [247] Lippincott-Schwartz, J.; Snapp, E. and Kenworthy, A. (2001): Studying protein dynamics in living cells, *Nat Rev Mol Cell Biol* 2 [6], pp. 444-56.
- [248] Bruneau, N.; Richard, S.; Silvy, F.; Verine, A. and Lombardo, D. (2003): Lectin-like Ox-LDL receptor is expressed in human INT-407 intestinal cells: involvement in the transcytosis of pancreatic bile salt-dependent lipase, *Mol Biol Cell* 14 [7], pp. 2861-75.
- [249] Howarth, M.; Takao, K.; Hayashi, Y. and Ting, A. Y. (2005): Targeting quantum dots to surface proteins in living cells with biotin ligase, *Proc Natl Acad Sci U S A* 102 [21], pp. 7583-8.
- [250] Drobnik, W.; Borsukova, H.; Bottcher, A.; Pfeiffer, A.; Liebisch, G.; Schutz, G. J.; Schindler, H. and Schmitz, G. (2002): Apo AI/ABCA1-dependent and HDL3-mediated lipid efflux from compositionally distinct cholesterol-based microdomains, *Traffic* 3 [4], pp. 268-78.
- [251] Hammond, A. T.; Heberle, F. A.; Baumgart, T.; Holowka, D.; Baird, B. and Feigenson, G. W. (2005): Crosslinking a lipid raft component triggers liquid ordered-liquid disordered phase separation in model plasma membranes, *Proc Natl Acad Sci U S A* 102 [18], pp. 6320-5.
- [252] Lichtenberg, D.; Goni, F. M. and Heerklotz, H. (2005): Detergent-resistant membranes should not be identified with membrane rafts, *Trends Biochem Sci* 30 [8], pp. 430-6.
- [253] Smart, E. J.; Ying, Y. S.; Mineo, C. and Anderson, R. G. (1995): A detergent-free method for purifying caveolae membrane from tissue culture cells, *Proc Natl Acad Sci U S A* 92 [22], pp. 10104-8.
- [254] Song, K. S.; Li, Shengwen; Okamoto, T.; Quilliam, L. A.; Sargiacomo, M. and Lisanti, M. P. (1996): Co-purification and direct interaction of Ras with caveolin, an integral membrane protein of caveolae microdomains. Detergent-free purification of caveolae microdomains, *J Biol Chem* 271 [16], pp. 9690-7.

- [255] Bickel, P. E.; Scherer, P. E.; Schnitzer, J. E.; Oh, P.; Lisanti, M. P. and Lodish, H. F. (1997): Flotillin and epidermal surface antigen define a new family of caveolae-associated integral membrane proteins, *J Biol Chem* 272 [21], pp. 13793-802.
- [256] Schiller, J.; Arnhold, J.; Benard, S.; Muller, M.; Reichl, S. and Arnold, K. (1999): Lipid analysis by matrix-assisted laser desorption and ionization mass spectrometry: A methodological approach, *Anal Biochem* 267 [1], pp. 46-56.
- [257] Pike, L. J.; Han, X.; Chung, K. N. and Gross, R. W. (2002): Lipid rafts are enriched in arachidonic acid and plasmenylethanolamine and their composition is independent of caveolin-1 expression: a quantitative electrospray ionization/mass spectrometric analysis, *Biochemistry* 41 [6], pp. 2075-88.
- [258] Pike, L. J.; Han, X. and Gross, R. W. (2005): Epidermal growth factor receptors are localized to lipid rafts that contain a balance of inner and outer leaflet lipids: a shotgun lipidomics study, *J Biol Chem* 280 [29], pp. 26796-804.
- [259] Petkovic, M.; Schiller, J.; Muller, M.; Benard, S.; Reichl, S.; Arnold, K. and Arnhold, J. (2001): Detection of individual phospholipids in lipid mixtures by matrix-assisted laser desorption/ionization time-of-flight mass spectrometry: phosphatidylcholine prevents the detection of further species, *Anal Biochem* 289 [2], pp. 202-16.
- [260] Ottico, E.; Prinetti, A.; Prioni, S.; Giannotta, C.; Basso, L.; Chigorno, V. and Sonnino, S. (2003): Dynamics of membrane lipid domains in neuronal cells differentiated in culture, *J Lipid Res* 44 [11], pp. 2142-51.
- [261] Parasassi, T.; De Stasio, G.; d'Ubaldo, A. and Gratton, E. (1990): Phase fluctuation in phospholipid membranes revealed by Laurdan fluorescence, *Biophys J* 57 [6], pp. 1179-86.
- [262] Parasassi, T.; Di Stefano, M.; Loiero, M.; Ravagnan, G. and Gratton, E. (1994): Cholesterol modifies water concentration and dynamics in phospholipid bilayers: a fluorescence study using Laurdan probe, *Biophys J* 66 [3 Pt 1], pp. 763-8.
- [263] Parasassi, T.; Di Stefano, M.; Loiero, M.; Ravagnan, G. and Gratton, E. (1994): Influence of cholesterol on phospholipid bilayers phase domains as detected by Laurdan fluorescence, *Biophys J* 66 [1], pp. 120-32.
- [264] Veatch, S. L. and Keller, S. L. (2003): Separation of liquid phases in giant vesicles of ternary mixtures of phospholipids and cholesterol, *Biophys J* 85 [5], pp. 3074-83.
- [265] Parasassi, T.; Di Stefano, M.; Ravagnan, G.; Saporita, O. and Gratton, E. (1992): Membrane aging during cell growth ascertained by Laurdan generalized polarization, *Exp Cell Res* 202 [2], pp. 432-9.
- [266] Levi, M.; Wilson, P. V.; Cooper, O. J. and Gratton, E. (1993): Lipid phases in renal brush border membranes revealed by Laurdan fluorescence, *Photochem Photobiol* 57 [3], pp. 420-5.
- [267] Morrot, G.; Cribier, S.; Devaux, P. F.; Geldwerth, D.; Davoust, J.; Bureau, J. F.; Fellmann, P.; Herve, P. and Frilley, B. (1986): Asymmetric lateral mobility of phospholipids in the human erythrocyte membrane, *Proc Natl Acad Sci U S A* 83 [18], pp. 6863-7.
- [268] Mukherjee, S.; Raghuraman, H.; Dasgupta, S. and Chattopadhyay, A. (2004): Organization and dynamics of N-(7-nitrobenz-2-oxa-1,3-diazol-4-yl)-labeled lipids: a fluorescence approach, *Chem Phys Lipids* 127 [1], pp. 91-101.
- [269] Huster, D.; Muller, P.; Arnold, K. and Herrmann, A. (2001): Dynamics of membrane penetration of the fluorescent 7-nitrobenz-2-oxa-1,3-diazol-4-yl (NBD) group attached to an acyl chain of phosphatidylcholine, *Biophys J* 80 [2], pp. 822-31.
- [270] Loura, L. M. and Ramalho, J. P. (2007): Location and dynamics of acyl chain NBD-labeled phosphatidylcholine (NBD-PC) in DPPC bilayers. A molecular dynamics and time-resolved fluorescence anisotropy study, *Biochim Biophys Acta* 1768 [3], pp. 467-78.
- [271] Raghuraman, H.; Shrivastava, S. and Chattopadhyay, A. (2007): Monitoring the looping up of acyl chain labeled NBD lipids in membranes as a function of membrane phase state, *Biochim Biophys Acta* 1768 [5], pp. 1258-67.
- [272] Arvinte, T.; Cudd, A. and Hildenbrand, K. (1986): Fluorescence Studies of the Incorporation of N-(7-Nitrobenz-2-Oxa-1,3-Diazol-4-Yl)-Labeled Phosphatidylethanolamines into Liposomes, *Biochimica Et Biophysica Acta* 860 [2], pp. 215-228.
- [273] Chattopadhyay, A. and Mukherjee, S. (1993): Fluorophore environments in membrane-bound probes: a red edge excitation shift study, *Biochemistry* 32 [14], pp. 3804-11.

- [274] Silvius, J. R. (2003): Fluorescence energy transfer reveals microdomain formation at physiological temperatures in lipid mixtures modeling the outer leaflet of the plasma membrane, *Biophys J* 85 [2], pp. 1034-45.
- [275] de Almeida, R. F.; Loura, L. M.; Fedorov, A. and Prieto, M. (2005): Lipid rafts have different sizes depending on membrane composition: a time-resolved fluorescence resonance energy transfer study, *J Mol Biol* 346 [4], pp. 1109-20.
- [276] Almeida, P. F.; Pokorny, A. and Hinderliter, A. (2005): Thermodynamics of membrane domains, *Biochim Biophys Acta* 1720 [1-2], pp. 1-13.
- [277] Jacobson, K.; Mouritsen, O. G. and Anderson, R. G. (2007): Lipid rafts: at a crossroad between cell biology and physics, *Nat Cell Biol* 9 [1], pp. 7-14.
- [278] Mendez, A. J.; Lin, G.; Wade, D. P.; Lawn, R. M. and Oram, J. F. (2001): Membrane lipid domains distinct from cholesterol/sphingomyelin-rich rafts are involved in the ABCA1-mediated lipid secretory pathway, *J Biol Chem* 276 [5], pp. 3158-66.
- [279] McMullen, T. P.; Lewis, R. N. and McElhaney, R. N. (2000): Differential scanning calorimetric and Fourier transform infrared spectroscopic studies of the effects of cholesterol on the thermotropic phase behavior and organization of a homologous series of linear saturated phosphatidylserine bilayer membranes, *Biophys J* 79 [4], pp. 2056-65.
- [280] Lange, Y.; Ye, J. and Steck, T. L. (2005): Activation of membrane cholesterol by displacement from phospholipids, *J Biol Chem* 280 [43], pp. 36126-31.
- [281] Lange, Y.; Ye, J. and Steck, T. L. (2007): Scrambling of phospholipids activates red cell membrane cholesterol, *Biochemistry* 46 [8], pp. 2233-8.
- [282] Radhakrishnan, A. and McConnell, H. M. (2000): Chemical activity of cholesterol in membranes, *Biochemistry* 39 [28], pp. 8119-24.
- [283] Lange, Y. and Steck, T. L. (2008): Cholesterol homeostasis and the escape tendency (activity) of plasma membrane cholesterol, *Prog Lipid Res* 47 [5], pp. 319-32.
- [284] Slotte, J. P. (1999): Sphingomyelin-cholesterol interactions in biological and model membranes, *Chem Phys Lipids* 102 [1-2], pp. 13-27.
- [285] Nagao, K.; Takahashi, K.; Hanada, K.; Kioka, N.; Matsuo, M. and Ueda, K. (2007): Enhanced apoA-I-dependent cholesterol efflux by ABCA1 from sphingomyelin-deficient Chinese hamster ovary cells, *J Biol Chem* 282 [20], pp. 14868-74.
- [286] Smith, J. D.; Waelde, C.; Horwitz, A. and Zheng, P. (2002): Evaluation of the role of phosphatidylserine translocase activity in ABCA1-mediated lipid efflux, *J Biol Chem* 277 [20], pp. 17797-803.
- [287] Hamilton, J. A. (2003): Fast flip-flop of cholesterol and fatty acids in membranes: implications for membrane transport proteins, *Curr Opin Lipidol* 14 [3], pp. 263-71.
- [288] Leventis, R. and Silvius, J. R. (2001): Use of cyclodextrins to monitor transbilayer movement and differential lipid affinities of cholesterol, *Biophys J* 81 [4], pp. 2257-67.
- [289] Müller, P. and Herrmann, A. (2002): Rapid transbilayer movement of spin-labeled steroids in human erythrocytes and in liposomes, *Biophys J* 82 [3], pp. 1418-28.
- [290] Risselada, H. J. and Marrink, S. J. (2008): The molecular face of lipid rafts in model membranes, *Proc Natl Acad Sci U S A* 105 [45], pp. 17367-72.
- [291] Wang, N.; Silver, D. L.; Costet, P. and Tall, A. R. (2000): Specific binding of ApoA-I, enhanced cholesterol efflux, and altered plasma membrane morphology in cells expressing ABC1, *J Biol Chem* 275 [42], pp. 33053-8.

Acknowledgement

At first, I would like to thank Prof. Dr. Andreas Herrmann for guiding me into the fascinating world of research and for teaching me the art of the scientific investigation. I appreciate his efforts in keeping up my motivation during the difficult times.

I am also very grateful to Prof. Dr. Thomas Pomorski for the time he donated me for discussion and for his useful suggestions. I also appreciate his way of facing challenges and problems.

I would like to thank Dr. Peter Müller for the time he spent discussing my data and for the encouragement and support he was able to give me.

I am obliged to Dr. Giovanna Chimini and Dr. Ana Zarubica for the successful collaboration and the constant exchange of information and discussion.

I especially want to thank Dr. Thomas Korte for introducing me into the field of microscopy and for his continuous help with electronic equipment.

I am also indebted to Sabine Schiller for her precious help in crucial experiments and for sharing with me her experience.

Many thanks also go to Dr. Martin Stöckl for introducing me into FLIM and for being always available for discussion.

I also want to express my gratitude to “das Mädchen Büro” - Silvia, Frau Dr. Gabi, Susann and Roland -, and to Susanne and Adrien. Thanks for the friendly and pleasant atmosphere.

Finally, I would like to thank my parents, Claudio and Vittoria, and my brother Matteo for their love and constant support. I am also grateful to Roberto for sharing with me this experience and for his constant presence. Many thanks also to Sawa and Francesca for being always there despite the distance.

Publications

Talks

“Phospholipid exposure in ABCA7-expressing cells”, Satellite Meeting *Flippases* of the FEBS Special Meeting “ATP-Binding Cassette (ABC) Proteins: from Multidrug Resistance to Genetic Diseases” (Innsbruck, Austria). 04.03.2006 – 10.03.2006

“Potential role of ABCA7 in lipid trafficking”, Annual Meeting Marie Curie RTN *Flippases* (Copenhagen, Denmark) 24.08.2006 – 28.08.2006

“Function of ABCA transporters in membrane organization”, Annual Meeting Marie Curie RTN *Flippases* (Granada, Spain) 21.03.2007 – 25.03.2007

“Function of ABCA1 in the plasma membrane micro-organization”, EMBO Practical Course “Imaging in 3-D and the F-techniques: FRET, FCS, FLIM and FRAP” (Singapore, Singapore) 17.06.2007 – 29.06.2007

“ABCA1 and plasma membrane lateral heterogeneity”, Annual Meeting Marie Curie RTN *Flippases* (Budapest, Hungary) 07.02.2008 – 09.02.2008

Posters

Plazzo, A.P., Alder-Baerens, N., Zarubica, A., Korte, T., Chimini, G., Pomorski, T. and Herrmann, A. “Role of ABCA proteins in lipid trafficking”, EMBO Workshop on Cell Membrane Organization and Dynamics (Bilbao, Spain) 03.06.2006 – 07.06.2006

Plazzo, A.P., Zarubica, A., Korte, T., Chimini, G., Pomorski, T. and Herrmann, A. “Potential role of ABCA7 in lipid trafficking”, FEBS Special Meeting “New Concepts in Lipidology: from Lipidomics to Disease” (Noordwijkerhout, The Netherlands) 21.10.2006 – 25.10.2006

Plazzo, A.P., Zarubica, Stöckl, M., Pomorski, T., Chimini, G. and Herrmann, A. “ABCA1 acts on membrane lipid packing”, 2nd FEBS Special Meeting “ATP-Binding Cassette (ABC) Proteins: from Multidrug Resistance to Genetic Diseases” (Innsbruck, Austria). 01.03.2008 – 08.03.2008

Plazzo, A.P., Zarubica, Stöckl, M., Müller, P., Pomorski, T., Chimini, G. and Herrmann, A. “ABCA1 modulates the physical properties of the cell surface”, *Flippases 2008: “How Lipids Cross a Membrane”* (Ascona, Switzerland) 02.11.2008 – 07.11.2008

Manuscripts

Stöckl M., Plazzo A.P., Korte T., Herrmann A. (2008). Detection of lipid domains in model and cell membranes by fluorescence lifetime imaging microscopy of fluorescent lipid analogues. *J Biol Chem.* 283 (45), 30828-30837.

Zarubica A*, Plazzo A.P.*, Stöckl M., Trombik T., Hamon Y., Müller P., Pomorski T., Herrmann A., Chimini G. (2009). Functional implications of the influence of ABCA1 on lipid microenvironment at the plasma membrane: a biophysical study. *FASEB J* 23, 1775-1785.

* equally contributed

Eidesstattliche Erklärung

Hiermit erkläre ich, die vorliegende Arbeit selbständig ohne fremde Hilfe verfasst und nur die angegebene Literatur verwendet zu haben. Ein Teil der beschriebenen Ergebnisse wurde in Zusammenarbeit mit anderen Mitarbeitern der Arbeitsgruppe Molekulare Biophysik und des “Center of Immunology of Marseille-Luminy” erzielt. Diese sind entsprechend gekennzeichnet.

Ich besitze keinen entsprechenden Doktorgrad und habe mich anderwärts nicht um einen Doktorgrad beworben.

Die dem Promotionsverfahren zugrunde liegende Promotionsordnung ist mir bekannt.

Anna Pia Plazzo